UNIVERSIDADE FEDERAL DE MINAS GERAIS
Escola de Engenharia
Programa de Pós-Graduação em Engenharia de Produção

Tainá Pôssas Abreu

COMPETITIVE MULTIPLE ALLOCATION P-HUB LOCATION PROBLEMS: models and exact algorithms

Belo Horizonte
2026

Tainá Pôssas Abreu

COMPETITIVE MULTIPLE ALLOCATION P-HUB LOCATION PROBLEMS: models and exact algorithms

Thesis presented to the Graduate Program in Production Engineering of the Federal University of Minas Gerais in partial fulfillment of the requirements for the degree of Doctor in Production Engineering.

Advisor: Ricardo Saraiva de Camargo

Co-Advisor: Luiza Bernardes Real

Belo Horizonte
2026

Abreu, Tainá Pôssas.
A162c Competitive multiple allocation p-hub location problems [recurso eletrônico] : models and exact algorithms / Tainá Pôssas Abreu. – 2026.
1 recurso online (128 f. : il., color.) : pdf.

Orientador: Ricardo Saraiva de Camargo.
Coorientadora: Luiza Bernardes Real.

Tese (doutorado) – Universidade Federal de Minas Gerais, Escola de Engenharia.

Inclui bibliografia.

1. Engenharia de produção – Teses. 2. Logística – Teses. 3. Aerovias – Teses. 4. Algoritmos – Simulação por computador – Teses. I. Camargo, Ricardo Saraiva de. II. Real, Luiza Bernardes. III. Universidade Federal de Minas Gerais. Escola de Engenharia. IV. Título.

CDU: 658.5(043)

Ficha catalográfica elaborada pelo bibliotecário Marcio A. A. Gomes CRB/6 2812
Biblioteca Prof. Mário Werneck, Escola de Engenharia da UFMG

UNIVERSIDADE FEDERAL DE MINAS GERAIS

Escola de Engenharia

Programa de Pós-Graduação em Engenharia de Produção

FOLHA DE APROVAÇÃO

Problemas competitivos de localização de p-hubs com alocação múltipla: modelos e algoritmos exatos

TAINÁ PÔSSAS ABREU

Tese submetida à Banca Examinadora designada pelo Colegiado do Programa de Pós-Graduação em ENGENHARIA DE PRODUÇÃO, como requisito para obtenção do grau de Doutor em ENGENHARIA DE PRODUÇÃO, área de concentração PESQUISA OPERACIONAL E INTERVENÇÃO EM SISTEMAS SOCIOTÉCNICOS, linha de pesquisa Otimização e Simulação de Sistemas Logíst. e de Grande Porte.

Aprovada em 13 de fevereiro de 2026, pela banca constituída pelos membros:

Prof(a). Ricardo Saraiva de Camargo - Orientador

UFMG

Prof(a). Elisangela Martins de Sá

CEFET/MG

Prof(a). Gilberto de Miranda Junior

UFOP

Prof(a). Fatima Machado de Souza Lima

UFMG

Prof(a). Andréa Cynthia Santos Duhamel

Université Le Havre Normandie

Belo Horizonte, 13 de fevereiro de 2026.

Documento assinado eletronicamente por **Gilberto de Miranda Junior**, **Usuário Externo**, em 13/02/2026, às 11:20, conforme horário oficial de Brasília, com fundamento no art. 5º do Decreto nº 10.543, de 13 de novembro de 2020.

Documento assinado eletronicamente por **Ricardo Saraiva de Camargo**, **Professor do Magistério Superior**, em 13/02/2026, às 11:32, conforme horário oficial de Brasília, com fundamento no art. 5º do Decreto nº 10.543, de 13 de novembro de 2020.

Documento assinado eletronicamente por **Fátima Machado de Souza Lima**, **Professora do Magistério Superior**, em 14/02/2026, às 11:08, conforme horário oficial de Brasília, com fundamento no art. 5º do Decreto nº 10.543, de 13 de novembro de 2020.

Documento assinado eletronicamente por **Elisangela Martins de Sá**, **Usuária Externa**, em 20/02/2026, às 08:58, conforme horário oficial de Brasília, com fundamento no art. 5º do Decreto nº 10.543, de 13 de novembro de 2020.

A autenticidade deste documento pode ser conferida no site https://sei.ufmg.br/sei/controlador_externo.php?acao=documento_conferir&id_orgao_acesso_externo=0, informando o código verificador **4956596** e o código CRC **9A7FB4C6**.

Referência: Processo nº 23072.208703/2026-83 SEI nº 4956596

Agradecimentos

Agradeço primeiramente a Deus, pela oportunidade que me foi confiada e por me lembrar, nas horas de dúvida, que tudo tem um propósito maior. Agradeço ao meu companheiro, Felipe Baracho, pelo amor e todo apoio durante a desafiadora jornada do doutorado. Agradeço aos meus pais, Hailton e Shirley, por serem a minha base e torcida mais fiel. Agradeço à minha irmã, Maíra, cuja amizade e sabedoria foram diferenciais para atravessar os momentos mais delicados deste percurso. Agradeço também ao meu cunhado e sobrinha, Brice e Chloë, pelas mensagens de força e carinho.

Agradeço aos meus orientadores, Prof. Ricardo Camargo e Profª. Luiza Bernardes, pela confiança, orientação, e suporte para a conclusão deste trabalho. Agradeço à banca examinadora, formada pelos professores Profª. Andrea Santos, Profª. Elisangela Martins, Profª Fátima Lima e Prof. Gilberto Miranda pela disponibilidade em avaliar e contribuir com este trabalho. Agradeço a todos os professores e funcionários do Programa de Pós-Graduação em Engenharia de Produção da UFMG, pelo trabalho dedicado e pela contribuição na formação de seus alunos. Agradeço aos colegas de curso, Thalles, Maressa e Darlan, que apesar de pouco convívio, sempre estiveram dispostos a ajudar.

Agradeço aos colegas de profissão do Departamento de Engenharia de Transportes do CEFET-MG, pelo incentivo, e ao próprio CEFET-MG, pela concessão do afastamento integral para a realização desta qualificação. Agradeço, ainda, à CAPES, pelo apoio financeiro concedido em parte desta jornada.

Por fim, encerro mais este capítulo da minha vida profundamente grata por todos os aprendizados obtidos ao longo destes anos, que ultrapassaram o campo técnico e alcançaram dimensões pessoais e humanas. Que o conhecimento aqui construído continue a se desdobrar em sabedoria, em prol do coletivo, sempre.

RESUMO

Esta tese aborda o problema competitivo de localização de p-hubs com múltiplos caminhos e alocação múltipla (MPMAPHLP), motivado por aplicações na indústria aérea, na qual uma nova companhia aérea busca competir com uma empresa estabelecida em um mercado consolidado. Nesse contexto, levamos em consideração a escolha de rota pelo passageiro, tornando o planejamento estratégico de redes hub-and-spoke um fator crucial para a conquista de mercado. Duas novas formulações matemáticas são propostas: a primeira reformula o problema original de maximização da literatura em um modelo equivalente de minimização. A segunda reforça restrições de acoplamento do problema alcançando maior escalabilidade. Este trabalho é o primeiro a tratar este tipo de problema através da perda de mercado e a utilizar restrições de acoplamento mais fortes, favorecendo a escalabilidade. Para resolver os problemas inteiros mistos não lineares, primeiramente utilizamos formulações cônicas equivalentes, em seguida, novos algoritmos exatos baseados na técnica de aproximação externa do tipo *Outer Approximation* são desenvolvidos. Ademais, o trabalho é pioneiro na combinação de reformulação cônica com *Outer Approximation* nesse contexto. Através de extensivos experimentos computacionais usando dados da *Civil Aeronautics Board* com até 70 nós, demonstramos que nossos modelos superam substancialmente todo o trabalho anterior. Através de um solucionador cônico comercial, nossas formulações propostas alcançaram ganhos computacionais notáveis em relação ao modelo da literatura: o modelo de minimização inicial atinge acelerações médias de 113 vezes, e a segunda formulação chega a acelerações médias de 1081 vezes, ambas mais rápidas que o modelo de maximização, estabelecendo um novo padrão em eficiência de soluções para MPMAPHLP competitivo. Ganhos de performance foram obtidos ao empregar algoritmos baseados em aproximação externa OA, demonstrando a eficiência dos novos algoritmos desenvolvidos.

Palavras-chave: Localização de hubs, localização competitiva, economias de escala, programação cônica de segunda ordem inteira mista, técnica de aproximação externa.

ABSTRACT

This thesis addresses the competitive multi-path multi-allocation p-hub location problem (MPMAPHLP), motivated by applications in the airline industry, in which a new airline seeks to compete with an established company in a consolidated market. In this context, we consider passenger route choice, making strategic hub-and-spoke network planning a crucial factor for market capture. Two new mathematical formulations are proposed: the first reformulates the original maximization problem from the literature into an equivalent minimization model. The second reinforces the problem's coupling constraints, achieving greater scalability. This work is the first to address this type of problem through market loss and to use stronger coupling constraints, favoring scalability. To solve mixed-integer non-linear problems, we first use equivalent conic formulations, followed by new exact algorithms based on the outer approximation technique. Furthermore, this work pioneers the combination of conic reformulation with outer approximation in this context. Through extensive computational experiments using Civil Aeronautics Board (CAB) data with up to 70 nodes, we demonstrate that our models substantially outperform all previous work. Using a commercial conic solver, our proposed formulations achieved remarkable computational gains compared to the literature model: the initial minimization model achieves average speedups of 113 times, and the second formulation reaches average speedups of 1081 times, both faster than the maximization model, establishing a new standard in efficiency for competitive MPMAPHLP solutions. Performance gains were obtained by employing algorithms based on external approximation, demonstrating the efficiency of the newly developed algorithms.

Keywords: Hub location, competitive location, economies of scale, mixed-integer second-order cone programming, outer approximation technique.

List of Figures

List of Tables

Contents

Chapter 1

Introduction

This thesis addresses the *Competitive Multi-Path Multi-Allocation p-Hub Location Problem* (MPMAPHLP), a challenging problem with both mathematical and practical relevance that arises when a new entrant seeks to establish a hub-and-spoke network in a market dominated by an incumbent operator. This problem encapsulates a strategic decision-making process, where the objective is not merely to optimize network efficiency but to do so in a competitive environment, in which customer choice is influenced by factors such as price, travel time, and service attractiveness. Such scenarios are commonplace in industries such as air transportation, freight logistics, and telecommunications, where the design of an efficient hub-and-spoke network becomes a decisive factor for competitiveness and market share acquisition.

Hubs are transshipment facilities responsible for consolidating flows from multiple origins before routing them either to their destinations or to other hubs for further redistribution (O'kelly, 1986; O'Kelly and Bryan, 1998). Unlike the classical $p-$*Hub Location Problem* ($p-$HLP) (O'kelly, 1986; Campbell et al., 2002), which assumes a monopolistic market and focuses solely on distance or cost minimization between the facilities and the demand points, the competitive variant introduces an additional layer of strategic complexity. Here, the network design decisions of the entrant are heavily influenced by the fixed presence of incumbent networks, whose existing hub configurations shape the competitive landscape. This research addresses a non-cooperative competitive hub location setting with a static incumbent network, where the incumbent's network is considered fixed, and the entrant optimizes its network configuration accordingly.

In the classical $p-$HLP, the goal is to select p hub facilities from a set of candidates to design a hub-and-spoke network that minimizes total costs. This network structure allows bundled flows on inter-hub connections to benefit from economies of scale, resulting in lower transportation costs compared to direct shipments between origin-destination pairs. It is typically assumed that demand is fixed and fully assigned to the designed network, without consideration of alternative services.

In competitive models, this assumption of captive demand no longer holds. The entrant operates in a market already served by an incumbent network, and customers typically select the most attractive service based on relative utilities of the alternatives

(Huff, 1964, 1966). Demand behavior is influenced by a set of predefined factors that characterize attraction mechanisms introduced in the modeling framework. As a result, the problem shifts from a pure cost minimization perspective to the challenge of optimizing market share. The success of an entrant company in capturing a larger market share is heavily dependent on the attractiveness of its hubs and their capacity to influence customer choices (Drezner and Drezner, 2001).

In the multiple allocation p-hub location problem, demand nodes can be assigned to multiple hubs, providing greater flexibility in route planning, as illustrated by Figure 1.1, in which the hubs (red nodes) are connected to every node in the map. This network configuration allows a multitude of paths to serve any pair of origin-destination points (Eiselt and Marianov, 2009; Tiwari et al., 2021a). The multi-path variant assumes that flows can be distributed through several alternative routes.

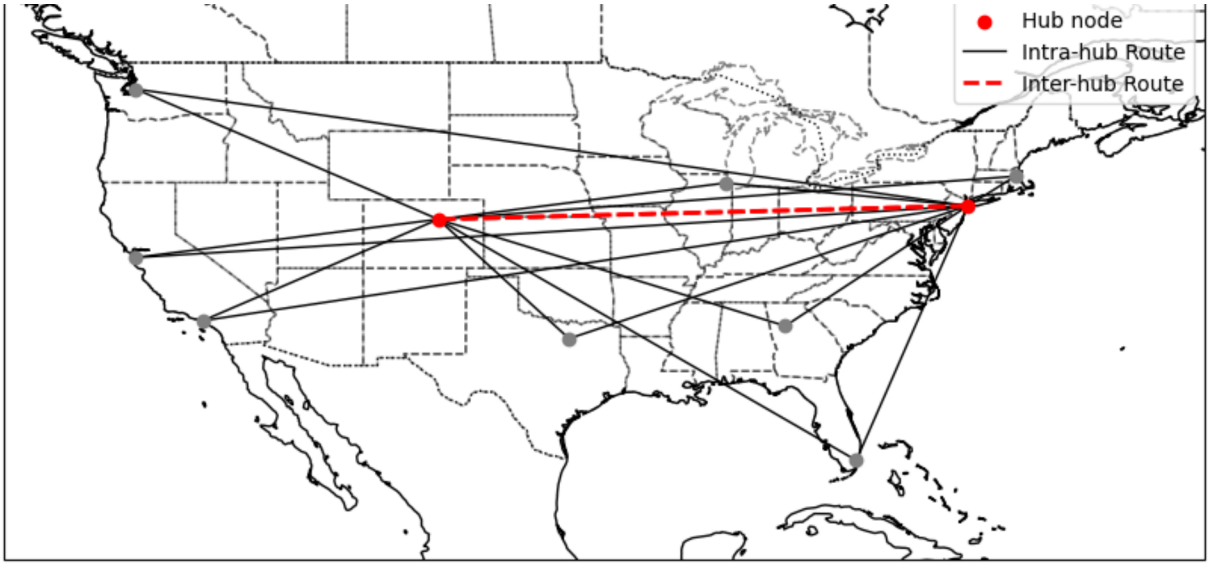

Figure 1.1: A multi-path network with 10 nodes and 2 hubs

The problem under study integrates three critical and computationally challenging dimensions: (i) *competitive market dynamics*, where demand allocation depends on the relative utility of paths; (ii) *multi-path routing*, which allows demand to be split over multiple origin-destination paths, enhancing network resilience and customer service levels; and (iii) *multi-allocation*, wherein origin-destination pairs are connected via multiple hub pairs, providing greater flexibility but exponentially increasing the solution space.

The first formal mathematical formulation of this problem, in the form we studied in this research, was proposed by Eiselt and Marianov (2009), who extended the earlier work of Marianov et al. (1999) by incorporating more sophisticated demand attraction functions based on customer utility models. This replaced the simple cost-based deterministic allocation employed in the original model. A key challenge in this problem lies in the presence of a nonlinear objective function, which models market share capture through gravity-like customer choice formulations. Traditional approaches rely on

linearization techniques, typically based on Big-M formulations, auxiliary variables, or finite constraint approximation (Elhedhli, 2005). These methods allow the problem to be reformulated as a mixed-integer linear program (MILP), leading to models with an extremely large number of variables and constraints, which grow combinatorially with the network size, and suffer from weak linear relaxations. This results in poor performance of branch-and-bound algorithms, characterized by large optimality gaps and excessive computational times, even for moderately sized instances.

Recognizing the computational challenges of solving the nonlinear integer program proposed by Eiselt and Marianov (2009), which had previously been tackled using heuristics such as genetic algorithms, Tiwari et al. (2021a) revisit the same formulation with a focus on solving large-scale instances to optimality. To this end, they propose and compare four alternative solution approaches that preserve convexity properties, effectively eliminating the need for fragile linearizations. As a result, their methods yield substantially stronger relaxations and improved computational efficiency. This enables the exact solution of larger instances within tight optimality gaps and reasonable computational times, a feat previously impractical using linearization-based methods.

Since the contribution of Tiwari et al. (2021a), no further methodological advances have been proposed for addressing this problem in competitive settings. Although significant progress has been made in other variants of competitive hub location problems (Drezner and Eiselt, 2024; Sharma et al., 2025), the development of scalable and mathematically robust formulations for the competitive multi-path multi-allocation p-hub location problem remains an open challenge. Existing models do not leverage convexity properties to strengthen relaxations while maintaining a structure suitable for efficient exact optimization. This thesis addresses this methodological gap by proposing novel formulations that are both optimization-wise stronger and capable of handling large-scale competitive instances effectively.

Our methodological framework begins with the development of two alternative mathematical formulations for the MPMAPHLP. The first reformulates the original maximization problem as an equivalent minimization model based on market loss, preserving its mathematical structure while enabling a reformulation into a convex conic form. The second formulation strengthens the coupling constraints between inter-hub connection and hub selection, resulting in tighter relaxations and improved scalability. Both formulations are explored under two mathematical programming paradigms: a convex mixed-integer nonlinear program (MINLP) and an equivalent mixed-integer second-order conic program (MISOCP), drawing conceptual inspiration from Tiwari et al. (2021a). Further, this modeling frameworks support the design of exact algorithms based on the outer approximation technique, developed in this research to solve both formulations efficiently.

To assess the computational viability of the proposed formulations, we first solve all SOCP versions of the three models, including the original maximization and the two

new minimization formulations, directly using the IBM ILOG CPLEX Optimization Studio, which supports mixed-integer second-order cone programming. This initial analysis provides valuable insights into the strengths and limitations of each conic formulation in terms of scalability and relaxation quality. Regarding computational performance, the minimization-based formulations achieved substantial gains compared to the maximization model from the literature: the original minimization model presented an average speed-up of 113 times, while the new tightened formulation reached an acceleration of approximately 1080 times. These results confirm the superior numerical efficiency of minimizing market loss over maximizing market share, establishing the new formulation as a benchmark reference for future studies.

Building on the structural insights gained from the conic formulations, we propose three exact solution approaches based on the *Outer Approximation* (OA) technique to improve the tractability of the new minimization models. These methods iteratively approximate the nonlinear market capture functions using linear constraints, while preserving the convexity of the underlying model. The first approach restructures the master problem by projecting the objective over decision variables to facilitate cut generation (called OA-Obj). The second introduces a scalar reformulation of the objective, allowing for a distinct OA strategy (called OA-rvar). The third applies OA directly to the conic formulation with an initial set of outer approximation cuts (called COACuts). These algorithms significantly reduce computation times and enhance scalability without compromising optimality. We obtained average speed-ups of 1143.84 times, 415.55 times, and 3451.79 times, respectively to OA-Obj, OA-rvar, and COACuts, when comparing the new formulation to the original minimization formulation processing times, confirming the effectiveness of the new formulation for optimizing hub-and-spoke networks in competitive environments. The models that showed the best performance were the OA-rvar, followed by the OA-Obj, and the uncut conic model, all applied to the new minimization formulation.

The computational study is based entirely on publicly available benchmark instances retrieved from the repository maintained at https://github.com/tainapossas/MPMAPHLP. The dataset includes the classical Civil Aeronautics Board (CAB) dataset, which contains inter-city distances and flows data for cities in the United States. Performance metrics considered include computational time, optimality gaps, the number of branch-and-bound nodes, and algorithmic scalability across different instance sizes and parameter settings.

1.1 Objectives and Contributions

The main objective of this research is to advance the mathematical modeling and exact solution methods for the Competitive Multi-Path Multi-Allocation p-Hub Location Prob-

lem, with emphasis on improving scalability and computational efficiency. Specifically, the research aims to:

- Propose alternative mathematical formulations for the MPMAPHLP, including a minimization-based model and an enhanced new formulation with tighter connectivity constraints;
- Develop exact solution algorithms based on the outer approximation strategy, specifically tailored to the proposed mathematical formulations;
- Assess the performance of the models and algorithms through a comprehensive computational study on benchmark instances.

The outcomes of these objectives are reflected in the main contributions of this work and their relevance to both the academic literature and real-world applications in competitive network design. This thesis contributes with (i) new convex and conic formulations for the competitive MPMAPHLP, (ii) an extended Outer Approximation framework with three algorithmic variants, and (iii) a comprehensive computational analysis demonstrating unprecedented speed-ups and complete optimal resolution of benchmark instances.

1.2 Thesis Structure

The remainder of this thesis is organized as follows. Chapter 2 presents a literature review on competitive hub location problems and revisits the original formulation of the MPMAPHLP as proposed in the literature. Chapter 3 presents our proposed mathematical formulations of the competitive Multi-Path Multi-Allocation p-Hub Location Problem (MPMAPHLP), including both the original nonlinear model, its mixed-integer second-order conic reformulation, and their alternative tightened formulations. Chapter 4 introduces the outer-approximation framework and details the three proposed algorithmic variants, explaining how each adapts the method to different problem representations. Chapter 5 reports the computational experiments and performance analyses, comparing the formulations and algorithms in terms of efficiency and solution quality. Moreover, it provides a structural and behavioral interpretation of the resulting networks Finally, Chapter 6 summarizes the main conclusions and outlines potential directions for future research.

Chapter 2

Literature Review

The concept of hub facilities has been extensively studied in the literature, initially characterized as interacting nodes responsible for consolidating and redistributing flows across different origin-destination pairs (O'kelly, 1986). These facilities play a crucial role in enhancing transportation efficiency by acting as switching and transshipment points. Over time, the definition has evolved to encompass a broader range of logistical functions, including sorting, consolidation, connection, and break-bulk operations, reflecting their central role in facilitating large-scale movement of goods and passengers (Alumur, 2019).

The benefits derived from effectively connecting hubs and nodes within a hub-and-spoke network range from reduced operational costs to enhanced system profitability. This network configuration forms the basis of the *Hub Network Design Problem* (HNDP), which focuses on optimizing the design of such networks. The HNDP remains closely tied to the broader *Facility/Hub Location Problems* (FLPs/HLPs) and is central to the field of *Location Science*. To gain insight into the literature surrounding HNDP, readers can refer to several noteworthy surveys and reviews in the field (Alumur and Kara, 2008; Campbell and O'Kelly, 2012; Farahani et al., 2013; Contreras and O'Kelly, 2019; Alumur et al., 2021; Basallo-Triana et al., 2021; Wandelt et al., 2022; Sharma et al., 2025). These surveys, along with influential technical papers, have contributed significantly to establishing well-defined and widely recognized categories of hub location problems.

Studying hub location scenarios without accounting for competition may lead to solutions that fail to capture the complexities of real-world conditions, where businesses operate in highly competitive markets. Ignoring the competitive aspect results in an incomplete and overly simplified understanding of the dynamics involved in HNDPs. However, over the years, various studies have addressed this competitive non-monopolistic market environments. Comprehensive reviews on competitive hub location models, such as those presented by Eiselt et al. (2019), Drezner and Eiselt (2024), and Sharma et al. (2025), provide valuable syntheses and classification of these contributions, emphasizing the necessity and benefits of explicitly incorporating competitive interactions into hub location modeling.

Drezner and Eiselt (2024) highlighted that competition involves multiple strategic dimensions, and identifying optimal sites for competing hubs is thus central to gaining

market advantage and has become a prominent research theme in the field. Although their review is a comprehensive reference, it was made honoring Tammy Drezner and emphasizing literature directly connected to her contributions either through direct citations or works referencing her publications. However, our bibliographic analysis intentionally adopts a broader perspective, therefore, despite covering a similar recent period, we include studies not necessarily addressed by the authors, thereby complementing and expanding upon existing syntheses of competitive location models.

To address this gap, we conducted a bibliographic analysis spanning five years (2020–2024). A search in ScienceDirect with the argument *"competitive AND hub AND location"* on title, abstract, or keywords resulted in 27 hits. However, this preliminary search includes studies from a broad spectrum of fields, many of which are not directly related to hub location models, especially those involving competitive scenarios.

As a next step, we perform a manual screening of the titles and abstracts to assess whether each work truly falls within the scope of the HNDP. In particular, we verify whether the articles explicitly deal with hub location models involving hub allocation, and whether competitive elements are present. We exclude from analysis papers with classic HLPs without competition, and unrelated uses of the term "hub" in logistics or data networks. The goal is to isolate the subset of studies that effectively contribute to the understanding of competitive hub location strategies, forming the analytical basis for the literature review that follows.

From the initial pool of 27 articles, only 5 were found to directly address the competitive HNDP, highlighting the relative scarcity of research in this specific domain. Table 2.1 presents the results chronologically. While relatively few authors have dedicated their efforts to studying competition in hub location problems, it has nonetheless remained an active area of research in recent years.

Table 2.1: Literature on competitive hub location problems

Reference	Modeling Approach			Solution Methods						
	MILP	MINLP	MISOCP	BB	CPA	LR	HEU	MTH	HYB	OA
de Araújo et al. (2020)	✓			✓			✓		✓	
Mahmoodjanloo et al. (2020)		✓						✓	✓	
Tiwari et al. (2021a)		✓	✓		✓	✓		¨		
Tiwari et al. (2021b)		✓	✓		✓	✓				
Sharma et al. (2021)	✓			✓						
This work		✓	✓							✓

(Modelling Approach) MILP :Mixed-Integer Linear Programming; MINLP: Mixed-Integer Nonlinear Programming; MISOCP: Mixed-Integer Second-Order Cone Programming.
(Solutions Methods) BB: Branch-and-Bound / Branch-and-Cut; CPA: Cutting Plane Algorithm; LR: Lagrangian Relaxation; HEU: Heuristic Methods; MTH: Metaheuristic Methods; HYB: Hybrid Approaches (e.g., Heuristic + Exact); OA: Outer Approximation

The progression in methodological complexity and diversity of modeling approaches over time suggests a growing sophistication in addressing these problems. Earlier studies predominantly relied on simpler models and solution methods, such as heuristics and

metaheuristics. In contrast, more recent research has introduced advanced approaches, reflecting significant advancements in modeling and computational capabilities. However, there remains a need for more robust, exact, and sophisticated methods to further enhance the practical applicability and theoretical contributions in this field.

de Araújo et al. (2020) address the discrete multiple allocation $(r|p)$ hub-centroid problem in a competitive scenario in which two non-cooperative firms sequentially position hubs aiming to maximize their respective captured flows. The authors propose two novel MILP formulations and develop exact branch-and-cut algorithms, integrating heuristic and exact separation procedures to efficiently generate violated cuts. The authors obtained fast convergence and optimal solutions for benchmark instances with 40 nodes.

Mahmoodjanloo et al. (2020) address a multi-modal competitive hub location and pricing problem under conditions of customer loyalty and elastic demand. They propose a bilevel MINLP framework, wherein the upper-level decisions involve selecting optimal hub locations and allocating flows, while the lower-level problem determines optimal pricing strategies using a multinomial logit model to capture customer preferences and demand elasticity. Due to the complexity arising from the nonlinear and hierarchical structure, the authors introduce a bilevel decomposition approach combining Scatter Search at the upper level and an enhanced gradient-based differential evolution metaheuristic at the lower level, solving instances up to 20 nodes.

Tiwari et al. (2021a,b) address two different formulations for the competitive hub location problem in which an entrant firm seeks to maximize its market share: a multi-path and a single-path multi-allocation p-hub location, respectively. The original MINLP formulations is tackled through four solution approaches: (i) linearization using outer approximation, which they called Kelley's cutting-plane method (CPA); (ii) a MISOCP reformulation; (iii) Lagrangian relaxation combined with CPA; and (iv) Lagrangian relaxation combined with a MISOCP. As discussed in the previous chapter, the present research builds upon and advances the multi-path formulation proposed by Tiwari et al. (2021a).

Tiwari et al. (2021b) have criticized the multi-path assumption arguing that it prevents the aggregation of flows at the installed hubs and, therefore, hinders the exploitation of scale economies in inter-hub connections. However, in our perspective, it does not necessarily undermine the ability to benefit from such economies. In practice, multi-path routing can offer greater flexibility and adaptability, allowing the system to balance loads more efficiently and avoid congestion at heavily used hubs. Moreover, by distributing flows strategically, it is still possible to concentrate traffic along cost-effective inter-hub links where scale economies are more pronounced. Thus, rather than hindering efficiency, the multi-path approach can enhance network robustness and performance under realistic competitive market conditions. This motivates our decision to adopt and

focus on the multi-path assumption as a more suitable representation for flexible and competitive network design.

Sharma et al. (2021) propose a MILP model to address a profit-maximizing hub location problem in the airline industry under coopetition. The model captures a two-phase process in which two carriers independently design domestic networks and then jointly optimize intercontinental connections while competing on shared routes. The authors strengthen the formulation using analytically derived valid inequalities and solve the problem exactly with IBM ILOG CPLEX. Computational experiments demonstrate the model's effectiveness, with instances of up to 50 nodes solved optimally.

In the next sections, we examine the key assumptions underlying competitive strategies in hub location problems and define the position of our work within the broader context of the literature. We begin by discussing the fundamental assumptions regarding decision-making models that consider either static or dynamic perspectives; the strategic interactions between firms; economies of scale, a critical factor in hub-and-spoke models; and assumptions on customer behavior models. Finally, we review the current competitive MPMAPHLP formulation, which is the object of study for the improvements proposed in this work. This discussion highlights the theoretical and practical foundations that guide research in this field, while aligning our work with established approaches in the literature.

2.1 Decision-Making Models: Static vs Dynamic

The decision making on competitive environment emerged with Hotelling (1929) that originated the primary approach to competitive facility location: a game-theoretic framework, in which firms simultaneously choose price and flexible locations. A second approach, known as sequential competitive location, is grounded in the work of Von Stackelberg (1951), who pioneered the analysis of duopolies characterized by a leader–follower dynamic (ReVelle and Eiselt, 2005). Our research aligns specifically with this second approach, focusing on the strategic selection of fixed locations under existing or potential competitive conditions.

Eiselt et al. (1993) provide a foundational perspective on competitive location models by classifying them according to the structure of market interaction and decision-making. Although their framework does not explicitly employ the terminology of static and dynamic models, it implicitly reflects this distinction through the taxonomy *'rules of the game'*. Most models surveyed fall under the static category, where competing firms make their location and pricing decisions simultaneously, assuming full information and stable market conditions. These models are analytically tractable and suitable for equilibrium analysis but fail to capture strategic adaptations over time. The authors also discuss sequential models, where one firm acts as a leader and the other as a follower, an

approach aligned with the Stackelberg competition structure. This implicitly introduces dynamic behavior, as the leader anticipates the competitor's response.

When applied to airline networks, the decision-making process for selecting hubs presents unique challenges. High operational and capital costs associated with changing hub locations make it difficult for companies to adjust their choices based on competitors' decisions. Once a hub is established, it involves significant investments in infrastructure, administrative facilities, and operational integration. The term "*brick-and-mortar facilities*" is commonly used in the literature to describe permanent, physical infrastructures, such as warehouses or transportation hubs, that are costly and challenging to relocate due to their fixed nature and associated investments. As Campbell and O'Kelly (2012) highlight, nearly all models to date have treated hub location problems as static cases, which is understandable given the substantial one-time expenses and sunk capital costs associated with large hub facilities. This static perspective aligns with the reality that airlines are often constrained in their ability to react dynamically to competitive shifts in the market.

In this study, we adopt a static decision-making framework applied to the air transportation industry, consistent with the predominant approach in the hub location literature. By assuming that competitors' decisions are fixed and do not react to the entry or strategic choices of the new firm, we can provide a straightforward analysis of the problem. This focus allows us to emphasize the direct impact of our proposed formulation without introducing the added complexity of dynamic interactions. Future research could expand on this work by incorporating dynamic elements to investigate how competitor responses might influence optimal solutions in more interactive settings.

2.2 Strategic Interactions in Competitive Markets

In an era of increasing interconnectedness, airlines cannot focus solely on competing to capture market share or on cooperating to grow the overall market. Instead, they may benefit from a framework that allows both collaboration and competition to coexist effectively. The relationship between firms engaging in simultaneous competition and cooperation is commonly referred to as "coopetition" (Walley, 2007).

Sharma et al. (2021) investigates three primary forms of strategic interactions among competing firms in the market: (1) competition-dominated markets, (2) cooperation-dominated markets, and (3) equal coopetition markets. Their findings indicate that while coopetition is not always the optimal strategy, it becomes increasingly advantageous as economies of scale grow more significant.

In this work, we focus on a non-cooperative scenario, consistent with the prevailing approach in the existing literature. This decision allows us to align with prior research, which predominantly examines competitive settings to understand market dy-

namics without collaborative influences. Furthermore, by proposing novel formulations for an established problem, we aim to build upon and extend the foundational work in this domain. Emphasizing non-cooperation enables a direct comparison with previous models, showcasing the contributions and innovations of the proposed approach. However, future studies could expand upon these analyses by incorporating cooperative or hybrid strategies to evaluate their impact on the proposed formulation.

2.3 Economies of Scale in Hub-and-Spoke Models

The adoption of hub-and-spoke systems were primarily motivated by the harness of economies of scale, achieved by the sharing of transportation costs. Nevertheless, many authors have already questioned its oversimplified constant discount factor form, $0 \leq \alpha \leq 1$, used in most of the literature in this area (O'Kelly and Bryan, 1998; Bryan, 1998; Kimms, 2006; Alumur and Kara, 2008; De Camargo et al., 2009; Campbell, 2013; Alumur et al., 2021; Real et al., 2021; Farham et al., 2023).

By definition, economies of scale in the transportation field refer to the cost advantages resulting from the bundling of flows, when the marginal cost per unit decreases, and the average cost per unit also decreases (O'Kelly and Bryan, 1998; Bryan, 1998; Kimms, 2006). In other words, as a company transports more goods or people, it can distribute its fixed costs over a larger number of units, leading to cost savings and improved efficiency. Economies of scale often result in increased profitability and a competitive advantage for businesses.

Some concepts that are also important to be highlighted, as emphasized by Alumur et al. (2021), are economies of density and economies of spatial scope. These terms were well defined by Basso and Jara-Díaz (2006a,b), and Jara-Díaz et al. (2013), respectively as cost reduction per unit of traffic as traffic density increases while keeping the network's route structure unchanged (similarly, economies of scale share this concept but do not assume a fixed route structure); economies of spatial scope can be defined as cost reductions per unit due to the introduction of new services or new origin-destination pairs.

Although Kimms (2006) was not the first work to highlight the mistake of assuming flow-independent costs in hub location models, his work is of great importance in firmly emphasizing (even in the title of his paper) that these models lead to incorrect decisions, no matter how good the resolution procedures used are. Traditional hub-and-spoke network design models often rely on simplifying assumptions regarding economies of scale, particularly the uniform application of cost reductions to inter-hub links (hub-to-hub) while excluding intra-hub connections (node-to-hub and hub-to-node). These assumptions, while convenient, fail to fully capture the operational complexities of real-world transportation systems. Kimms (2006) challenge these conventions by arguing that such models misrepresent the true nature of economies of scale, leading to suboptimal network

designs and cost estimations. These connections may handle significantly lower traffic volumes than the hub-node or node-node links, as proved by Campbell (2013).

To address these limitations, Kimms (2006) propose a more realistic modeling approach incorporating nonlinear, concave cost functions that reflect economies of scale across all types of connections. This approach better represents the cost structures by introducing flow-dependent costs and allowing economies of scale to extend beyond inter-hub links. This line of research not only enhances the accuracy of network cost estimations but also opens new avenues for optimizing hub placement and allocation decisions under realistic economic conditions.

Despite all this, we use economies of scale as a fixed parameter applied exclusively to inter-hub links. This assumption allows for a direct comparison with the reference models in the literature analyzed in this work.

2.4 Modeling Customer Choice Behavior

The final key descriptor of competitive location models pertains to customer behavior. A primary distinction in this context lies between demand allocation models and customer choice models. As the names suggest, demand allocation models allow the firm to determine which facility is assigned to a given customer, as highlighted by Laporte et al. (2019). In contrast, customer choice models incorporate customer preferences and decision-making processes, offering a more realistic depiction of demand distribution in competitive environments.

A comprehensive overview of customer behavior modeling in location analysis is provided by Ricard and Bierlaire (2025), who survey fifty years of research on probabilistic and deterministic choice models in competitive settings. The paper provides a historical perspective on the development of behavioral optimization models in transportation and logistics. The authors emphasized a growing consensus that integrating operations research techniques with discrete choice theory is not only essential but also opens up a wide array of intellectually stimulating challenges for the modeling of competitive systems.

Empirical evidence supporting our approach can be found in recent studies such as Ahn (2023), which emphasize that preferences in airport services, both for passengers and cargo, are shaped by multidimensional factors beyond traditional metrics like cost and distance. In their analysis of Yangyang International Airport, factors such as geographic location, regional demand potential, specialized cargo infrastructure, and public policy support were identified as essential determinants of logistics competitiveness. These insights reinforce the necessity of incorporating such attractiveness indicators into utility-based demand models.

In the broader context of customer behavior, an essential dimension of market dynamics is demand elasticity. O'Kelly et al. (2015) provide a foundational framework for

hub location problems with price-sensitive demands, demonstrating how demand diminishes or shifts across different service levels based on routing costs. However, it must be clear that the present research does not consider demand elasticity or price sensitivity.

Building on this perspective, our study adopts a customer choice framework to explore competitive hub location strategies. We use a gravity-based formulation, as introduced by Eiselt and Marianov (2009), to model customer allocation decisions, in which the utility function of paths is proportional to the attractiveness of inter-hub connections and inversely related to generalized travel costs. This choice is motivated not only by its behavioral plausibility and analytical tractability, but also by the need to maintain methodological consistency with the benchmark study of Tiwari et al. (2021a), used for validation and performance comparison. The following topics elaborate on the structure of these models and the theoretical foundations of choice-based formulations used in this research.

Gravitational Model

The gravity-type spatial interaction model, initially introduced by Huff (1964), has been widely used to represent customer choice behavior in competitive facility location problems. This model belongs to a broader class of stochastic utility models, often referred to as "*brand choice models*" in the marketing literature.

In this framework, the attractiveness of a facility, A_j, and the travel distance, d_{ij}, influence the perceived utility of a customer located at demand point i when using facility j. The utility, u_{ij}, can be expressed as:

$$u_{ij} = \frac{F(A_j)}{H(d_{ij})}, \quad \forall i, j$$

where F and H are non-decreasing functions associated with the attractiveness and the travel distance, respectively. A commonly used functional form is:

$$u_{ij} = \frac{A_j^{\alpha}}{d_{ij}^{\beta}}, \quad \alpha, \beta > 0.$$

This relationship has been extensively applied in hub-and-spoke network optimization, as demonstrated by Drezner and Eiselt (2024). However, the recent work of Wang et al. (2024) point out that many air transportation studies have relied on predetermined α and β values in the Huff model without adequate justification, even though airport-specific differences make such uniform parameters unreliable for catchment-area estimation. In their work, they instead calibrated these parameters using mobile-location data from the New York metropolitan region to minimize the model's predictive error. We therefore recommend that future research utilizing real-world data follow this data-driven calibration approach, from empirical location data, to ensure context-specific validity and enhance the robustness of Huff-based analyses. As the present work is based on benchmark datasets, we adopt the parameter values established in the reference literature.

Latent Class Choice Models

Latent Class Choice Models (LCCMs) represent a flexible approach to capturing taste heterogeneity and unobservable decision protocols in discrete choice analysis (Ben-Akiva et al., 1997). These models assume that individuals belong to different latent classes, each characterized by specific decision rules or preferences. The probability of an individual n choosing alternative i is given by:

$$P_n(i) = \sum_{s=1}^{S} P_n(i|s)Q_n(s),$$

where $P_n(i|s)$ represents the probability of choosing i given membership in class s, and $Q_n(s)$ is the probability of individual n belonging to class s.

This framework allows for the modeling of varying sensitivities of attraction across different passenger segments, as business and leisure passengers. Business passengers, for instance, often prioritize time efficiency and direct connections, making them more sensitive to travel time and hub accessibility. In contrast, leisure passengers may place greater emphasis on cost savings and are generally more flexible with route options and travel times. By accounting for these differences in attraction sensitivities, the model can provide a more accurate representation of passenger behavior, ultimately improving the reliability of hub location decisions in competitive transportation markets. This segmentation allows for tailored strategies to optimize network performance while meeting the diverse preferences of passenger groups.

Hybrid Logit Model

The Hybrid Logit Model integrates the flexibility of multinomial probit with the computational efficiency of logit models. It partitions the utility function into systematic, random, and error components, enabling the modeling of taste variation and heteroscedasticity (Ben-Akiva et al., 1997). The utility U_n for individual n can be expressed as:

$$U_n = X_n\beta + Z_nS\eta_n + \epsilon_n,$$

where X_n captures observed attributes, $Z_nS\eta_n$ represents random effects, and ϵ_n follows a Gumbel distribution. This structure allows for a wide range of applications in discrete choice problems.

2.5 Competitive Multi-Path Multi-Allocation p-Hub Location Problem

The problem of locating hubs in a competitive environment was first introduced by Marianov et al. (1999) as a strategy for capturing demand from pre-existing competitor hubs. In such settings, customers dynamically choose between competing services based on the

path relative utility, which are influenced by the network configuration. When a new hub is introduced and offers a more attractive route, i.e. by shortening the overall distance or time from origin to destination, a shift in user preference may occur, resulting in the reallocation of demand toward the new operator. This underlying mechanism motivates the development of optimization models that explicitly account for such competitive interactions in hub location decisions.

The competitive hub location problem addresses two practically relevant scenarios frequently encountered in transportation networks. In the first, a major airline has established a set of hub airports at an earlier point in time, and latter the underlying passenger or cargo demand matrix may have increased. Faced with shifting traffic patterns and increasing pressure from competitors, the airline seeks to reassess its hub configuration, exploring opportunities to relocate or add hubs in order to reduce operational costs while accounting for the presence of rival facilities. In the second scenario, a smaller airline aims to strategically enter a market dominated by larger players. These dominant airlines often base their network decisions on aggregate demand, which may overlook customers whose specific travel needs are not well served. By identifying these underserved users, a new airline can place hubs strategically to attract part of this demand. In both cases, the competitive hub location model serves as a valuable tool to identify configurations that can either improve service efficiency or enable market share capture.

The model present in this section was proposed by Eiselt and Marianov (2009), which extends earlier work of Marianov et al. (1999) by incorporating a customer allocation function that accounts for the relative attractiveness of competing hub-to-hub routes. They also eliminate the traditional *"winner-take-all"* assumption, under which all customers traveling between origin i and destination j are allocated to a single route. The mathematical structure introduced in the next topic provides the basis for the reformulated models presented later in this thesis.

Notation, Definitions and Problem Formulation

Let N be the set of nodes scattered in a geographic region, a network space, in which each point $i \in N$ is both a hub candidate, and an origin or a destination for some demands. Let $W = \{(i,j) \in N \times N : i \neq j\}$ be the set of pair of origin-destination nodes with each pair $(i,j) \in W$ exchanging $w_{ij} > 0$ units of flow. Let also $I = \{(k,l) \in N \times N\}$ be the set of all possible inter-hub connections or hub-pairs. The inter-hub connection (k,k) is allowed and concerns the case where the route has only one hub, that is, when $k = l$. There are also a set C of competitors that are already operating with a hub-and-spoke structure and competing for their respective market share, and an entrant company e that wishes to enter this market. Although demand information is common knowledge for all competitors, no other information is shared between them, i.e., the companies do not

cooperate. Moreover, each company $a \in C \cup \{e\}$ must operate its own sets $H^a \subset N$ and $I^a = \{(k,l) \in H^a \times H^a\}$ of installed hubs and active inter-hub connections, respectively, that may be used to form paths to route the captured demands.

Traditionally, it is assumed that any path connecting a pair of origin-destination points includes one or at most two hubs, but this does not necessarily stem from a modeling assumption. In fact, in many instances, the emergence of paths with two hubs is a natural consequence of the optimization process itself, particularly under the original cost structure of the multiple allocation p-hub problem. When optimizing market share, the model tends to concentrate flows through the most cost-efficient hub pairs, often resulting in at most two active hubs in the optimal solution, even when more are allowed. Finally, whenever two different hubs are used to transport the bundle of demand flows, scale economies can be exploited.

Any entrant company seeks to capture the maximum market share possible by installing p hubs to form paths that can attract most of the demands of the origin-destination nodes $(i,j) \in W$. Note that each path $i-k-l-j$, with $(i,j) \in W$ and $(k,l) \in I^a$, operated by a company $a \in C \cup \{e\}$ has a perceived utility u^a_{iklj} for the demand w_{ij}, which follows a probabilistic choice model based on a gravitational utility function, that can be written as:

$$u^a_{iklj} = \frac{A^a_{kl}}{\gamma(T^a_{iklj})^\beta + (1-\gamma)(B^a_{iklj})^\delta}$$

A^a_{kl} represents the attractiveness of the inter-hub connection $(k,l) \in I^a$ and its respective hubs, while B^a_{iklj} and T^a_{iklj} are the cost and travel time, respectively, of the path. Parameters β and δ are scalar values that estimate the impact of travel time and cost, respectively, on the selection behavior of the demands. Higher power values indicate a dislike for longer travel times or higher transportation costs. Parameter γ represents the weight of the relative importance of each factor (time and cost) in the utility of the path. Moreover, parameters B^a_{iklj} and T^a_{iklj} are equal to $c_{ik} + \alpha c_{kl} + c_{lj}$ and $t_{ik} + t_{kl} + t_{lj}$, respectively, for all $(i,j) \in W$, $(k,l) \in I^a$, and $a \in C \cup \{e\}$, where c_{ij} and t_{ij}, $i,j \in N$, are the unitary transportation cost and the travel time between nodes i,j, respectively. Here, scale economies are represented by the scalar parameter $\alpha \in [0,1]$, simplified as a fixed discount factor for transshipment on inter-hub legs.

The utility parameters are then used in an attraction function f^e_{ij} that returns the fraction of the flow w_{ij} of the origin-destination pair $(i,j) \in W$ that the entrant company e will capture with its available paths formed by its set I^e of inter-hub connections:

$$f^e_{ij} = w_{ij} \frac{\sum\limits_{(k,l)\in I^e} u^e_{iklj}}{\sum\limits_{a\in C\cup\{e\}} \sum\limits_{(k,l)\in I^a} u^a_{iklj}} = w_{ij} \frac{\sum\limits_{(k,l)\in I^e} u^e_{iklj}}{\sum\limits_{(k,l)\in I^e} u^e_{iklj} + \mathcal{U}^c_{ij}}$$

in which $\mathcal{U}_{ij}^{c} = \sum_{a \in C} \sum_{(k,l) \in I^a} u_{iklj}^{a}$ is introduced to simplify notation hereafter. Table 2.2 summarizes the main notation.

Table 2.2: Summary of the main notation

Main Notation	
N	Set of nodes. $\lvert N \rvert = n$.
C	Set of competitors.
e	Entrant company.
I	$I = \{(k,l) \in N \times N\}$, or set of inter-hub connections.
H^a	Set of operating hubs of company $a \in C \cup \{e\}$.
I^a	Set of operating inter-hub connections of company $a \in C \cup \{e\}$.
W	$W = \{(i,j) \in N \times N : i \neq j\}$, or set of demand pairs of origin-destination nodes that exchange flows.
w_{ij}	Demand of origin-destination pair $(i,j) \in W$.
p	Number of hubs to install.
u_{iklj}^{a}	Utility or attractiveness of path (i,k,l,j) for company $a \in C \cup \{e\}$, $(i,j) \in W$ and $(k,l) \in I^a$.
$\mathcal{U}_{ij}^{c}$	$\mathcal{U}_{ij}^{c} = \sum_{a \in C} \sum_{(k,l) \in I^a} u_{iklj}^{a}$, the competitors' total attractiveness for the pair of origin-destination $(i,j) \in W$.

Note that while sets H^a and I^a are known for competitors $a \in C$, sets H^e and I^e that maximize the total captured demand must be found for the entrant company e. Note also that the cardinality of set H^e is equal to p, since exactly p hubs will be installed for the entrant company e. Furthermore, to find these sets or the underlined configuration of hubs and active inter-hub connections, function f_{ij}^{e} needs to be properly adjusted to comply with the respective assumptions of the MPMAPHLP problem..

To formulate the MPMAPHLP, Eiselt and Marianov (2009) have defined the decision variables of activation of hub-pairs or inter-hub connections $x_{kl} \in \{0,1\}$, which assumes a value of 1 if the inter-hub connection or hub-pair $(k,l) \in I^e$ is set, and zero otherwise. Note that the decision variables x_{kl} assemble the set I^e of the entrant company. With the aid of these decision variables, Eiselt and Marianov (2009) have adjusted the attraction function for the pair of origin-destination nodes $(i,j) \in W$ as

$$f_{ij}^{e}(x) = w_{ij} \frac{\sum\limits_{(k,l) \in I^e} u_{iklj}^{e} x_{kl}}{\sum\limits_{(k,l) \in I^e} u_{iklj}^{e} x_{kl} + \mathcal{U}_{ij}^{c}}$$

They also defined the decision variable of location $y_k \in \{0,1\}$, which assumes a value of 1 if a hub is installed at a point $k \in N$, and zero otherwise. The problem is modeled as follows:

$$\textbf{MAX MPMAPHLP} \begin{cases} \max \displaystyle\sum_{(i,j)\in W} w_{ij} \frac{\displaystyle\sum_{(k,l)\in I^e} u^e_{iklj}\, x_{kl}}{\displaystyle\sum_{(k,l)\in I^e} u^e_{iklj}\, x_{kl} + \mathcal{U}^c_{ij}} & & (2.1) \\ \text{s.t.: } x_{kl} \le y_k & \forall\, k,l \in H^e & (2.2) \\ x_{kl} \le y_l & \forall\, k,l \in H^e & (2.3) \\ \displaystyle\sum_{k\in N} y_k = p & & (2.4) \\ y_k \in \{0,1\} & \forall\, k \in N & (2.5) \\ x_{kl} \in \{0,1\} & \forall\, (k,l) \in I^e & (2.6) \end{cases}$$

The objective function (2.1) maximizes the captured demand of the entrant company. Constraints (2.2) and (2.3) are the activation constraints, that stablish that the hub-pair or inter-hub connection $(k,l) \in I^e$ can only be active if the respective hubs are installed. Constraint (2.4) guarantees that p hubs will be installed. The domain of the decision variables are shown in constraints (2.5) and (2.6).

Note that the MAXMPMAPHLP formulation is an integer nonlinear program (INLP) that can be transformed into a mixed-integer nonlinear program (MINLP) by relaxing the decision variables $x_{kl} \in [0,1]$, $(k,l) \in I^e$. Since all utilities in the model are positive and the attractiveness function is concave, smooth, and differentiable, and given that the objective is to maximize captured market share, it follows that whenever y_k and y_l are equal to one, the corresponding variable x_{kl} will also take the value one – see constraints (2.2) and (2.3). Nevertheless, whenever either y_k or y_l is equal to zero, x_{kl} assumes the value of zero. Hence, we shall replace constraints (2.6) hereafter with their relaxations:

$$x_{kl} \in [0,1], \quad \forall (k,l) \in I^e \tag{2.7}$$

The formal definition of the maximization form of the MPMAPHLP provides the basis for the development of alternative modeling perspectives. The next chapter is dedicated to present our proposed reformulations to this problem, aiming to improve the mathematical properties and computational performance of this class of competitive hub location problems.

Chapter 3

Mathematical Reformulations of the Competitive MPMAPHLP

This chapter presents the mathematical reformulations developed for the Competitive Multi-Path Multi-Allocation p-Hub Location Problem. While Chapter 2 provided an overview of the problem as originally introduced in the literature, here we formalize the optimization models employed throughout this work.

3.1 Our Minimization Form of the MPMAPHLP Problem

We assume that the sum of the captured market with the loss of market share is equal to the total demand. So we can model MPMAPHLP problem as the minimization of the loss of market share. Note that, for any pair of origin-destination nodes $(i,j) \in W$ in the MPMAPHLP problem, we have the following relation:

$$
\begin{aligned}
& f_{ij}(x) + \phi_{ij}(x) = w_{ij} \\
& \phi_{ij}(x) = w_{ij} - w_{ij} \frac{\sum\limits_{(k,l)\in I^e} u^e_{iklj} x_{kl}}{\sum\limits_{(k,l)\in I^e} u^e_{iklj} x_{kl} + \mathcal{U}^c_{ij}} = w_{ij} \left(1 - \frac{\sum\limits_{(k,l)\in I^e} u^e_{iklj} x_{kl}}{\sum\limits_{(k,l)\in I^e} u^e_{iklj} x_{kl} + \mathcal{U}^c_{ij}} \right) \\
& = w_{ij} \frac{\mathcal{U}^c_{ij}}{\sum\limits_{(k,l)\in I^e} u^e_{iklj} x_{kl} + \mathcal{U}^c_{ij}}
\end{aligned}
$$

in which $\phi_{ij}(x)$ is the loss of market share. After dividing the right-hand side by $\mathcal{U}^c_{ij}$ we get

$$
\phi_{ij}(x) = \frac{w_{ij}}{\sum\limits_{(k,l)\in I^e} \pi^e_{iklj} x_{kl} + 1}
$$

in which $\pi^e_{iklj} = \frac{u^e_{iklj}}{\mathcal{U}^c_{ij}}$, $\forall (i,j) \in W$, $(k,l) \in I^e$.

Therefore, here we present our first proposal for the MPMAPHLP, based on a remodeling the (2.1)-(2.5), (2.7) maximization problem, presented in the literature as a equivalent minimization problem, as follows:

$$
\text{MIN MPMAPHLP} \begin{cases}
\min \displaystyle\sum_{(i,j)\in W} \frac{w_{ij}}{\sum_{(k,l)\in I^e} \pi^e_{iklj}\, x_{kl} + 1} & & (3.1)\\
\text{s.t.: } x_{kl} \leq y_k & \forall\, k,l \in H^e & (3.2)\\
x_{kl} \leq y_l & \forall\, k,l \in H^e & (3.3)\\
\displaystyle\sum_{k\in N} y_k = p & & (3.4)\\
y_k \in \{0,1\} & \forall\, k \in N & (3.5)\\
x_{kl} \in [0,1] & \forall\, (k,l) \in I^e & (3.6)
\end{cases}
$$

The objective function (3.1) minimizes the loss of demand for the entrant company. Constraints are the same as in the maximization model presented earlier. Constraints (3.2) and (3.3) are the activation constraints. The hub-pair or inter-hub connection $(k,l) \in I^e$ can only be active if the respective hubs are installed. Constraint (3.4) guarantees that p hubs will be installed. The domain of the decision variables are shown in constraints (3.5) and (3.6).

The formulations MAXMPMAPHLP and MINMPMAPHLP are MINLPs that cannot be directly solved by most off-the-shelf solvers. Nevertheless, they are amenable to being recast into conic programs, which can be efficiently solved by solvers like Gurobi and CPLEX. In the next section, we will present the conic reformulation of these problems.

3.2 Conic Programming of the MPMAPHLP

The competition on MPMAPHLP gives rise to difficult mixed-integer nonlinear programs that challenges existing commercial solvers. Thus, to solve this problem, one needs to rely on different solution strategies. For the first MPMAPHLP application, Eiselt and Marianov (2009) have proposed a multi-start two-phase metaheuristic. For their turn, Tiwari et al. (2021a) have proposed four different approaches: the Cutting Plane Algorithm (CPA), the Mixed-Integer Second-Order Cone Programming (MISOCP), and two Lagrangian-relaxation-based versions, namely LR-CPA and LR-MISOCP. Although they identified LR-CPA as the most effective method for their nonlinear maximization model, the conic minimization formulations proposed in this thesis present structural advantages that enable efficient solution through MISOCP solvers and OA-based exact methods. As such, the integration of Lagrangian Relaxation techniques is not pursued in the present work but may be considered in future research.

Building upon this foundation, this section presents their and our conic programming formulations. These approach are not only relevant for their theoretical properties, such as convexity preservation and relaxation strength, but also for their practical performance in solving larger instances of the MPMAPHLP.

Second-order cone programming (SOCP) is a subclass of conic optimization in which the feasible region is defined by second-order cones. Formally, a standard SOCP problem optimizes a linear objective function subject to linear constraints and a set of second-order cone constraints, expressed as:

$$\|A_i x + b_i\|_2 \leq c_i^\top x + d_i, \quad \forall i = 1, \ldots, m, \tag{3.7}$$

where $A_i \in \mathbb{R}^{n_i \times n}$, $b_i \in \mathbb{R}^{n_i}$, $c_i \in \mathbb{R}^n$, and $d_i \in \mathbb{R}$.

The rotated second-order cone, also known as the Lorentz cone or ice-cream cone, is formally defined as:

$$\mathcal{Q}^n = \left\{(t, x) \in \mathbb{R} \times \mathbb{R}^{n-1} : \|x\|_2 \leq t\right\}. \tag{3.8}$$

In the general form, an SOCP can be expressed as:

$$\min_x \quad f^\top x \tag{3.9}$$

$$\text{s.t.} \quad \|A_i x + b_i\|_2 \leq c_i^\top x + d_i, \quad i = 1, \ldots, m, \tag{3.10}$$

$$Gx = h, \tag{3.11}$$

$$x \in \mathbb{R}^n, \tag{3.12}$$

where $f \in \mathbb{R}^n$ is the objective coefficient vector, and $Gx = h$ represents linear equality constraints.

SOCP generalizes both linear programming (LP) and convex quadratic programming (QP), providing a flexible framework for modeling convex optimization problems. Despite being nonlinear in form, SOCP possesses a special conic structure that enables its solution via efficient interior-point methods implemented in commercial solvers (Akturk et al., 2014), such as Gurobi and CPLEX.

This modeling framework has attracted considerable attention due to its ability to represent a wide range of convex optimization problems, including supply chain design, scheduling, robust optimization, and specific classes of location and facility planning models (Atamtürk et al., 2012). A comprehensive treatment of the mathematical foundations and applications of SOCP can be found in Ben-Tal and Nemirovski (2001).

The extension of SOCP to problems involving discrete decisions leads to mixed-integer second-order cone programming (MISOCP). This class of problems combines the

convexity of conic constraints with the combinatorial nature of integer variables. A detailed overview of MISOCP, including modeling techniques and advances in solution algorithms, is provided by Benson and Ümit Sağlam (2014).

3.2.1 Recasting MAXMPMAPHLP Formulation into a Conic Program

Using Atamtürk et al. (2012)'s guidelines, Tiwari et al. (2021a) have recast the MAXMPMAPHLP problem into a MISOCP after introducing auxiliary variables $Q_{ij} \geq 0$ and $V_{ij} \geq 0$, $(i,j) \in W$, in which $Q_{ij} = \frac{1}{\sum_{(k,l)\in I^e} u^e_{iklj}\, x_{kl} + \mathcal{U}^c_{ij}}$ and $V_{ij} = Q_{ij} \sum_{(k,l)\in I^e} u^e_{iklj}\, x_{kl}$. They have then reworked the former relation as $Q_{ij} \sum_{(k,l)\in I^e} u^e_{iklj}\, x_{kl} + Q_{ij}\mathcal{U}^c_{ij} = 1$ to obtain a new relation $V_{ij} + Q_{ij}\mathcal{U}^c_{ij} = 1$, $(i,j) \in W$. Returning yet to the first relation, Tiwari et al. (2021a) have introduced other decision variables $r_{ij} \geq 0$ to replace its denominator or $r_{ij} = \sum_{(k,l)\in I^e} u^e_{iklj}\, x_{kl} + \mathcal{U}^c_{ij}$, $(i,j) \in W$. To enable the use of second-order cone programming techniques, the equality $Q_{ij} = \frac{1}{r_{ij}}$ is relaxed to the inequality $Q_{ij} \geq \frac{1}{r_{ij}}$. This transformation is a standard convexification approach that ensures the feasibility region becomes convex, while still preserving the structural behavior of the original model. The relaxed inequality can be equivalently written as $Q_{ij} r_{ij} \geq 1$, which is a rotated second-order cone constraint. This formulation allows the problem to be cast as a MISOCP, making it solvable by modern conic solvers with guarantees of convergence under convexity assumptions. Observing the second relation, they have rewritten it as $V_{ij} \geq \frac{\sum_{(k,l)\in I^e} u^e_{iklj}\, x_{kl}}{r_{ij}}$ or $V_{ij} r_{ij} \geq \sum_{(k,l)\in I^e} u^e_{iklj}\, x_{kl}$.

As the decision variables x_{kl} were originally defined as binary variables, the last two relations can be transformed to standard second-order constraints or $(Q_{ij} + r_{ij})^2 \geq 2 + {Q_{ij}}^2 + {r_{ij}}^2$ and $(V_{ij} + r_{ij})^2 \geq 2 \sum_{(k,l)\in I^e} u^e_{iklj}\, x_{kl} + {V_{ij}}^2 + {r_{ij}}^2$, for all $(i,j) \in W$. Gathering all these relations, Tiwari et al. (2021a) have proposed their following mixed-integer second-order conic program for the MAXMPMAPHLP formulation:

$$
\text{Conic MAXMPMAPHLP} \begin{cases}
\max \sum_{(i,j)\in W} w_{ij}\, V_{ij} & & (3.13)\\
\text{s.t.: } x_{kl} \le y_k & \forall\, k,l \in H^e & (3.14)\\
x_{kl} \le y_l & \forall\, k,l \in H^e & (3.15)\\
\sum_{k\in N} y_k = p & & (3.16)\\
r_{ij} = \sum_{(k,l)\in I^e} u^e_{iklj}\, x_{kl} + \mathcal{U}^c_{ij} & \forall\, (i,j) \in W & (3.17)\\
Q_{ij} = \dfrac{1}{r_{ij}} & \forall\, (i,j) \in W & (3.18)\\
V_{ij} + \mathcal{U}^c_{ij}\, Q_{ij} = 1 & \forall\, (i,j) \in W & (3.19)\\
(V_{ij} + r_{ij})^2 \ge 2 \sum_{(k,l)\in I^e} u^e_{iklj}\, x_{kl} + V^2_{ij} + r^2_{ij} & \forall\, (i,j) \in W & (3.20)\\
(Q_{ij} + r_{ij})^2 \ge 2 + Q^2_{ij} + r^2_{ij} & \forall\, (i,j) \in W & (3.21)\\
Q_{ij}, V_{ij}, r_{ij} \ge 0 & \forall\, (i,j) \in W & (3.22)\\
y_k \in \{0,1\} & \forall\, k \in N & (3.23)\\
x_{kl} \in [0,1] & \forall\, (k,l) \in I^e & (3.24)
\end{cases}
$$

The objective function (3.13) maximizes the total market share captured by the entrant company, represented by variables V_{ij}. Constraints (3.14) and (3.15) ensure that routes x_{kl} are only allowed between open hubs. The number of hub selection is enforced by Equation (3.16), which guarantees that exactly p hubs are activated. Equation (3.17) defines the total utility r_{ij} of all possible paths between origin-destination pairs (i,j), incorporating both the entrant's and competitor's attributes. To handle the fractional structure of the objective, Equation (3.18) introduces Q_{ij} as the inverse of r_{ij}, and Equation (3.19) expresses the market share condition in a linearized form. The standard second-order cone constraints (3.20) and (3.21) preserve the convexity of the reformulated model. Finally, Equations (3.22)–(3.24) define the domains of the decision variables.

3.2.2 Recasting MINMPMAPHLP Formulation into a Conic Program

The rotated cone in our reformulation takes the following form $x \le yz \iff ||(2x, y-z)||_2 \le y+z$, where $||\cdot||_2$ is the L_2 norm, x, y, z are decision variables of suitable sizes. Let the denominator of the attractiveness function be equal to $r_{ij} = \sum_{(k,l)\in I^e} \pi^e_{iklj}\, x_{kl} + 1$, then we define $\eta_{ij} = \frac{w_{ij}}{r_{ij}}$. Note that $r_{ij} \ge 1$. Now, we define $\eta_{ij} \ge \frac{w_{ij}}{r_{ij}}$ or the rotated cone inequality $\eta_{ij} r_{ij} \ge w_{ij}$, for $(i,j) \in W$. Therefore, the MINMPMAPHLP problem is equivalent to the following conic program:

$$
\textbf{Conic MINMPMAPHLP}\begin{cases}
\min \displaystyle\sum_{(i,j)\in W} \eta_{ij} & & (3.25)\\
\text{s.t.: } x_{kl} \le y_k & \forall\, k,l \in H^e & (3.26)\\
x_{kl} \le y_l & \forall\, k,l \in H^e & (3.27)\\
\displaystyle\sum_{k\in N} y_k = p & & (3.28)\\
r_{ij} = \displaystyle\sum_{(k,l)\in I^e} \pi^e_{iklj}\, x_{kl} + 1 & \forall\, (i,j) \in W & (3.29)\\
\eta_{ij} r_{ij} \ge w_{ij} & \forall\, (i,j) \in W & (3.30)\\
r_{ij} \ge 1 & \forall\, (i,j) \in W & (3.31)\\
\eta_{ij} \ge 0 & \forall\, (i,j) \in W & (3.32)\\
y_k \in \{0,1\} & \forall\, k \in N & (3.33)\\
x_{kl} \in [0,1] & \forall\, (k,l) \in I^e & (3.34)
\end{cases}
$$

The objective function (3.25) minimizes the total loss of demand, represented by the auxiliary variables η_{ij}, which express the portion of unserved market for each origin–destination pair. Constraints (3.26)–(3.27) are the classical activation conditions. Equation (3.28) enforces the installation of exactly p hubs in the network. Equation (3.29) defines the attractiveness denominator r_{ij}. The conic constraint (3.30) replaces the fractional term of the original nonlinear objective by the rotated cone inequality $\eta_{ij} r_{ij} \ge w_{ij}$, which preserves convexity while capturing the inverse relationship between η_{ij} and r_{ij}. Constraint (3.31) sets a lower bound of 1 on each r_{ij}, whereas constraint (3.32) restricts η_{ij} to be non-negative. Finally, domain restrictions (3.33)–(3.34) define the binary nature of the hub-selection variables y_k and the continuous relaxation of the inter-hub activation variables x_{kl}. Together, these relations transform the original fractional model into a convex mixed-integer second-order conic program (MISOCP), directly solvable by modern conic optimization solvers.

While these formulations ensure convexity and improve numerical tractability, their relaxation can still exhibit weaknesses that affect computational performance, particularly for large-scale instances. In this context, further structural refinement becomes essential to enhance model tightness and strengthen the coupling between hub location and connection decisions. The following section introduces a tightened version of the conic minimization model, designed to improve relaxation quality and accelerate the convergence of exact optimization methods.

3.3 The New Tightened Formulations for the MINMPMAPHLP

Despite the classical formulations of the MPMAPHLP capture the core elements of competitive hub location modeling, it exhibit certain structural weaknesses that may hinder computational performance, especially for large-scale instances. In particular, the pairwise connectivity constraints, $x_{kl} \leq y_k$ **(r1)** and $x_{kl} \leq y_l$ **(r2)**, $\forall\ k, l \in H^e$, employed in the original model lead to a relatively loose linear relaxation, which can increase the effort required in exact solution methods such as branch-and-bound.

This structural limitation stems from the fact that the flow allocation sub-models (indexed by origin-destination pairs) are only indirectly connected through complicating variables such as hub activations, as seen in constraints **(r1)** and **(r2)** of the original MPMAPHLP formulation. These constraints define local binary relationships between route activation variables and hub selection variables, ensuring that a connection between two nodes is only allowed if both endpoints are selected as hubs. Although these constraints are intuitive and easy to interpret, they result in a dispersed and fragmented coupling structure, which increases the density and interdependence of the constraint matrix.

To address this issue, we propose a tightened formulation that introduces a more integrated coupling between inter-hub and hub selection, aiming to strengthen the relaxation and improve computational efficiency in direct solution approaches. It can be obtained by replacing **(r1)** and **(r2)** constraints with a single global constraints that regulates the total number of hub-level connections incident to each hub. The new coupling strategy enforces that, for each node $k \in N$, the total number of incoming and outgoing activated connections must be consistent with its hub status. Specifically, we impose:

$$\sum_{l \in N} x_{kl} + \sum_{l \in N : l \neq k} x_{lk} = (2p - 1)\ y_k, \qquad \forall k \in N \tag{3.35}$$

Constraint (3.35) ensures that each active node k, when stated as hub ($y_k = 1$), is involved in exactly $(2p - 1)$ hub-level connections, consistent with the structure of a complete directed subgraph formed by the p selected hubs. As a result, the feasible region defined by this global coupling constraint is strictly contained within the region defined by the local constraints **(r1)** and **(r2)**, leading to a tighter polyhedral relaxation of the model.

[***Proposition***] Let $\mathcal{P}_1$ be the feasible region defined by constraints **(r1)** and **(r2)**, and let $\mathcal{P}_2$ be the feasible region defined by constraint (3.35). Then, $\mathcal{P}_2 \subset \mathcal{P}_1$ and the formulation using constraint (3.35) defines a tighter polyhedron.

Proof. We first show that any solution satisfying constraint (3.35) also satisfies constraints **(r1)** and **(r2)**.

Let (x, y) be a feasible solution under (3.35). The constraint implies that each active hub k (i.e., $y_k = 1$) must be incident to exactly $(2p - 1)$ hub-level arcs. Therefore, any arc (k, l) with $x_{kl} = 1$ must necessarily satisfy $y_k = y_l = 1$, as the total number of such arcs is limited and strictly enforced. This implies $x_{kl} \leq y_k$ and $x_{kl} \leq y_l$, satisfying both **(r1)** and **(r2)**.

Now, we show that the converse is not true. Consider a fractional solution (x, y) such that $y_k = \frac{p}{n}$ and all arcs $x_{kl} = \frac{p}{n}$. This solution satisfies **(r1)** and **(r2)**, trivially. However, it violates (3.35) because the required number of incident arcs on node k is not satisfied.

Hence, the feasible region defined by (3.35) is strictly contained within that defined by **(r1)** and **(r2)**, which proves the proposition. □

This alternative formulation imposes a global constraint on the number of active connections incident to each hub, determined by the total number of hubs selected. Unlike the original local constraints that act individually on each route variable, constraint (3.35) aggregates these connectivity requirements in a compact, node-centric form. This aggregation results in a more regular and centralized coupling structure, where the interaction between flow and hub selection decisions is enforced through a single equation per node.

By replacing the dispersed binary dependencies of constraints **(r1)** and **(r2)** with the unified global condition (3.35), the model benefits from a more compact constraint matrix and a reduction in redundant feasible configurations. This refinement not only improves the strength of the continuous relaxation but also enhances numerical stability and convergence in exact optimization algorithms. Latter in this work, we show through extensive computational experiments that this new formulation yields considerable gains, particularly in solving large-scale instances of the problem.

We now present the revised version of the minimization model, called NEW MINMPMAPHLP, or simply NEW:

$$
\text{NEW MINMPMAPHLP} \begin{cases}
\min \displaystyle\sum_{(i,j)\in W} \frac{w_{ij}}{\sum_{(k,l)\in I^e} \pi^e_{iklj}\, x_{kl} + 1} & & (3.36)\\
\text{s.t.:} \displaystyle\sum_{l\in N} x_{kl} + \sum_{l\in N: l\neq k} x_{lk} = (2p-1)\, y_k & \forall k \in N & (3.37)\\
\displaystyle\sum_{k\in N} y_k = p & & (3.38)\\
y_k \in \{0,1\} & \forall\, k \in N & (3.39)\\
x_{kl} \in [0,1] & \forall\, (k,l) \in I^e & (3.40)
\end{cases}
$$

The objective function (3.36) minimizes the total market loss of the entrant company, preserving the same rational structure as in the original minimization model. Constraints (3.37) introduces the strengthened coupling relation that replaces the two local activation constraints of the classical formulation. This global constraints enforce that each active hub k participates in exactly $(2p-1)$ hub-level connections, thereby ensuring network consistency and producing a tighter continuous relaxation. Equation (3.38) guarantees that exactly p hubs are installed in the network. Constraints (3.39)–(3.40) define the binary domain of the hub-selection variables y_k and the bounded continuous domain of the inter-hub activation variables x_{kl}. By integrating the global connectivity condition into the original market-loss objective, this new formulation achieves a more compact and numerically stable structure, reducing redundant feasible configurations and improving convergence in exact solution methods.

The tightened formulation can also be directly applied to the conic representation of the problem. The model maintains the conic structure while incorporating the stronger coupling constraints developed earlier. The formulation is as follows.

$$
\textbf{Conic NEW MINMPMAPHLP}
\begin{cases}
\min \displaystyle\sum_{(i,j)\in W} \eta_{ij} & & (3.41)\\
\text{s.t.:} \displaystyle\sum_{l\in N} x_{kl} + \sum_{l\in N: l\neq k} x_{lk} = (2p-1)\, y_k & \forall k \in N & (3.42)\\
\displaystyle\sum_{k\in N} y_k = p & & (3.43)\\
r_{ij} = \displaystyle\sum_{(k,l)\in I^e} \pi^e_{iklj}\, x_{kl} + 1 & \forall\, (i,j) \in W & (3.44)\\
\eta_{ij} r_{ij} \geq w_{ij} & \forall\, (i,j) \in W & (3.45)\\
r_{ij} \geq 1 & \forall\, (i,j) \in W & (3.46)\\
\eta_{ij} \geq 0 & \forall\, (i,j) \in W & (3.47)\\
y_k \in \{0,1\} & \forall\, k \in N & (3.48)\\
x_{kl} \in [0,1] & \forall\, (k,l) \in I^e & (3.49)
\end{cases}
$$

The objective function (3.41) minimizes the total loss of market share represented by the auxiliary variables η_{ij}, which measure the unserved portion of demand between each origin–destination pair. Constraints (3.42) are the tightened global connectivity condition that enforces structural consistency among activated hubs. Equation (3.43) ensures that exactly p hubs are installed in the network. Equations (3.44) define the attractiveness denominator r_{ij}. Constraints (3.45) represent the conic rotated inequality $\eta_{ij} r_{ij} \geq w_{ij}$, preserving convexity while capturing the inverse relationship between attractiveness and market loss. Constraints (3.46) and (3.47) ensure the non-negativity and lower bounds of the conic variables, while Equations (3.48)–(3.49) define the domains of the binary

hub-selection variables y_k and continuous route activation variables x_{kl}. Collectively, these relations produce a tighter conic MISOCP formulation that maintains convexity, enhances numerical stability, and yields superior computational performance compared with the original conic model.

In summary, the proposed formulations — a convex minimization model based on market loss (MINMPMAPHLP) and its tightened version with enhanced coupling constraints (NEW MINMPMAPHLP) — constitute the methodological core of this thesis. Both are represented as convex MINLPs and further recast into MISOCPs, enabling the use of advanced conic optimization tools. Notably, the structural properties of the tightened formulation also favor decomposition-based strategies, which may be explored in future research. The Chapter 5 presents computational results of the conic formulations using commercial solvers, providing a baseline for evaluating the performance of the proposed formulations.

Building upon these mathematical models, the next chapter develops the solution methodology designed to efficiently handle both the conic and nonlinear versions of the problem. Chapter 4 introduces the Outer Approximation (OA)–based algorithms proposed in this work, which exploit the convex structure of the formulations to generate exact solutions through iterative master–subproblem interactions. These algorithms establish the computational foundation for the analyses and comparisons presented in the subsequent chapters.

Chapter 4

Review of Exact Solution Outer Approximation Method

The mathematical formulations presented in last chapter define the competitive MPMAPHLP as a mixed-integer nonlinear convex optimization problem that can be reformulated and solved through modern MISOCP solvers. However, given the nonlinear and combinatorial nature of the problem, alternative exact strategies can also be explored to improve tractability and to better understand its structural behavior. In this context, the present chapter introduces the Outer Approximation (OA) framework as an exact iterative method for convex MINLPs, which alternates between solving linearized master problems and nonlinear subproblems to progressively approximate the feasible region.

The objective of this chapter is to present the theoretical foundations and algorithmic structure of the OA method, along with its adaptations to the specific formulations developed. Therefore, three algorithmic variants are detailed, each associated with a distinct modeling perspective, to demonstrate the application of OA principles to both nonlinear and conic formulations of the problem. These formulations and their corresponding algorithms establish the methodological basis for the computational analyses conducted in subsequent chapters.

The OA algorithm was first proposed by Duran and Grossmann (1986), extending the cutting-plane algorithm (CPA) of Kelley (1960) to handle convex MINLPs involving both continuous and integer variables. While Kelley's method addressed continuous convex problems, Duran and Grossmann generalized the concept to mixed-integer domains by alternating between nonlinear continuous subproblems and linearized MILP master problems. Although Tiwari et al. (2021a) refer to their use of Kelley's CPA in their modeling framework, the presence of integer variables and master–subproblem iterations clearly characterizes their approach as an OA implementation.

The OA approach is particularly effective when the nonlinearities are continuous and convex, and the discrete variables can be separated from the nonlinear structure. This framework allows separating the discrete design decisions from the continuous nonlinear optimization. The method alternates between solving nonlinear programming (NLP) subproblems, where discrete variables are fixed, and MILP master problems that accumulate

outer approximation cuts. As described by Floudas (1995), at each iteration, it generates an upper bound and a lower bound on the MINLP solution. The upper bound results from the solution of the problem with fixed discrete variables (in our case, the variable y). The lower bound results from the solution of the master problem, derived using the primal information of the solution point based upon a linearization (outer approximation) of the nonlinear objective around that point.

These cuts progressively refine piecewise linear outer approximations of the nonlinear feasible region or objective function. A comprehensive survey of MINLP techniques by Grossmann and Kravanja (1995) highlights OA as one of the most effective method for convex MINLPs.

Let us consider a general convex MINLP formulation:

$$\min_{x\in\mathbb{R}^n,\, y\in\mathbb{Z}^p} \quad f(x,y) \tag{4.1}$$

$$\text{s.t.} \quad g_i(x,y) \le 0, \quad i = 1,\dots,m \tag{4.2}$$

$$x \in X \subseteq \mathbb{R}^n, \quad y \in Y \subseteq \mathbb{Z}^p \tag{4.3}$$

At iteration h, fix the integer variables $y^h \in Y$, and solve the resulting continuous nonlinear subproblem:

$$\min_{x\in X} \quad f(x,y^h) \tag{4.4}$$

$$\text{s.t.} \quad g_i(x,y^h) \le 0, \quad i = 1,\dots,m \tag{4.5}$$

Let $x^h \in X$ be the optimal solution to this subproblem. If this point is feasible and improves the incumbent solution, update the upper bound and store the incumbent.

From the subproblem solution (x^h, y^h), we construct linear approximations (first-order Taylor expansions) of the nonlinear functions. These cuts are valid outer approximations of the convex feasible region.

For the objective function:

$$\xi \ge f(x^h,y^h) + \nabla_x f(x^h,y^h)^T(x-x^h) + \nabla_y f(x^h,y^h)^T(y-y^h) \tag{4.6}$$

For each constraint g_i, generate:

$$g_i(x^h,y^h) + \nabla_x g_i(x^h,y^h)^T(x-x^h) + \nabla_y g_i(x^h,y^h)^T(y-y^h) \le 0 \tag{4.7}$$

These linear inequalities are added to the master problem to enforce an outer approximation of the nonlinear feasible region.

The master problem accumulates all cuts generated in previous iterations:

$$\min_{x,y,\xi} \quad \xi \tag{4.8}$$

$$\text{s.t.} \quad \text{OA cuts from previous iterations (Eqs. 4.6–4.7)} \tag{4.9}$$

$$x \in X, \quad y \in Y \tag{4.10}$$

Let (x^{h+1}, y^{h+1}) be the optimal solution of the master problem. If the objective value provides a better lower bound and the gap with the incumbent solution is within a specified tolerance ε, the algorithm terminates.

The OA method generates a sequence of outer approximations that converge to the true convex feasible region. The upper bound UB is updated by feasible solutions of the subproblems, and the lower bound LB is given by the master problem.

$$\text{Convergence condition:} \quad UB - LB \leq \varepsilon$$

Because the master problem only grows in size by one or a few cuts per iteration, the OA method is often efficient in practice, especially when gradients are cheap to compute and the subproblem is fast to solve. It is particularly appealing when the nonlinearity is only present in the continuous variables, or when the discrete variables appear linearly in $f(x, y)$ and $g(x, y)$, as the outer approximations become increasingly tighter and the convergence is faster.

In the following sections, the OA structure is adapted to the specific formulations of MINMPMAPHLP, simplified to the nomenclature MPMAPHLP for the sake of brevity, since from now on we will only focus on minimization models. We propose three tailored algorithmic variants, which differ in how the nonlinear objective function is approximated and how auxiliary variables are introduced to construct the polyhedral relaxation. Each variant reflects a distinct modeling perspective, leading to different structures of master and subproblems.

The first variant, OA-Obj, represents the simplest implementation of the OA scheme, applied directly to the original nonlinear formulations and linearizing the objective function with respect to the continuous x-variables, without using any initial cuts. The second variant, OA-rvar, applies the same OA principles to the MINLP structure but performs the linearization through the auxiliary variables r_{ij}, which represent the nonlinear denominators of the objective function. This version remains purely linear and convex, and it also employs initial cuts to improve the quality of the early approximations. Finally, the COACuts algorithm extends the OA framework to our conic formulations of the MPMAPHLP, embedding the linearization within a MISOCP structure and incorporating only initial cuts to strengthen the first master problem and accelerate convergence. Together, these three variants establish the methodological foundation for the computational analyses presented in the following chapter.

The OA-based formulations presented in this chapter are all derived from the same MINLP structures introduced in Chapter 3, which defines the competitive MPMAPHLP. Hence, the basic sets, variables, and connectivity constraints follow exactly the same notation and interpretation as before. The distinction among the proposed OA variants lies exclusively in the way the nonlinear term is approximated: directly in the x-variables (in the case of OA-Obj), or in the auxiliary denominators r_{ij} (in the case of OA-rVar

and COACuts). For this reason, the models are fully reproduced for completeness, but their equations are not described again in detail, since their meaning remains unchanged from the previous chapter. Instead, the focus of this chapter is on the methodological differences in how the outer approximation is constructed and applied in each variant.

4.1 OA-Obj Algorithm: Outer Approximation on the Original Objective

We begin this section by recalling our MINLP formulation previously developed for the MPMAPHLP, which serves as the starting point for the application of the OA-Obj algorithm:

$$
\textbf{MINLP}\ \textbf{MPMAPHLP}
\begin{cases}
\min \displaystyle\sum_{(i,j)\in W} w_{ij}\ \frac{1}{\sum_{(k,l)\in I^e} \pi^e_{iklj}\ x_{kl} + 1} & & (4.11)\\
\text{s.t.: } x_{kl} \le y_k & \forall\ k,l \in H^e & (4.12)\\
x_{kl} \le y_l & \forall\ k,l \in H^e & (4.13)\\
\displaystyle\sum_{k\in N} y_k = p & & (4.14)\\
y_k \in \{0,1\} & \forall\ k \in N & (4.15)\\
x_{kl} \in [0,1] & \forall\ (k,l) \in I^e & (4.16)
\end{cases}
$$

The OA-Obj algorithm corresponds to the original problem enhanced with additional outer approximation cuts. The nonlinearity arises in the objective function (4.11), which aggregates the entrant's market share loss terms of the form:

$$\phi_{ij}(x) = \frac{1}{\sum_{(k,l)\in I^e} \pi^e_{iklj} x_{kl} + 1}$$

To linearize this expression around a previously evaluated point $\bar{x}^h_{kl}$, a first-order Taylor expansion is applied, yielding the so-called OA cut at iteration h (Duran and Grossmann, 1986; Floudas, 1995):

$$\eta_{ij} \ge \phi_{ij}(\bar{x}^h) + \sum_{(k,l)\in I^e} \nabla_{kl}\phi_{ij}(\bar{x}^h)\ (x_{kl} - \bar{x}^h_{kl}) \quad \forall (i,j) \in W,\ h \in H \tag{4.17}$$

where η_{ij} denotes an auxiliary variable representing the contribution of pair (i,j) to the linearized objective function, and $\nabla_{kl}\phi_{ij}(\bar{x}^h)$ is the component of the gradient of ϕ_{ij} with respect to variable x_{kl}, evaluated at point $\bar{x}^h$. The set H indexes the OA iterations, each corresponding to a distinct linearization point generated throughout the algorithm. This strategy enables the approximation of the nonlinear objective through an evolving polyhedral relaxation. The gradient components are given by:

$$\nabla_{kl}\phi_{ij}(\bar{x}^h) = -\frac{\pi^e_{iklj}}{\left(\sum_{(k,l)\in I^e}\pi^e_{iklj}\,\bar{x}^h_{kl}+1\right)^2} \tag{4.18}$$

where the negative sign reflects the decreasing nature of ϕ_{ij} with respect to each x_{kl}. Using all OA cuts accumulated up to iteration h, the linearized master problem of the OA-Obj algorithm can be written as follows:

OA-Obj MPMAPHLP

$$\begin{cases}
\min & \displaystyle\sum_{(i,j)\in W} w_{ij}\,\eta_{ij} & \\
\text{s.t.:} & x_{kl} \le y_k & \forall\, k,l \in H^e \\
& x_{kl} \le y_l & \forall\, k,l \in H^e \\
& \displaystyle\sum_k y_k = p & \\
& \eta_{ij} \ge \phi_{ij}(\bar{x}^h) + \displaystyle\sum_{(k,l)\in I^e} \nabla_{kl}\phi_{ij}(\bar{x}^h)(x_{kl}-\bar{x}^h_{kl}) & \forall (i,j)\in W,\ h\in H \\
& \eta_{ij} \ge 0 & \forall\,(i,j)\in W \\
& y_k \in \{0,1\} & \forall\, k \in N \\
& x_{kl} \in [0,1] & \forall\,(k,l)\in I^e
\end{cases}$$

The OA-Obj algorithm can also be applied to the tightened formulation of the MPMAPHLP, replacing the local activation constraints by the global coupling condition introduced in Section 3.3.

OA-Obj New MPMAPHLP

$$\begin{cases}
\min & \displaystyle\sum_{(i,j)\in W} w_{ij}\,\eta_{ij} & \\
\text{s.t.:} & & \\
& \displaystyle\sum_{l\in N} x_{kl} + \sum_{l\in N: l\neq k} x_{lk} = (2p-1)\,y_k & \forall k \in N \\
& \displaystyle\sum_k y_k = p & \\
& \eta_{ij} \ge \phi_{ij}(\bar{x}^h) + \displaystyle\sum_{(k,l)\in I^e} \nabla_{kl}\phi_{ij}(\bar{x}^h)(x_{kl}-\bar{x}^h_{kl}) & \forall (i,j)\in W,\ h\in H \\
& \eta_{ij} \ge 0 & \forall\,(i,j)\in W \\
& y_k \in \{0,1\} & \forall\, k \in N \\
& x_{kl} \in [0,1] & \forall\,(k,l)\in I^e
\end{cases}$$

The steps of this algorithm are summarized in Algorithm 1. The OA-Obj method iteratively refines a linear approximation of the nonlinear objective by generating supporting hyperplanes based on first-order derivatives. At each iteration, the relaxed master

problem is solved, if the optimality gap between the linear approximation and the true objective exceeds 0.01%, a new cut is generated using the gradient at the current solution point. This process continues until the approximation accurately represents the nonlinear function within the specified tolerance.

Algorithm 1 OA-Obj Algorithm

1: Initialize $h \leftarrow 0$ and feasible solution $\bar{x}^h$
2: **repeat**
3: Solve the master problem with current OA cuts
4: Compute $\phi_{ij}(\bar{x}^h)$ and its gradient $\nabla\phi_{ij}(\bar{x}^h)$
5: Add OA cut at x^h:

$$\eta_{ij} \geq \phi_{ij}(\bar{x}^h) + \sum_{(k,l)\in I^e} \nabla_{kl}\phi_{ij}(\bar{x}^h)(x_{kl} - \bar{x}^h_{kl})$$

6: $h \leftarrow h + 1$
7: **until** optimality gap $\leq 0.01\%$
8: **Output:** best incumbent solution x^h

The OA-Obj algorithm therefore serves as the baseline implementation of the OA framework for the MPMAPHLP, preserving the structure of the original MINLP and enabling a direct assessment of the benefits introduced by the subsequent variants.

4.2 OA-rvar Algorithm: Outer Approximation on Auxiliary Variables r

The OA-rvar algorithm builds upon the OA-Obj approach and applies the Outer Approximation method to the MINLP formulation of the MPMAPHLP by expressing the nonlinear terms in the objective function through the auxiliary variables r_{ij}, which represent the denominators of the fractional objective function:

$$r_{ij} = \sum_{(k,l)\in I^e} \pi^e_{ijkl} x_{kl} + 1, \tag{4.19}$$

Thus, the nonlinearity is shifted to the function $\phi_{ij}(r_{ij}) = \frac{1}{r_{ij}}$, leading to the following MINLP formulation of the MPMAPHLP:

$$
\text{MINLP}\ \text{MPMAPHLP}\ \begin{cases}
\min \displaystyle\sum_{(i,j)\in W} w_{ij}\ \phi_{ij} & \\
\text{s.t.: } x_{kl} \leq y_k & \forall\ k,l \in H^e \\
x_{kl} \leq y_l & \forall\ k,l \in H^e \\
\displaystyle\sum_{k\in N} y_k = p & \\
r_{ij} = \displaystyle\sum_{(k,l)\in I^e} \pi^e_{iklj}\ x_{kl} + 1 & \forall\ (i,j) \in W \\
\phi_{ij}(r_{ij}) = \dfrac{1}{r_{ij}} & \forall\ (i,j) \in W \\
r_{ij} \geq 1 & \forall\ (i,j) \in W \\
y_k \in \{0,1\} & \forall\ k \in N \\
x_{kl} \in [0,1] & \forall\ (k,l) \in I^e
\end{cases}
$$

Although the auxiliary variables r_{ij} were originally introduced in the conic formulation, their use here remains within the MINLP structure of the problem. The linearization is therefore performed with respect to r_{ij}, instead of the inter-hub connection variables x_{kl}, resulting in a more stable and accurate approximation of the nonlinear objective.

This reformulation simplifies the computation of derivatives and separates the nonlinear objective term from the combinatorial structure. The outer approximation is then applied through the general OA cut formulation:

$$\eta_{ij} \geq \phi_{ij}(\bar{r}^h_{ij}) + \phi'_{ij}(\bar{r}^h_{ij})\,(r_{ij} - \bar{r}^h_{ij}) \qquad \forall (i,j) \in W,\ h \in \mathcal{H} \tag{4.20}$$

$\phi'_{ij}(\bar{r}^h_{ij})$ denotes the derivative of ϕ_{ij} with respect to r_{ij}, evaluated at the point $\bar{r}^h_{ij}$, and is given by $\phi'_{ij}(\bar{r}^h_{ij}) = -\frac{1}{(\bar{r}^h_{ij})^2}$. The set $\mathcal{H}$ contains all cuts generated throughout the algorithm, divided, in this variant, into two subsets: $\mathcal{H}_0$, which represents the initial cuts generated prior to the first OA iteration, and H, which corresponds to the cuts added iteratively during the optimization process ($\mathcal{H} = \mathcal{H}_0 \cup H$). The OA cut at iteration h linearizes the objective function around the point $\bar{r}^h_{ij}$ by means of a first-order Taylor expansion:

$$\eta_{ij} \geq \frac{1}{\bar{r}^h_{ij}} - \frac{1}{(\bar{r}^h_{ij})^2}\,(r_{ij} - \bar{r}^h_{ij}) \quad \forall\ (i,j) \in W,\ h \in \mathcal{H}$$

The resulting master problem for the OA-rvar variant applied to the original minimization MPMAPHLP form is defined as follows:

OA-rvar MPMAPHLP

$$
\begin{cases}
\min \displaystyle\sum_{(i,j)\in W} w_{ij}\,\eta_{ij} & \\
\text{s.t.: } x_{kl} \le y_k & \forall\, k,l \in H^e \\
\quad x_{kl} \le y_l & \forall\, k,l \in H^e \\
\quad \displaystyle\sum_{k\in N} y_k = p & \\
\quad r_{ij} = \displaystyle\sum_{(k,l)\in I^e} \pi^e_{iklj}\, x_{kl} + 1 & \forall\, (i,j) \in W \\
\quad \eta_{ij} \ge \dfrac{1}{\bar{r}^h_{ij}} - \dfrac{1}{(\bar{r}^h_{ij})^2}\,(r_{ij} - \bar{r}^h_{ij}) & \forall\, (i,j) \in W,\ h \in \mathcal{H} \\
\quad r_{ij} \ge 1 & \forall (i,j) \in W \\
\quad \eta_{ij} \ge 0 & \forall (i,j) \in W \\
\quad y_k \in \{0,1\} & \forall\, k \in N \\
\quad x_{kl} \in [0,1] & \forall\, (k,l) \in I^e
\end{cases}
$$

The same OA-rvar logic can be extended to the tightened version of the MPMAPHLP:

OA-rvar New MPMAPHLP

$$
\begin{cases}
\min \displaystyle\sum_{(i,j)\in W} w_{ij}\,\eta_{ij} & \\
\text{s.t.: } \displaystyle\sum_{l\in N} x_{kl} + \sum_{l\in N: l\neq k} x_{lk} = (2p-1)\, y_k & \forall k \in N \\
\quad \displaystyle\sum_{k\in N} y_k = p & \\
\quad r_{ij} = \displaystyle\sum_{(k,l)\in I^e} \pi^e_{iklj}\, x_{kl} + 1 & \forall\, (i,j) \in W \\
\quad \eta_{ij} \ge \dfrac{1}{\bar{r}^h_{ij}} - \dfrac{1}{(\bar{r}^h_{ij})^2}\,(r_{ij} - \bar{r}^h_{ij}) & \forall\, (i,j) \in W,\ h \in \mathcal{H} \\
\quad r_{ij} \ge 1 & \forall (i,j) \in W \\
\quad \eta_{ij} \ge 0 & \forall (i,j) \in W \\
\quad y_k \in \{0,1\} & \forall\, k \in N \\
\quad x_{kl} \in [0,1] & \forall\, (k,l) \in I^e
\end{cases}
$$

Appendix A details the procedure for constructing the set of initial cuts, also generated for the variables r_{ij} before the first OA iteration. These cuts provide an initial piecewise-linear approximation of the nonlinear term, improving the quality of the first master problem and accelerating convergence in early iterations. The generation process follows the piecewise linearization approach proposed by Elhedhli (2005).

The pseudo-code for the OA-rvar variation solving the MPMAPHLP is shown in Algorithm 2.

Algorithm 2 OA-rvar Algorithm

1: Generate initial cuts $\mathcal{H}_0$ for each $(i,j) \in W$
2: For each $(i,j) \in W$ and $h \in \mathcal{H}_0$, add cut

$$\eta_{ij} \geq \phi_{ij}(\bar{r}_{ij}^h) + \phi'_{ij}(\bar{r}_{ij}^h)(r_{ij} - \bar{r}_{ij}^h), \qquad \forall (i,j) \in W, h \in \mathcal{H}_0$$

3: Initialize $H \leftarrow \emptyset$, $h \leftarrow 0$, and feasible solution $\bar{r}^h$
4: **repeat**
5: Solve the master problem with initial cuts $\mathcal{H}_0$
6: Evaluate $\phi_{ij}(\bar{r}_{ij}^h)$ and $\phi'_{ij}(\bar{r}_{ij}^h)$
7: Add new OA cut:

$$\eta_{ij} \geq \phi_{ij}(\bar{r}_{ij}^h) + \phi'_{ij}(\bar{r}_{ij}^h)(r_{ij} - \bar{r}_{ij}^h), \qquad \forall (i,j) \in W, h \in H$$

8: Update $H \leftarrow H \cup \{h\}$ and $h \leftarrow h + 1$
9: **until** optimality gap $\leq \varepsilon$
10: **Return** incumbent solution $\bar{r}^h$

The OA-rvar algorithm combines the convexity of the continuous relaxation with a strengthened initialization strategy, resulting in a fully linear and computationally efficient implementation of the OA framework for the MPMAPHLP. This variant therefore serves as a bridge between the purely MINLP-based OA-Obj and the conic COACuts algorithm presented in next section.

4.3 COACuts Algorithm: Outer Approximation to the Conic Form

The COACuts algorithm extends the OA strategy to the conic formulation of the MPMAPHLP. In this variant, the nonlinearity is embedded within the second-order cone structure, and the OA cuts are incorporated directly into the conic model to strengthen its initial linear approximation. Unlike the OA-rvar algorithm, which iteratively refines the linearization within a purely linear setting, the COACuts approach keeps the conic representation intact and applies the OA principle only through an set of supporting cuts. Let us now recall the conic form of the MPMAPHLP:

$$\textbf{Conic MPMAPHLP} \begin{cases} \min \sum_{(i,j)\in W} w_{ij}\ \eta_{ij} & \\ \text{s.t.: } x_{kl} \le y_k & \forall\ k,l \in H^e \\ x_{kl} \le y_l & \forall\ k,l \in H^e \\ \sum_{k\in N} y_k = p & \\ r_{ij} = \sum_{(k,l)\in I^e} \pi^e_{iklj}\ x_{kl} + 1 & \forall\ (i,j) \in W \\ \eta_{ij} r_{ij} \ge 1 & \forall\ (i,j) \in W \\ r_{ij} \ge 1 & \forall\ (i,j) \in W \\ \eta_{ij} \ge 0 & \forall\ (i,j) \in W \\ y_k \in \{0,1\} & \forall\ k \in N \\ x_{kl} \in [0,1] & \forall\ (k,l) \in I^e \end{cases}$$

The COACuts formulation retains the conic structure of the original MPMAPHLP formulation. As in the OA-rvar model, the construction of the outer approximation cuts in the COACuts formulation follows the same linearization structure with respect to the auxiliary variables r_{ij}. The COACuts is defined as follows:

$$\textbf{COACuts MPMAPHLP} \begin{cases} \min \sum_{(i,j)\in W} w_{ij}\ \eta_{ij} & \\ \text{s.t. } x_{kl} \le y_k & \forall\ k,l \in H^e \\ x_{kl} \le y_l & \forall\ k,l \in H^e \\ \sum_{k\in N} y_k = p & \\ r_{ij} = \sum_{(k,l)\in I^e} \pi^e_{iklj}\ x_{kl} + 1 & \forall (i,j) \in W \\ \eta_{ij} r_{ij} \ge 1 & \forall\ (i,j) \in W \\ \eta_{ij} \ge \phi_{ij}(\bar{r}^h_{ij}) + \phi'_{ij}(\bar{r}^h_{ij})(r_{ij} - \bar{r}^h_{ij}) & \forall (i,j) \in W,\ h \in \mathcal{H}_0 \\ r_{ij} \ge 1 & \forall (i,j) \in W \\ \eta_{ij} \ge 0 & \forall (i,j) \in W \\ y_k \in \{0,1\} & \forall k \in N \\ x_{kl} \in [0,1] & \forall\ (k,l) \in I^e \end{cases}$$

where $\phi_{ij}(r_{ij}) = \frac{1}{r_{ij}}$ and $\phi'_{ij}(r_{ij}) = -\frac{1}{r^2_{ij}}$.

Since the nonlinear term $\phi_{ij}(r_{ij})$ is convex and continuously differentiable, its first-order approximation around a given point $\bar{r}^h_{ij}$ provides a valid supporting hyperplane for the conic feasible region. Therefore, the OA cuts are generated using the same derivative

information as in the OA-rvar case, but are incorporated directly into the conic model as additional linear constraints.

Unlike the OA-rvar algorithm, which iteratively refines the approximation by adding new cuts, the COACuts model applies the outer-approximation principle only once, through a single set of pre-generated cuts. This design choice reflects the already convex nature of the conic formulation, where iterative refinements are not imposed. The COACuts algorithm was therefore conceived as a non-iterative variant, intended to evaluate how the inclusion of initial OA cuts interacts with the conic representation of the MPMAPHLP.

The same approach can also be applied to the tightened version of the MPMAPHLP introduced in Section 3.3, leading to the COACuts on New MPMAPHLP formulation, as presented below:

$$
\textbf{COACuts New MPMAPHLP} \left\{
\begin{array}{lll}
\min & \displaystyle\sum_{(i,j)\in W} w_{ij}\ \eta_{ij} & \\
\text{s.t.} & \displaystyle\sum_{l\in N} x_{kl} + \sum_{l\in N: l\neq k} x_{lk} = (2p-1)\ y_k & \forall k \in N \\
& \displaystyle\sum_{k\in N} y_k = p & \\
& r_{ij} = \displaystyle\sum_{(k,l)\in I^e} \pi^e_{iklj}\ x_{kl} + 1 & \forall (i,j) \in W \\
& \eta_{ij} r_{ij} \geq 1 & \forall\ (i,j) \in W \\
& \eta_{ij} \geq \phi_{ij}(\bar{r}^h_{ij}) + \phi'_{ij}(\bar{r}^h_{ij})(r_{ij} - \bar{r}^h_{ij}) & \forall (i,j) \in W,\ h \in \mathcal{H}_0 \\
& r_{ij} \geq 1 & \forall (i,j) \in W \\
& \eta_{ij} \geq 0 & \forall (i,j) \in W \\
& y_k \in \{0,1\} & \forall k \in N \\
& x_{kl} \in [0,1] & \forall\ (k,l) \in I^e
\end{array}
\right.
$$

In summary, the COACuts algorithm serves as the conic counterpart to the linear OA-based variants. Its non-iterative structure, based solely on pre-generated cuts, provides a methodological reference for evaluating the behavior of outer-approximation techniques within a conic optimization framework.

The main steps of the COACuts algorithm are summarized in Algorithm 3. In this variant, a finite set of linearization points for the variables r_{ij} is also selected according to the procedure described in Appendix A. For each of these points, an outer-approximation cut of the function $\phi_{ij}(r_{ij}) = \frac{1}{r_{ij}}$ is generated and added as an additional linear constraint to the conic formulation of the MPMAPHLP (or its tightened version). The resulting mixed-integer second-order conic problem, reinforced by this *a priori* set of cuts, is then solved once using a MISOCP solver.

Algorithm 3 COACuts Algorithm

1: Generate initial linearization points $\bar{r}_{ij}^h$ for $(i,j) \in W$, $h \in \mathcal{H}_0$
2: For each $(i,j) \in W$ and $h \in \mathcal{H}_0$, add cut

$$\eta_{ij} \geq \phi_{ij}(\bar{r}_{ij}^h) + \phi'_{ij}(\bar{r}_{ij}^h)(r_{ij} - \bar{r}_{ij}^h)$$

3: Build the COACuts formulation with conic constraints and all initial cuts
4: Solve the resulting MISOCP
5: **Return** the optimal solution

In summary, the OA-Obj, OA-rvar, and COACuts algorithms constitute three complementary implementations of the outer-approximation framework for the MPMAPHLP. The following chapter reports the computational experiments and comparative analysis performed to evaluate their performance and practical efficiency.

Chapter 5

Computational Results and Performance Analysis

This section presents and discusses the computational results obtained from the formulations proposed for the *Multiple Allocation p-Hub Location Problem in a Competitive Scenario* (MPMAPHLP). The experiments were designed to evaluate the performance of the formulations under different modeling perspectives, encompassing both the conic formulations and the Outer Approximation (OA)-based formulations, which are presented later in this chapter.

All formulations reported in this work were implemented in `C++` and solved using `IBM ILOG CPLEX Optimization Studio`, version `22.1.2.0`, without any callback routines. Therefore, all computational improvements reported stem from the proposed model structures. All experiments were conducted on a personal laptop (*ASUS VivoBook X513EA*) running `Ubuntu 24.04.2 LTS`, equipped with an `Intel(R) Core(TM) i7-1165G7` processor (2.80 GHz) and 19 GB of RAM, using a single processing thread.

All test instances are derived from the well-established *Civil Aeronautics Board* (CAB) benchmark dataset, widely used in the hub location literature. This dataset provides intercity distances and passenger flows among U.S. cities. Initially, we tested instances with 10, 15, 20, 25, 30, and 40 nodes. Larger instances with 50, 60, and 70 nodes were later tested for the best-performing models and are discussed in a dedicated subsection. All instances are available at: https://github.com/tainapossas/MPMAPHLP.

Customer utility values were computed as described in Section 2.5, assuming a single incumbent operator with a fixed hub network, which are randomly selected, and an entrant aiming to capture market share by deploying the same number of p hubs. The parameters used in the attractiveness and cost functions are as follows: $\beta = 1$, $\delta = 1$, $\gamma = 0.5$, and the attractiveness index A^a_{kl} is set to 1.25 for single-hub routes ($k = l$), reflecting their higher perceived convenience, and 1 otherwise. Travel times are assumed proportional to distances, with total route time computed as $T^a_{iklj} = d_{ik} + d_{kl} + d_{lj}$. Transportation costs are modeled by $B^a_{iklj} = \chi d_{ik} + \alpha d_{kl} + \zeta d_{lj}$, where $\chi = \zeta = 1$. The same travel times and costs are considered for both the incumbent and entrant over identical routes ($i \to k \to l \to j$).

This chapter presents the main summarized results obtained, while the detailed results are placed in Appendices B, C, and D. For each network size n, different numbers of hubs (p) and economies of scale (α) were tested. The value of α varied from 0.1 to 1.0, in increments of 0.1, in order to assess the impact of different discount levels on inter-hub connections and their influence on market capture. The column *Market Share (%)* represents the entrant's weighted market share across all origin–destination (O–D) pairs, calculated as the ratio between the total captured demand and the overall network demand. In all tables the entries marked with '-' mean ***unavailable/impossible-to-determine/out-of-memory***, while empty entries mean values equal to ***zero***.

To enable a fair performance comparison between the approaches, the original conic maximization and minimization models were executed without time limits for instances up to 25 nodes, ensuring a consistent comparison with the OA-based models, which were also solved to optimality. For the 30- and 40-node instances, however, a maximum time limit of 3600 seconds (1 hour) was imposed to the conic formulations due to limitation on the operational research time constraints. Therefore, in these cases, relative speed-ups between models were not considered for analysis, but the optimality gaps observed are briefly discussed.

5.1 Results of the Conic Formulations

This section presents the computational performance of the three conic formulations proposed for the MPMAPHLP: the original maximization model (MAXMPMAPHLP, or simply MAX), the original minimization model (MINMPMAPHLP, or simply MIN), and the new strengthened minimization model (NEW MINMPMAPHLP, or simply NEW). The purpose of this analysis is to compare their relative performance in terms of average CPU time and the average number of branch-and-bound nodes explored across different instance sizes.

The MAXMPMAPHLP model corresponds to the original market-share maximization conic model proposed by Tiwari et al. (2021a). It is important to highlight a critical implementation issue identified in the source code made publicly available by the authors. The variable intended to model the scale-economy parameter (α) was mistakenly defined as an `integer` instead of a `floating-point` parameter. As a result, the hub-level network structure remained constant across all tested values of α, compromising the validity of their reported results. To address this issue, we corrected the implementation and re-executed all instances to ensure consistency and validity in the comparative analysis.

Detailed computational results for each tested value of α are provided in the Appendix on Tables B.1 and B.2. Each row corresponds to a specific test configuration defined by the number of nodes (n), the number of hubs to be installed (p), and the value of the economy-of-scale parameter (α). For each test, we report the achieved market share

by the entrant, the CPU time (in seconds) and the optimality gap (%) at termination in parenthesis, when not null, in Table B.1, and the number of branch-and-bound nodes explored (#bbn) in Table B.2. This table offers a granular view of how the formulations behave across different α parameter settings and provides evidence of the superior efficiency of the new minimization-based model in most configurations. The winning formulations with respect to the total computational time have their entries in bold.

At the end of each set of ten runs, which differ according to the value of the economy-of-scale parameter α, for a given (n, p) configuration, we compute the average performance metrics (CPU time, gap, and number of branch-and-bound nodes) over all values of α. This averaging process provides a representative summary of each model's computational behavior under different levels of instance complexity, capturing how performance scales with increasing network size and number of hubs. Based on these averaged metrics, Table 5.1 summarizes the overall results obtained for the three formulations.

Considering first the average computational times (Avg. cpu (s)) reported in Table 5.1, it can be observed that for all tested instances, the average processing times of the maximization model are consistently higher than those of the minimization model, which in turn are higher than those of the new minimization formulation. The latter is therefore the fastest among all, solving instances with up to 40 nodes in less than 40 seconds on average. When analyzing the average number of branch-and-bound nodes (Avg. #bbn) considering only the instances solved to optimality, the results show that the maximization and minimization models required a comparable order of magnitude of explored nodes, whereas the new minimization formulation needed substantially fewer nodes, further confirming its superior computational efficiency.

From the detailed results in Tables B.1, it can also be observed that the maximization model reached proven optimality within the 1-hour time limit in 115 out of 180 tests (63.89%). It did not converge within 1 hour of processing time in 25% of the cases (45 tests), specifically for five tests with 25 nodes and 4 hubs (when $\alpha = 0.1, 0.3, 0.4, 0.6, 1.0$), all tests with 30 nodes, and all tests with 40 nodes and 4 hubs. Furthermore, the model failed to solve all tests with 40 nodes, and 5 and 6 hubs (11.11% of the tests). In contrast, the minimization model solved all tests, reaching proven optimality within 1 hour in 150 out of 180 cases (83.33%), while presenting gaps for all tests with 40 nodes (16.67%). The new minimization-based formulation, on the other hand, successfully solved 100% of the tests to proven optimality. These results underscore the limited scalability of the original maximization formulation and strongly support the effectiveness of the minimization-based approaches, especially the new formulation even in complex configurations.

It can be observed that as instance size increases, particularly for larger values of p, all processing times tend to grow. Although this pattern is not strictly monotonic across all combinations, a clear trend emerges when p is held constant and n increases. Figure 5.1 offers a visual representation of the comparative results across processing times

when varying instance sizes and number of hubs for the three conic formulations — a) MAXMPMAPHLP, b) MINMPMAPHLP, and c) NEW MINMPMAPHLP. The vertical axis corresponds to the logarithmic transformation of average solution times, specifically, $\log_{10}(t+1)$, applied to accommodate the wide variability in magnitude while preserving interpretability, particularly for values below one second. This transformation ensures that all time values are plotted on a consistent, positive scale.

The Figures 5.1a and 5.1b show clear evidence that computational time increases with instance complexity for both the MAX and MIN formulations, since as the number of nodes (n) and hubs (p) increases, the average processing times also rise significantly. In contrast, Figure 5.1c reveals a more nuanced behavior on terms of solution times of the NEW formulation. While it consistently outperforms the original ones across all tested values of n and p, the magnitude of time improvement does not necessarily increase with the number of nodes. For instance, in the case of $p = 4$, the average time for $n = 25$ surpasses ones for $n = 30$, suggesting that the relative efficiency gain of the tightened formulation is not strictly proportional to the nominal complexity added by increasing n. These findings confirm the computational advantages of the proposed tight formulation and highlight its practical potential for solving large-scale instances of the problem efficiently.

Table 5.1: General computational results comparing the conic formulations in terms of average CPU time and branch-and-bound nodes.

n	**p**	**MAXMPMAPHLP**		**MINMPMAPHLP**		**NEW MINMPMAPHLP**	
		Avg. cpu (s)	**Avg. #bbn**	**Avg. cpu (s)**	**Avg. #bbn**	**Avg. cpu (s)**	**Avg. #bbn**
10	2	1.21	35.10	0.20	39.40	0.15	1.50
10	3	2.11	54.20	0.20	49.90	0.12	1.90
10	4	6.37	47.60	0.18	45.10	0.07	0.00
15	2	14.59	65.80	1.42	67.90	0.40	0.00
15	3	19.61	115.30	1.34	105.00	0.38	0.00
15	4	27.43	133.50	1.53	133.30	0.54	0.70
20	2	86.64	105.90	5.41	108.20	0.50	0.00
20	3	252.59	174.40	7.71	178.10	1.98	0.00
20	4	910.13	241.00	8.37	235.30	1.03	0.00
25	2	536.19	205.00	20.38	191.30	2.08	0.00
25	3	1122.46	448.40	32.83	398.60	1.30	0.00
25	4	4414.99	597.30	47.45	591.40	6.89	3.40
30	4	3593.52	606.20	624.69	8134.50	5.81	1.50
30	5	3595.72	397.50	1015.97	11828.90	2.31	0.50
30	6	3594.64	312.20	1502.25	17200.80	2.65	0.50
40	4	3591.96	1.10	3597.19	9146.00	37.14	5.40
40	5	-	-	3597.69	8523.70	23.61	4.80
40	6	-	-	3597.96	7606.80	16.74	2.70

To better quantify the efficiency improvements achieve by our proposed formulations, Table B.3 reports the detailed results of the relative speed-ups among formulations for each tested combination of (n, p, α) only for instances solved to proven optimality. These results quantify the computational gains when comparing the maximization model with the minimization ones, and between the two minimization formulations. For each instance size (n, p), the reported averages were computed over the ten tested values of the economy-of-scale parameter α, ensuring a consistent comparison across all models.

Table 5.2 provides a summarized view of these comparisons, presenting both the average and maximum speed-up values obtained for each (n, p) configuration. Analyzing these results, it can be observed that the minimization models exhibit remarkable performance gains over the maximization model. The highest average speed-up (Avg. Speed-up) recorded by the ratio between MAX and MIN running times is 113.19 times, corresponding to the instance with $n = 20$ and $p = 4$. The maximum speed-up (Max. Speed-up) in this case reaches 407.25 times, observed for $\alpha = 1.0$ in the same instance configuration, as reported in Table B.3. The NEW minimization model, in turn, achieves even greater improvements: it accelerates the MAX model by up to 1080.78 times on average, reaching a maximum speed-up of 4359.30 times in the same instance ($n = 20$, $p = 4$, $\alpha = 1.0$). When the two minimization formulations are compared, a lower but still significant performance differences are also observed. The NEW formulation achieves an average speed-up of 596.98 times over the original MIN model, with a maximum speed-up of 829.39 times obtained for the instance with $n = 30$, $p = 6$, and $\alpha = 0.6$.

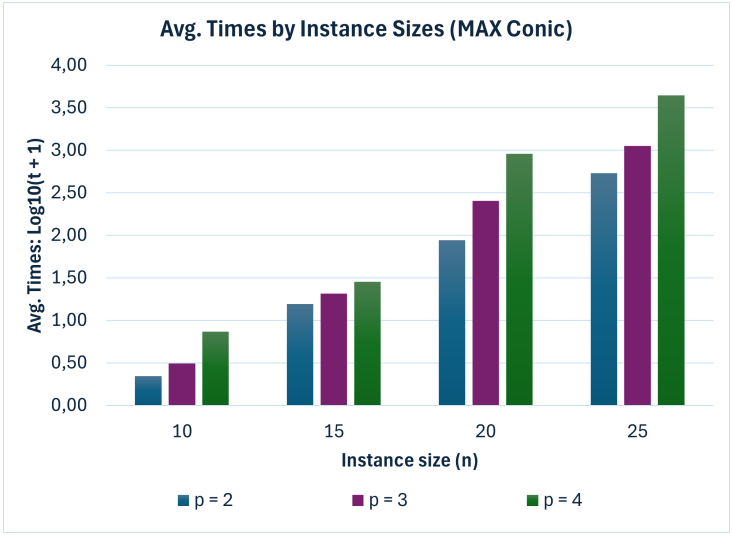

(a) MAXMPMAPHLP conic formulation — average CPU times by n and p

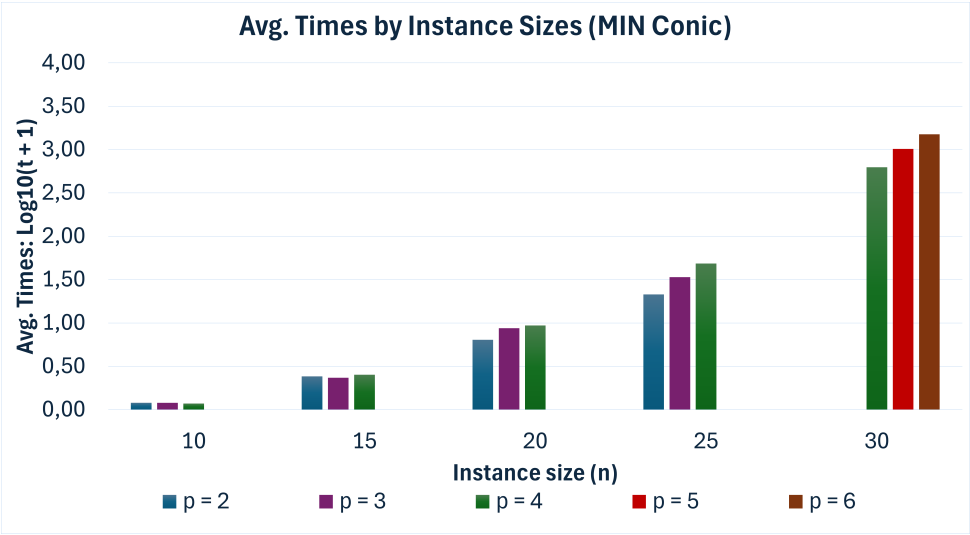

(b) MINMPMAPHLP conic formulation — average CPU times by n and p

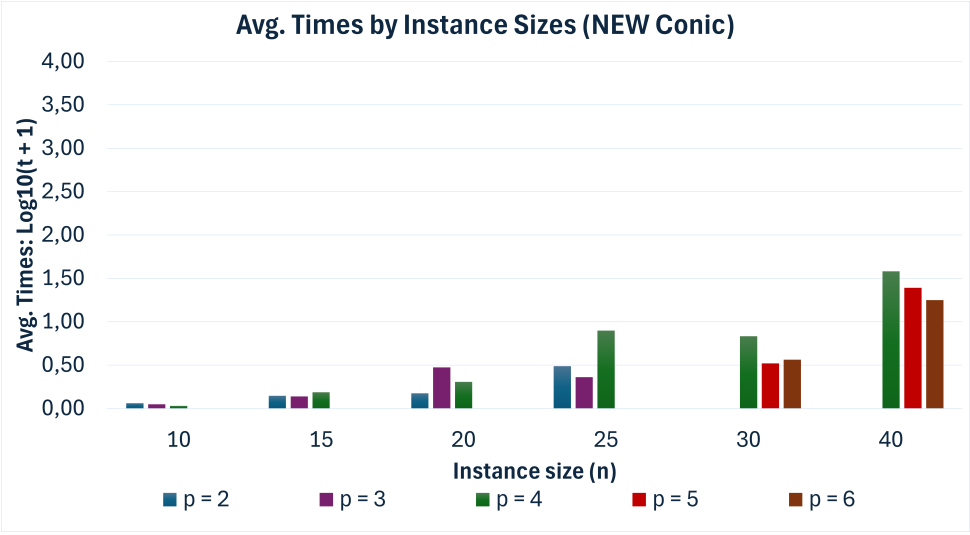

(c) NEW MINMPMAPHLP conic formulation — average CPU times by n and p

Figure 5.1: Average computational times by instance complexity for conic formulations

Table 5.2: General computational results comparing the conic formulations in terms of average and maximum speed-ups.

n	**p**	**Avg. Speed-up**			**Max Speed-up**		
		MAX/MIN	**MAX/NEW**	**MIN/NEW**	**MAX/MIN**	**MAX/NEW**	**MIN/NEW**
10	2	6.17	9.40	1.51	9.53	14.73	2.08
10	3	10.76	18.48	1.74	20.53	36.36	2.18
10	4	36.79	91.35	2.77	118.56	237.13	4.25
15	2	10.43	51.08	5.68	19.13	83.50	9.94
15	3	14.79	75.03	4.63	42.08	263.95	6.31
15	4	17.63	87.40	4.31	39.46	252.22	7.88
20	2	16.89	175.27	10.95	37.43	306.06	14.07
20	3	36.66	194.52	6.84	116.40	763.80	25.72
20	4	113.19	1080.78	10.25	407.25	4359.30	15.10
25	2	26.50	398.40	14.97	34.33	550.22	18.85
25	3	35.69	863.50	25.39	74.22	1379.22	29.98
25	4	93.52	1000.17	11.38	200.59	2287.61	17.97
30	4			114.42			161.96
30	5			441.29			560.78
30	6			596.98			829.39

To evaluate and compare the performance of different algorithms across the set of test instances, we adopt the benchmarking framework introduced by Dolan and Moré (2002), used to render Figure 5.2. This methodology relies on the concept of performance profiles, which are defined as cumulative distribution functions that measure the fraction of problems for which a given solver performs within a factor τ of the best performance. Formally, let P be the set of problems and S the set of solvers. For each problem $p \in P$ and solver $s \in S$, let $t_{p,s}$ denote the performance measure (e.g., runtimes) of solver s on problem p. The performance ratio is defined as:

$$r_{p,s} = \frac{t_{p,s}}{\min\limits_{s' \in S} t_{p,s'}}$$

The performance profile for solver s is then given by the function:

$$\rho_s(\tau) = \frac{1}{|P|} \left| \{ p \in P : r_{p,s} \leq \tau \} \right|$$

where $\tau \geq 1$ and $\rho_s(\tau)$ indicates the proportion of problems for which solver s performs within a factor τ of the best solver. It provides additional evidence that our minimization approaches tend to outperform its maximization counterpart for the competitive multiple-path multiple-allocation $p-$hub location problem.

Figure 5.2 shows the performance profile of the three conic formulations under a one-hour time limit. As expected, the MAX model displays the weakest computational performance, with the slowest convergence and the lowest proportion of solved instances. In contrast, the two minimization models exhibit more robust and stable behavior, with the NEW MINMPMAPHLP formulation clearly dominating the others. This superiority is attributed to the use of aggregated connectivity constraints and a tighter conic structure, which significantly reduce both the number of explored nodes and the overall processing time. The curve for MINMPMAPHLP remains flat at $\rho(\tau) \approx 0.83$, indicating that it solved around 83% of the instances and consistently outperformed the MAX model. Meanwhile, the MAXMPMAPHLP curve grows slowly and plateaus near $\rho(\tau) = 0.64$ at $\tau \approx 1000$, confirming it was only able to solve about 64% of the instances within the time limit. The NEW formulation, represented by the green curve, reaches $\rho(\tau) = 1$ early and remains dominant across all values of τ, highlighting its superior robustness and computational efficiency.

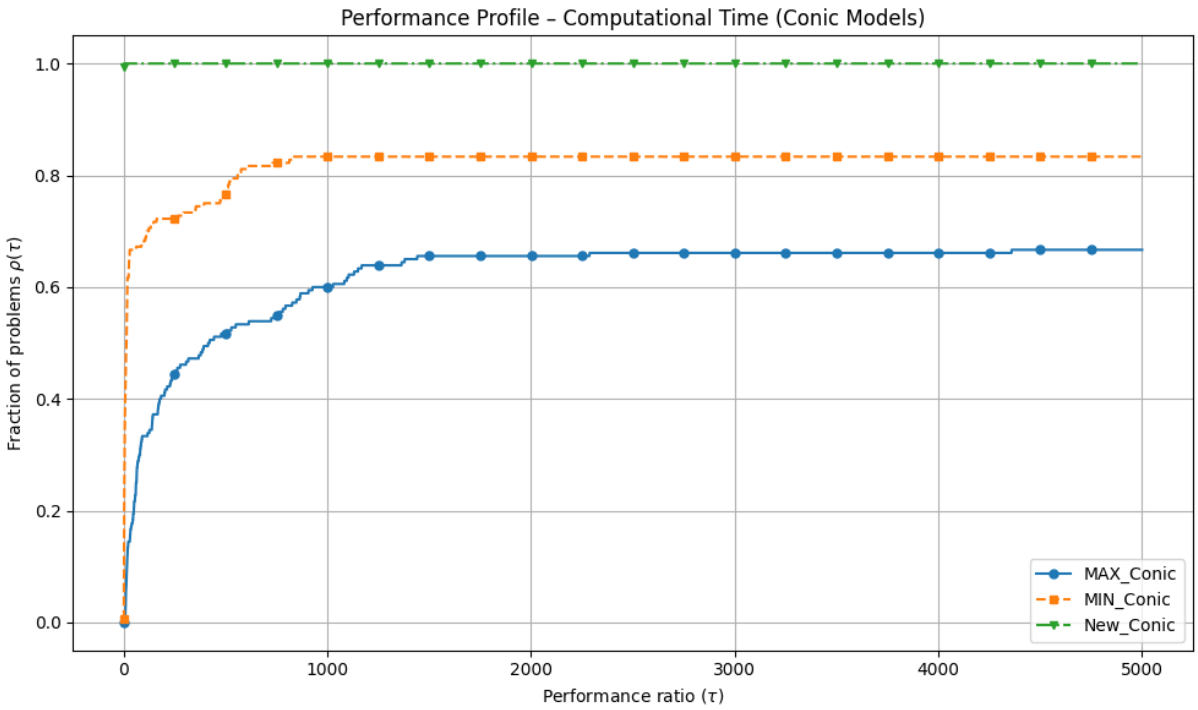

Figure 5.2: Performance profile for the all formulations on conic models

As previously mentioned, the original maximization and minimization conic formulations were unable to reach proven optimality for some of the larger instances within the established time limit, resulting in positive optimality gaps, as reported in Table 5.3. Since the MIN model successfully solved all 30-node instances, presenting in some cases negligible gaps of 0.01% imposed by the solver tolerance within the 1-hour limit, no values are reported for these configurations. In contrast, for the same instances, the maximization model exhibited average gaps of 36.06%, 44.36%, and 29.62% for $p = 4$, $p = 5$, and $p = 6$, respectively, which highlights the superior performance of our minimization formulation.

For the 40-node instances, the maximization model reached an average gap of 71.43% for the case with four hubs and failed to solve any of the tests with five or six hubs — the symbol "-" denotes *unavailable/impossible-to-determine/or out-of-memory* results, as explained at the beginning of this chapter. The minimization model, on the other hand, achieved a considerably smaller average gap of 49.51% for $n = 40$ and $p = 4$, and was able to solve the configurations with $p = 5$ and $p = 6$, obtaining average gaps of 48.06% and 43.80%, respectively.

The reported optimality gaps correspond to the relative difference between the best feasible solution found and the best bound available at termination. It is important to note that this metric does not necessarily reflect the distance to the true optimum, since the bound quality may vary across instances. Although direct comparison of optimality gaps across different instance sizes may be considered as not meaningful, analyzing them within the same (n, p) configuration reveals that the minimization formulation systemat-

ically achieves lower termination gaps than the maximization model, suggesting stronger relaxations and faster bound convergence. A deeper analysis based on bound evolution would provide a more precise view of solver convergence, however, this information was not available in the recorded logs for all runs.

Table 5.3: Average gaps (%) reported by MAX and MIN conic formulations

		Avg. Gap (%)	
n	**p**	**MAX**	**MIN**
30	4	36.06	
	5	44.36	
	6	29.62	
40	4	71.43	49.51
	5	-	48.06
	6	-	43.80

In conclusion, the minimization-based formulations proposed in this work offer streamlined and computationally efficient alternatives to the original maximization conic model of Tiwari et al. (2021a). Instead of maximizing the market share captured by the entrant, the equivalent yet more tractable approach of minimizing the market share lost to incumbent companies proved to be a more stable and effective strategy, yielding faster convergence across a wide range of instances without compromising optimality. Among these, the new strengthened minimization formulation (NEW MINMPMAPHLP) demonstrated the most remarkable performance, solving all instances to proven optimality, requiring significantly fewer processing times and branch-and-bound nodes, and achieving speed-ups of up to 1080 times in average compared to the original maximization model.

Having established the superiority of the minimization framework, the next section shifts the focus from comparisons with the literature to internal comparisons among our own models. We now investigate the potential of outer-approximation–based approaches to further enhance computational efficiency and reduce solution times while preserving the accuracy and robustness observed in the conic formulations.

5.2 Results of the Outer Approximation-Based Models

This section presents the computational results obtained by applying three outer approximation-based approaches to solve the original and new formulations of the MINMPMAPHLP model. The formulations under evaluation are: OA-Obj, OA-rvar, and COACuts. All instances and experimental conditions follow the same structure adopted in the previous section, but no time limit is imposed this time.

For each formulation, each test configuration we report market share (%), cpu time (s), final optimality gap (%), number of branch-and-bound nodes (#bbn) explored, and the ratio between solution times of the two formulations, which are the relative speed-ups obtained by the NEW model over the MIN one. Tests results are presented by instance size (n), number of hubs (p), and economy-of-scale parameter (α).

Tables C.1, C.2, and C.3 present the detailed results obtained for the OA-Obj, OA-rvar, and COACuts models respectively, and are provided in the Appendix to maintain a more concise flow of discussion throughout this section. All formulations successfully solved 100% of the tested instances to optimality, enabling direct and fair comparisons between the original and enhanced models. Across all three approaches, the NEW formulation consistently outperformed the traditional one in 100% of the tests, in terms of processing times. The summarized results provide a overview of the average and maximum running times.

The most remarkable case for OA-Obj (Table 5.4) occurs on the test with 40 nodes, 6 hubs, and $\alpha = 0.8$, with the NEW formulation completing in 15.12 seconds versus 22,647 seconds spent by the MIN model, yielding a speed-up of 1498 times. Despite the new model's gains in terms of computational times, we observed in these formulations that the average number of branch-and-bound nodes followed the same order of magnitude, tying in 16.66% of cases, while in the remainder, the NEW model uses fewer nodes.

On the OA-rvar (Table 5.5) the most notable result was for 40 nodes, 6 hubs, and $\alpha = 0.1$, where the NEW model solved the instance in 33.72 seconds, compared to 20,337.98 seconds required by the original formulation, a speed-up of 603.14 times. This time, the models tie in terms of the average number of branch-and-bound nodes across all cases.

Finally, on COACuts (Table 5.6), the most significant gain occurred for the instance with 40 nodes, 6 hubs, and $\alpha = 0.3$, where the NEW formulation solved the problem in just 24.26 seconds, compared to 120,905.97 seconds for the traditional minimization model, a speed-up of 4984 times faster. In relation to the average number of branch-and-bound nodes, the NEW formulation stands out in 100% of the tests.

The behavior of the MIN and NEW formulations reveals that, in some cases, both models explored a comparable number of branch-and-bound nodes, although the NEW model consistently achieved shorter computational times. This indicates that the two formulations followed similar branching strategies and exhibited comparable combinatorial complexity, yet the NEW formulation handled each node more efficiently. The reduced processing time per node suggests that the new model benefits from a stronger and more compact structure, yielding better-conditioned relaxations and faster convergence of the continuous subproblems solved at each node. Therefore, the computational gains observed for the NEW formulation are not due to a reduction in the search tree size, but rather to its superior numerical stability and internal solver efficiency.

Table 5.4: General computational results comparing MIN and NEW OA-Obj formulations

n	p	MIN			NEW		
		Avg. Time (s)	**Max. Time (s)**	**Avg. #bbn**	**Avg. Time (s)**	**Max. Time (s)**	**Avg. #bbn**
10	2	0.17	0.20	4.00	0.03	0.04	3.00
10	3	0.15	0.20	4.50	0.05	0.06	3.40
10	4	0.11	0.12	4.00	0.03	0.03	3.00
15	2	0.56	0.83	3.00	0.12	0.13	3.00
15	3	0.77	0.99	4.00	0.12	0.12	3.00
15	4	0.80	0.86	4.00	0.19	0.29	3.40
20	2	1.84	2.36	3.00	0.42	0.45	3.00
20	3	3.31	3.54	4.00	0.44	0.47	3.00
20	4	4.11	4.73	4.00	0.47	0.52	3.00
25	2	5.15	6.07	3.00	1.27	1.30	3.00
25	3	15.04	18.37	3.90	1.29	1.34	3.00
25	4	44.66	57.98	5.40	4.57	5.62	4.60
30	4	526.73	817.74	5.10	4.50	7.39	3.30
30	5	332.01	720.30	4.10	3.01	3.27	3.00
30	6	712.85	1418.44	4.20	3.82	6.99	3.20
40	4	6333.02	7423.67	5.00	33.19	52.73	4.20
40	5	34585.76	66951.30	6.10	56.64	83.57	5.10
40	6	42162.16	76638.82	5.00	35.71	53.89	4.20

Table 5.5: General computational results comparing MIN and NEW OA-rvar formulations

n	p	MIN			NEW		
		Avg. Time (s)	**Max. Time (s)**	**Avg. #bbn**	**Avg. Time (s)**	**Max. Time (s)**	**Avg. #bbn**
10	2	0.11	0.13	2.00	0.05	0.05	2.00
10	3	0.11	0.13	2.50	0.06	0.08	2.50
10	4	0.07	0.08	2.00	0.04	0.04	2.00
15	2	0.57	0.69	2.00	0.14	0.14	2.00
15	3	0.47	0.52	2.00	0.13	0.14	2.00
15	4	0.45	0.48	2.00	0.16	0.19	2.00
20	2	2.17	2.78	2.00	0.43	0.46	2.00
20	3	2.07	2.42	2.00	0.46	0.47	2.00
20	4	2.05	2.37	2.00	0.54	0.58	2.00
25	2	5.36	5.59	2.00	0.95	0.98	2.00
25	3	8.03	9.08	2.00	1.25	1.26	2.00
25	4	13.05	14.98	2.80	2.03	2.29	2.80
30	4	163.58	217.01	2.10	3.02	4.05	2.10
30	5	241.93	322.07	2.00	2.95	3.00	2.00
30	6	321.22	630.16	2.20	2.80	4.05	2.20
40	4	1952.09	2979.26	2.20	13.63	18.27	2.20
40	5	11621.90	15851.18	4.00	27.91	32.00	4.00
40	6	11150.41	20337.98	2.70	26.88	43.72	2.70

Table 5.6: General computational results comparing MIN and NEW COACuts formulations

n	p	MIN			NEW		
		Avg. Time (s)	**Max. Time (s)**	**Avg. #bbn**	**Avg. Time (s)**	**Max. Time (s)**	**Avg. #bbn**
10	2	0.36	0.43	36.60	0.13	0.15	1.00
10	3	0.35	0.47	44.80	0.11	0.16	0.90
10	4	0.26	0.40	38.00	0.06	0.06	0.00
15	2	2.46	3.45	63.10	0.24	0.25	0.00
15	3	2.09	2.72	107.50	0.34	0.54	0.00
15	4	2.58	3.06	114.60	0.44	0.91	0.30
20	2	7.26	10.27	113.20	0.75	0.95	0.00
20	3	9.76	12.33	166.20	0.69	0.71	0.00
20	4	12.25	15.61	237.30	1.03	1.31	0.00
25	2	30.60	35.54	217.90	1.85	1.92	0.00
25	3	48.05	56.56	432.90	2.34	2.65	0.00
25	4	65.74	85.41	581.70	9.61	18.84	2.80
30	4	632.31	743.01	7884.20	9.13	24.45	1.00
30	5	1058.23	1401.79	11730.70	4.70	5.77	0.80
30	6	1616.17	2052.01	16712.50	3.47	4.93	0.60
40	4	7456.37	8755.05	26886.40	433.31	672.94	28.10
40	5	31939.76	52360.68	68016.50	75.61	429.51	11.70
40	6	94788.63	121014.65	107069.90	72.27	488.99	6.40

Figures 5.3, 5.4, and 5.5 provides a comparative visualization of average solution times (logarithmic scale) between the original MINMPMAPHLP (a), and the improved NEW MINMPMAPHLP (b) formulations, for the OA-Obj, OA-rvar models, and COA-Cuts, respectively. The goal of the graphical analysis presented in this figures is to evaluate whether computational performance of the original MIN and NEW formulations are affected by instance complexity, for each solution method, by fixing the number of hubs p and varying the instance size n. This approach allows us to isolate the effect of instance scale on model performance, highlighting how the average solution time evolve as the problem grows.

In the OA-Obj formulations (Figure 5.3), there is evidence that, only for MIN model, the network size (n) has a consistent direct influence on the computational time, while variations in the number of hubs do not exhibit the same effect, for both models, as illustrated by the 30-node instances. In the OA-rvar formulations (Figure 5.4), a similar pattern is observed, particularly for the 40-node instances, reinforcing the influence of network size over hub quantity on the overall computational performance. Based on the plots presented in Figure 5.5, it can be observed that, in the COACuts formulations, the increase in instance complexity directly affects the computational time of the MIN model, whereas this effect is not evident for the NEW model. This behavior is particularly noticeable for the instances with 30 and 40 nodes, where the increase in the number of hubs (p) does not correspond to a increase in the average solution times.

Table 5.7 presents the average and maximum speed-ups achieved by the NEW formulation over the MIN formulation for the three approaches based on the Outer Approximation framework. Overall, the results confirm the consistent behavior already observed in the conic formulations, with the NEW model outperforming the MIN model in all tested instances. In the COACuts formulation, the average speed-ups range from 2.8 times to 3451.8 times, with maximum values reaching 4983.8 times for the instance with $n = 40$ and $p = 6$ at $\alpha = 0.3$. In the OA-Obj formulation, the gains are also very pronounced, with average speed-ups of up to 1143.8 times and a maximum of 1497.9 times for the instance with $n = 40$, $p = 6$, and $\alpha = 0.8$, demonstrating the outstanding performance of the NEW model even under more intensive cut-generation structures. In the OA-rvar formulation, the speed-ups remain high, with average gains close to 400 times for the largest instances and maximum values above 600 times, reinforcing the consistent advantage of the NEW model across different structural variants of the OA method. This pattern indicates that the structural strength of the new formulation not only reduces the per-node solution time but also maintains high computational efficiency even when combined with iterative cut-based algorithms. Therefore, the NEW model stands out as the most stable and scalable among all tested OA-based formulations.

The performance metrics used in this section are calculated following the benchmarking methodology proposed by Dolan and Moré (2002), described previously. These

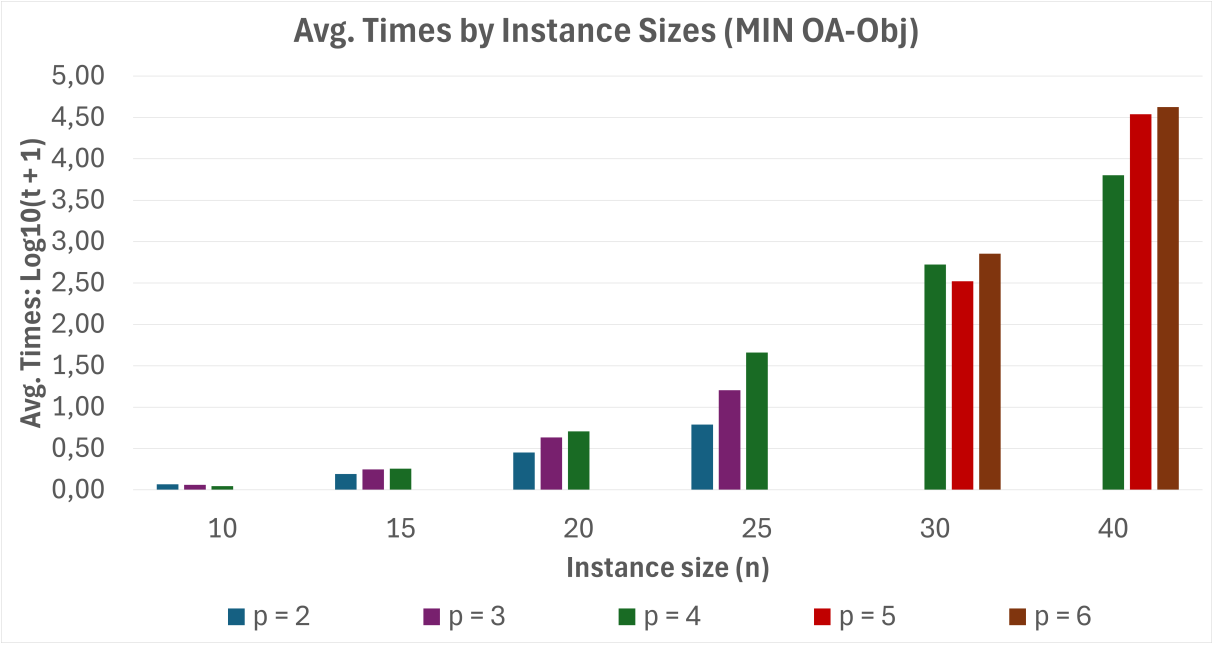

(a) MINMPMAPHLP OA-Obj formulation — average CPU times by n and p

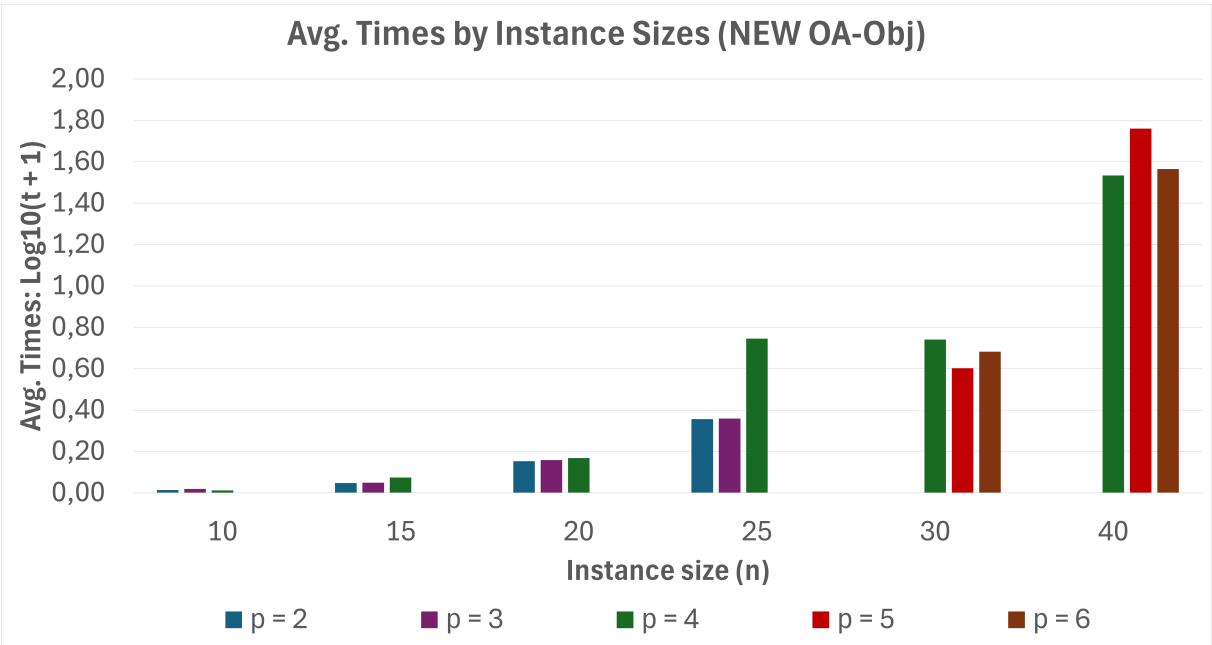

(b) NEW MINMPMAPHLP OA-Obj formulation — average CPU times by n and p

Figure 5.3: Average computational times by instance complexity for OA-Obj formulations

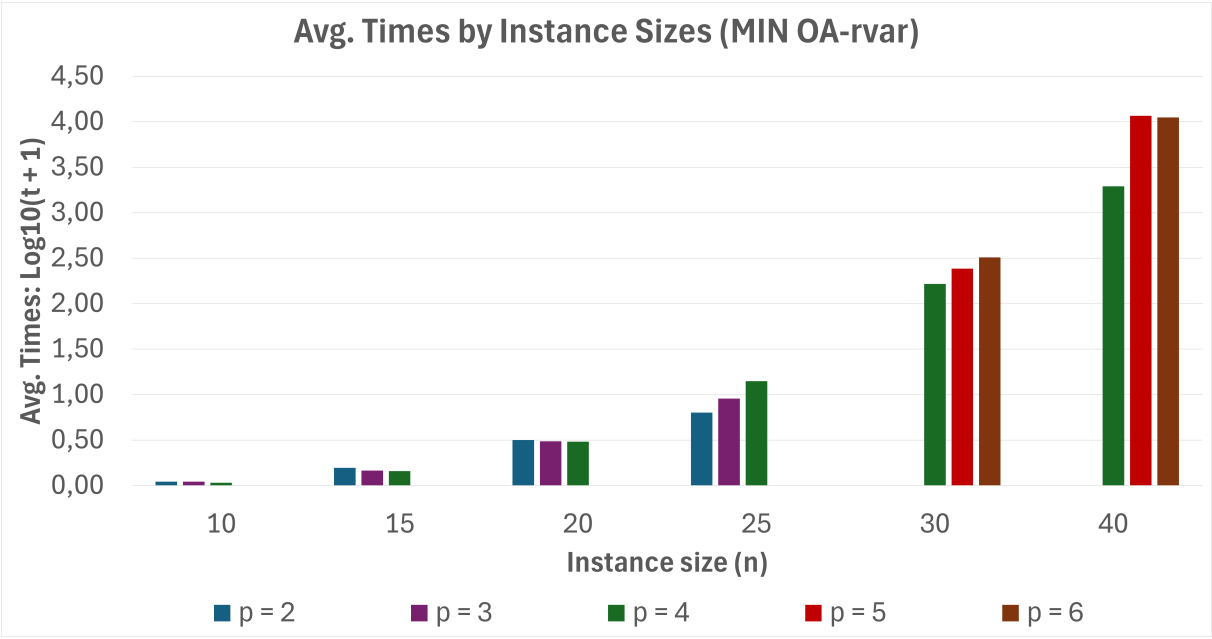

(a) MINMPMAPHLP OA-rvar formulation — average CPU times by n and p

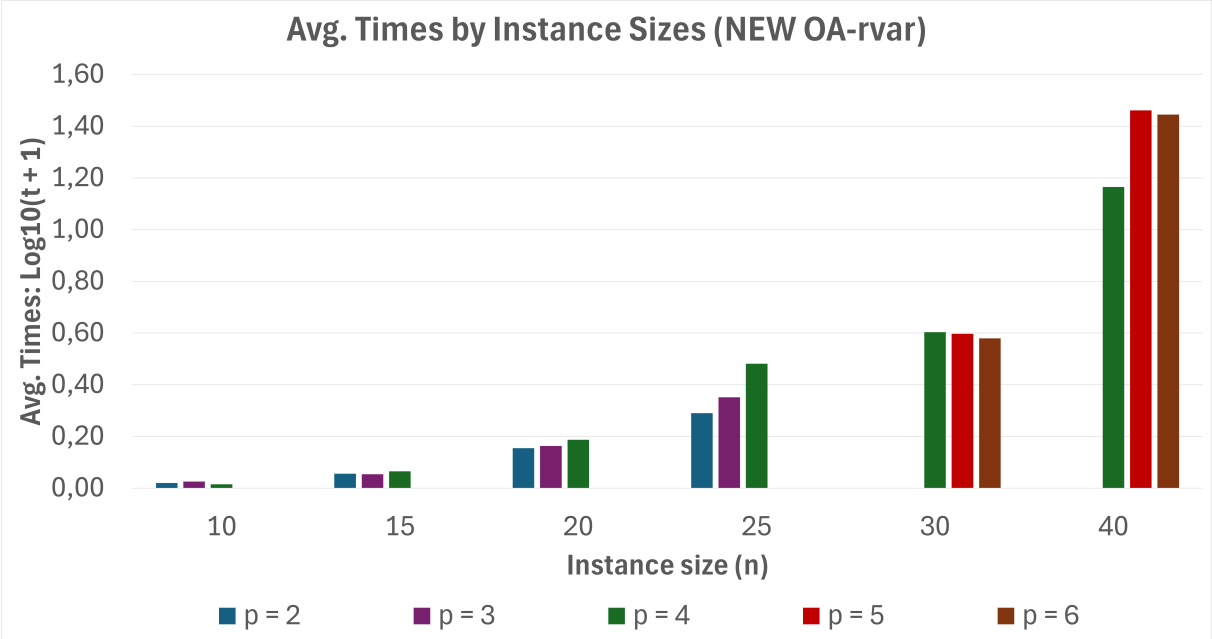

(b) NEW MINMPMAPHLP OA-rvar formulation — average CPU times by n and p

Figure 5.4: Average computational times by instance complexity for OA-rvar formulations

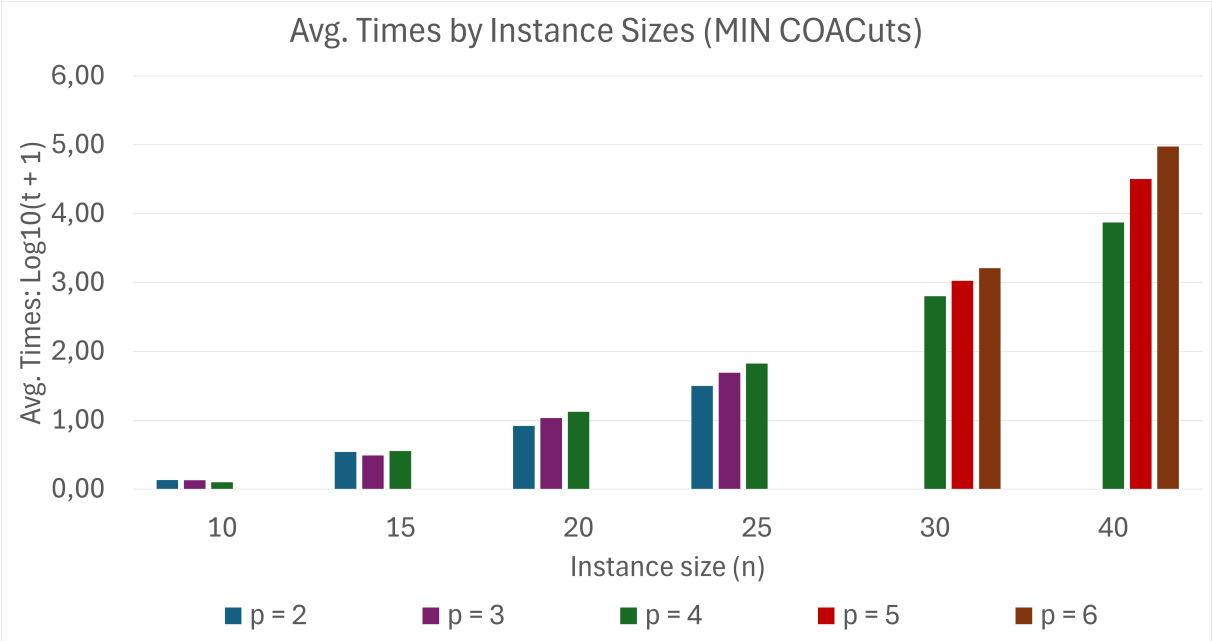

(a) MINMPMAPHLP COACuts formulation — average CPU times by n and p

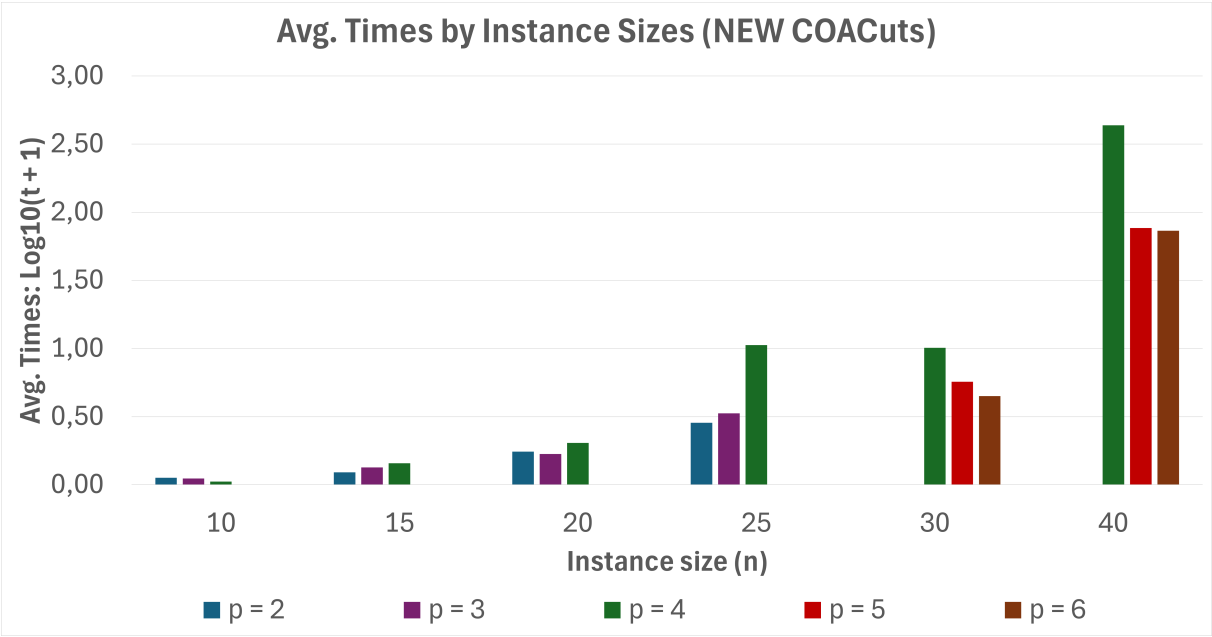

(b) NEW MINMPMAPHLP COACuts formulation — average CPU times by n and p

Figure 5.5: Average computational times by instance complexity for COACuts formulations

Table 5.7: General computational results comparing average and maximum speed-ups achieved by the NEW over MIN formulations

n	p	COACuts		OA-Obj		OA-rvar	
		Average	Maximum	Average	Maximum	Average	Maximum
10	2	2.81	3.50	5.39	6.50	2.28	3.25
10	3	3.41	5.33	3.39	4.50	1.74	2.00
10	4	4.60	6.67	3.88	5.50	2.13	2.67
15	2	10.47	15.68	4.81	7.55	4.15	5.31
15	3	6.28	8.50	6.43	8.25	3.56	4.00
15	4	6.71	10.13	4.94	6.92	2.79	3.00
20	2	10.05	18.34	4.36	5.62	5.11	6.62
20	3	14.22	17.37	7.54	8.19	4.54	5.26
20	4	12.25	17.50	8.74	10.28	3.81	4.65
25	2	16.53	19.53	4.05	4.71	5.63	5.88
25	3	20.61	25.29	11.68	14.09	6.44	7.21
25	4	6.48	11.07	9.78	11.12	6.33	6.93
30	4	82.22	121.47	134.88	244.83	55.00	63.66
30	5	236.37	352.83	110.34	238.51	82.05	111.83
30	6	482.15	678.42	184.23	204.92	109.61	159.53
40	4	69.27	289.52	200.24	244.52	141.69	163.07
40	5	1104.85	2837.90	600.52	1010.33	415.55	585.56
40	6	3451.79	4983.76	1143.84	1497.88	398.29	603.14

metrics are based exclusively on the processing times required to solve each instance, since all models reach optimality and share the same objective values. Figure 5.6 enables the comparison of performance profiles of the MINMPMAPHLP and NEW MINMPMAPHLP models for each of the three outer approximation-based techniques. Figure (a) presents the results for the OA-Obj models, Figure (b) for the OA-r variant, and Figure (c) for COACuts. The x-axis are performance ratios τ, while the y-axis represents the cumulative proportion of problems solved within τ times the best performance. In all graphs, the blue curve indicates the traditional MINMPMAPHLP model, and the orange curve represents the NEW MINMPMAPHLP formulation, the one with tighter connectivity constraints.

Figure 5.6a presents the performance profile of the models considering the OA-Obj formulation. The original MPMAPHLP model exhibits a slower growth in its performance curve, requiring a ratio $\tau > 1400$ to reach approximately total coverage of the tests. In all cases, the NEW MPMAPHLP model's profile curves reaches $\rho(\tau) = 1$ very close to $\tau = 1$, demonstrating consistent and stable behavior.

Figure 5.6b presents the performance profile comparing the formulations under the OA-rvar approach. The NEW formulation also demonstrates a clearly dominant performance, solving 100% of the instances with the best CPU times. Its curve reaches the upper bound ($y = 1$) near $\tau = 1$ and remains flat, indicating that it consistently outperformed the original model in all cases. In contrast, the original formulation only reaches 100% at $\tau \approx 600$, with a significant portion of instances requiring considerably

more time than the best-known solution.

Finally, the performance profile in Figure 5.6c clearly shows that the proposed NEW model solved under the COACuts consistently outperforms the original minimization MPMAPHLP formulation. Moreover, the curve for MPMAPHLP grows more slowly, indicating that its computational runtimes are significantly higher in many cases, with a performance ratio τ reaching values near 5000 to match the NEW formulation.

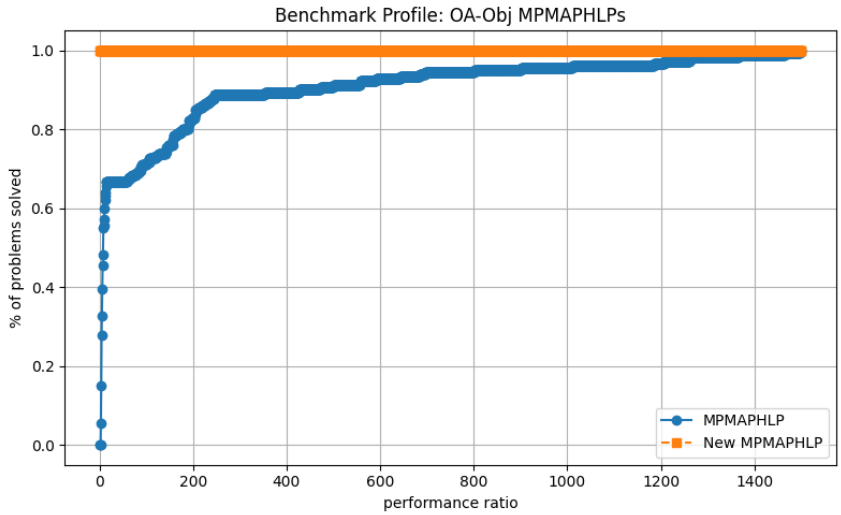

(a) Performance profile of OA-Obj models

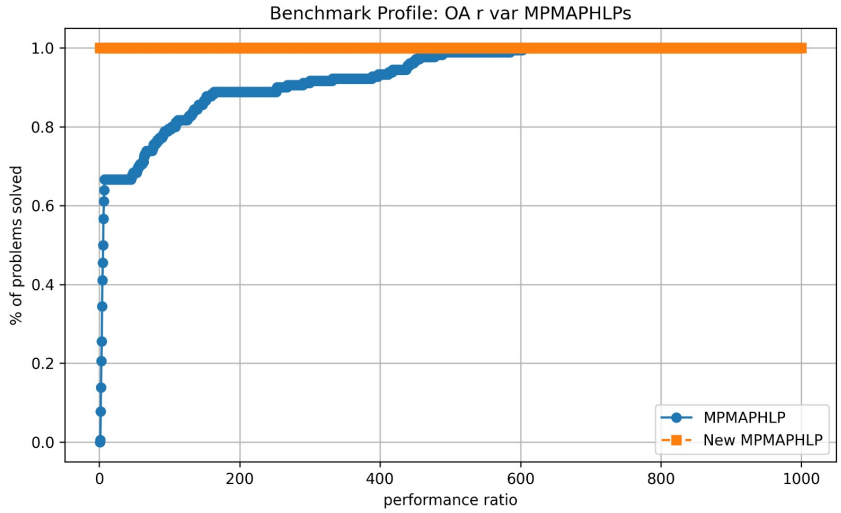

(b) Performance profile of OA-rvar models

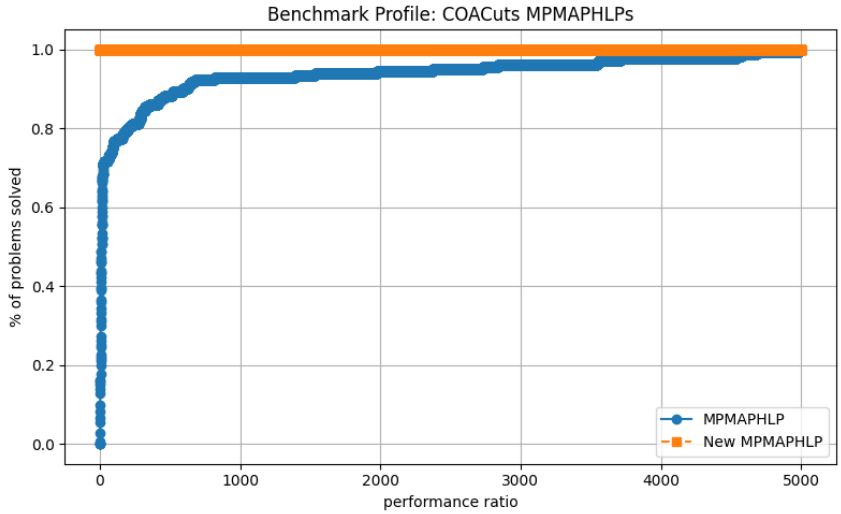

(c) Performance profile of COACuts models

Figure 5.6: Performance profile of OA-based models on original and NEW MPMAPHLP

This behavior reflects that NEW MPMAPHLP is not only superior in computational runtimes but also more robust across the tested scenarios when solved with all outer approximation based models. The results reinforce the recommendation of adopting the new tight formulation as the preferred approach for solving the MPMAPHLP problems.

In order to directly compare all models, we constructed a consolidated performance profile, shown in Figure 5.7, which includes all OA-based variants. The analysis confirms the superiority of the NEW model on OA formulations over the original MIN ones, as they are able to solve 100% of the instances rapidly for low values of τ. Among the traditional minimization MPMAPHLP models, the OA-rvar formulation stands out for its performance, reaching full instance coverage at a performance ratio slightly under $\tau = 1000$. In contrast, the COACuts and OA-Obj formulations solve approximately 90% of the instances only for τ values above 1000. Furthermore, between these two, the COACuts model consistently shows inferior performance in most cases.

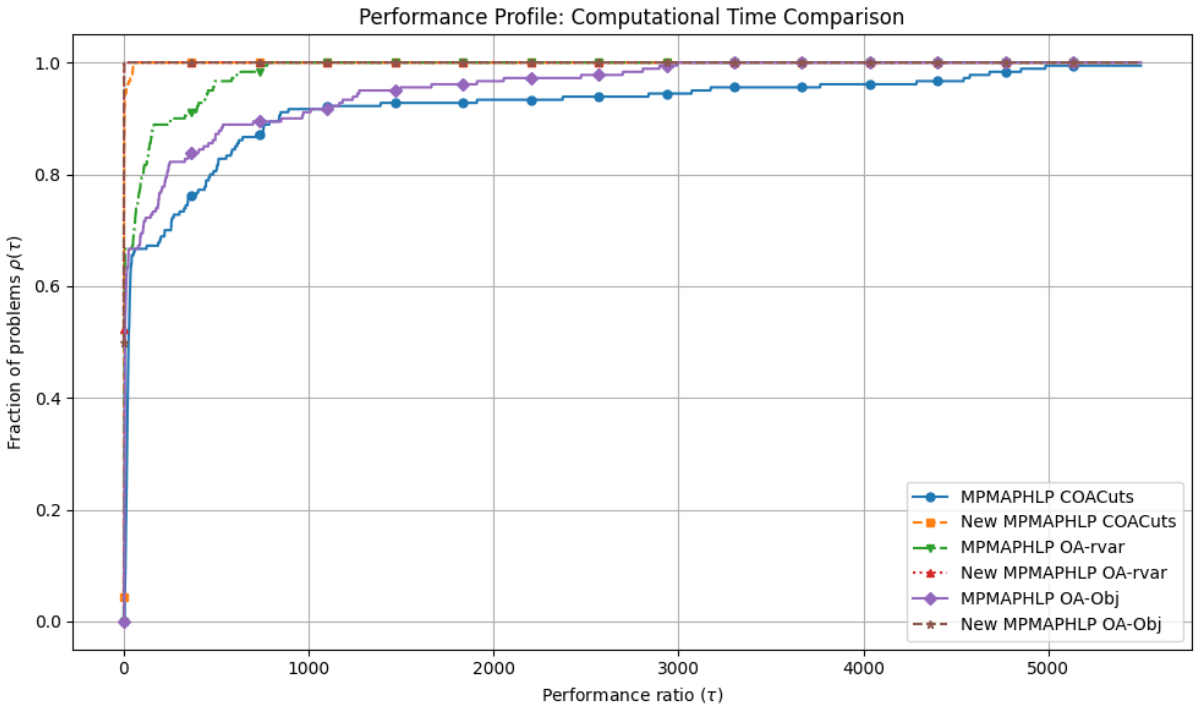

Figure 5.7: Performance profile of all models with OA-based formulations.

Finally, a chart was generated to compare the performance of the NEW OA formulations exclusively, as shown in Figure 5.8. The best performance is achieved by the OA-rvar formulation, followed by the OA-Obj model. The COACuts formulation performs the worst among the three, reaching 100% of the instances only for τ values over 50. It is important to note that, unlike the other two OA-based formulations, the OA-Obj model does not include any initial cuts in its master problem. As a result, the algorithm starts without a warm-start approximation of the nonlinear feasible region, which can lead to a larger number of iterations before convergence. Although this limitation may partially

explain its longer computational times in some configurations, the OA-Obj formulation still demonstrated competitive performance across all tested instances. Future work could explore the inclusion of initial cuts to further accelerate convergence and reduce the total solution time.

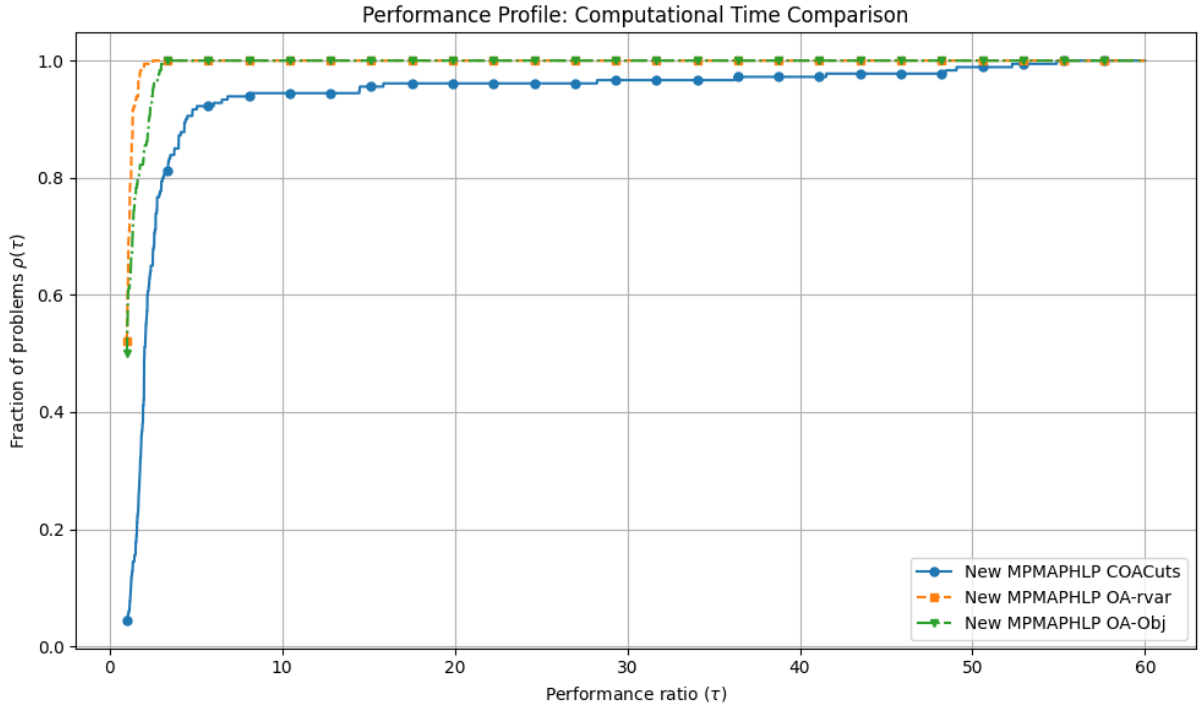

Figure 5.8: Performance profile of *NEW MPMAPHLP* models with OA-based formulations

Finally, we compare the relative performances of all models, including both conic and OA-based models, for all instances solved to proven optimality with up to 25 nodes. Figure 5.9 presents the performance profile of the nine evaluated formulations in terms of computational time. It can be observed that the maximization model remains the worst performer by a large margin, while the minimization formulations exhibit clearly superior behavior. Its curve increases gradually, reaching only about 80% of the instances for $\tau = 1000$ and approaching full coverage only for very large values of $\tau > 6000$. This behavior confirms that the maximization formulation is computationally demanding, while the minimization-based formulations consistently demonstrate superior efficiency and robustness across all tests.

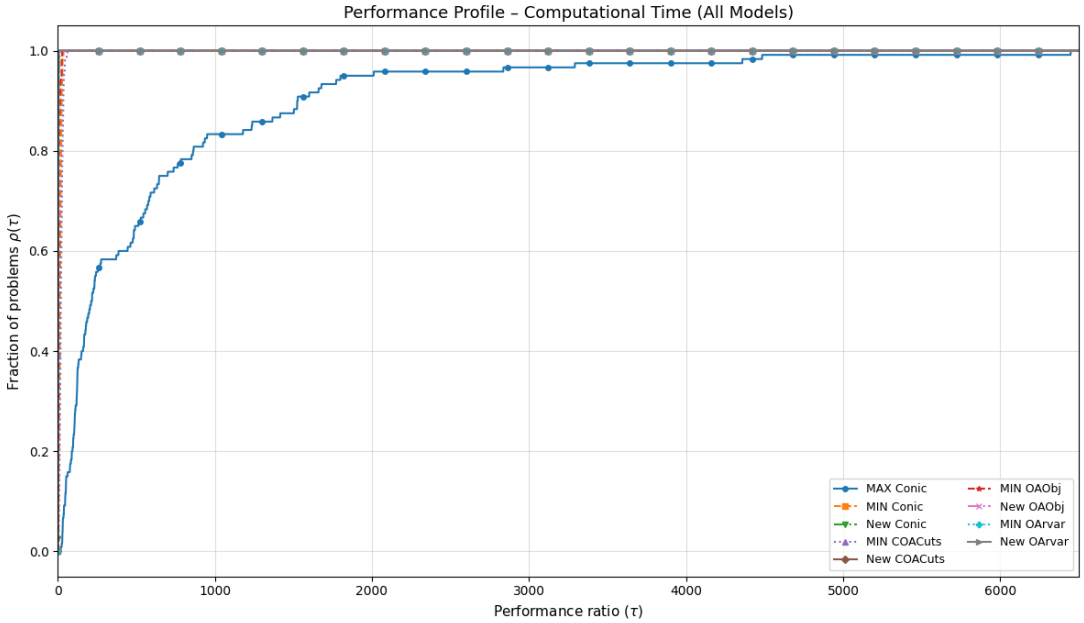

Figure 5.9: Performance profile for all 9 models up to 25 nodes

Excluding the maximization case, Figure 5.10 focuses on the eight remaining models, considering all instances solved to optimality up to 30 nodes. Interestingly, the MIN Conic and MIN COACuts formulations exhibit the worst performance, with their curves being very close. This suggests that there is no computational advantage in applying OA cuts in the conic minimization formulation.

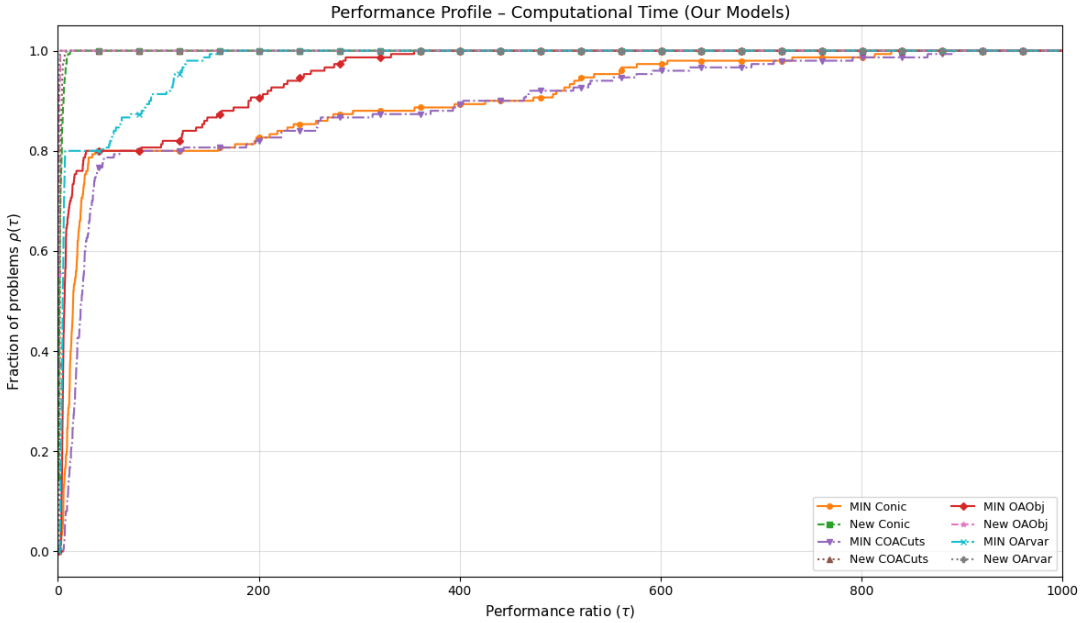

Figure 5.10: Performance profile for our models up to 30 nodes

5.3 Results of NEW formulations on Large Instances

Finally, we extended our analysis to larger-scale instances (n = 50, 60, and 70) using the four solution approaches studied on this work (Conic, COACuts, OA-rvar, and OA-Obj) based on the strengthened formulation (NEW MINMPMAPHLP, with aggregated connectivity constraints). The detailed results are reported in Tables D.1, D.2, and D.3, while Table 5.8 presents a summary of average and maximum CPU times for each instance group. From these results, we observe that all four methods were able to solve the instances with up to 60 nodes within minutes. For the largest instances (n = 70), one can notice that the OA-Obj are not able to solve any test with 4 or 6 hubs, and the OA-rvar model showed the best overall performance, solving even the most challenging case (with $p = 6$ and $\alpha = 0.8$) in under 1,040 seconds. To complement these observations, performance profiles are presented next, offering a broader perspective on the relative efficiency and consistency of the models across all tested instances.

Table 5.8: General computational results of New MPMAPHLP formulations on large scale instances.

n	p	Conic (s)		COAcuts (s)		OA r var (s)		OA-Obj (s)	
		Avg. Time	Max. Time	Avg. Time	Max. Time	Avg. Time	Max. Time	Avg. Time	Max. Time
50	4	115.956	150.97	124.74	148.15	119.76	124.16	248.359	408.7
50	5	38.533	66.4	53.759	68.76	85.831	88.82	94.378	98.17
50	6	86.606	113.03	154.049	412.83	129.725	145.86	430.156	457.46
60	4	202.577	477.08	234.233	312.2	197.692	356.19	238.053	251.56
60	5	227.565	453.62	383.024	799.4	256.043	344.61	988.195	1086.68
60	6	175.712	595.89	235.979	607.59	191.761	276	527.062	1028.35
70	4	6106.282	23581.1	16048.532	36266.7	677.69	835.6	-	-
70	5	9930.509	19912.27	2586.297	11459.34	709.819	804.45	632.36	1372.73
70	6	12056.383	27960.19	13515.326	51891.06	1010.364	1035.07	-	-

To plot the performance profile shown in Figure 5.11, we considered only the results for instances with up to 60 nodes, in order to include all formulations in the comparison, since OA-Obj could not be executed for the largest cases. Among the formulations applied to the NEW model, OA-rvar achieved the best overall performance, followed by OA-Obj, the direct conic formulation, and finally COACuts. This result confirms the robustness of the OA-rvar structure, which combines the advantages of the outer-approximation framework with a more stable variable-based representation, resulting in faster and more consistent convergence across different network sizes. Overall, these findings highlight the scalability of the NEW model structures for medium and large-sized networks, and consolidate OA-rvar as the most efficient approach among all tested formulations.

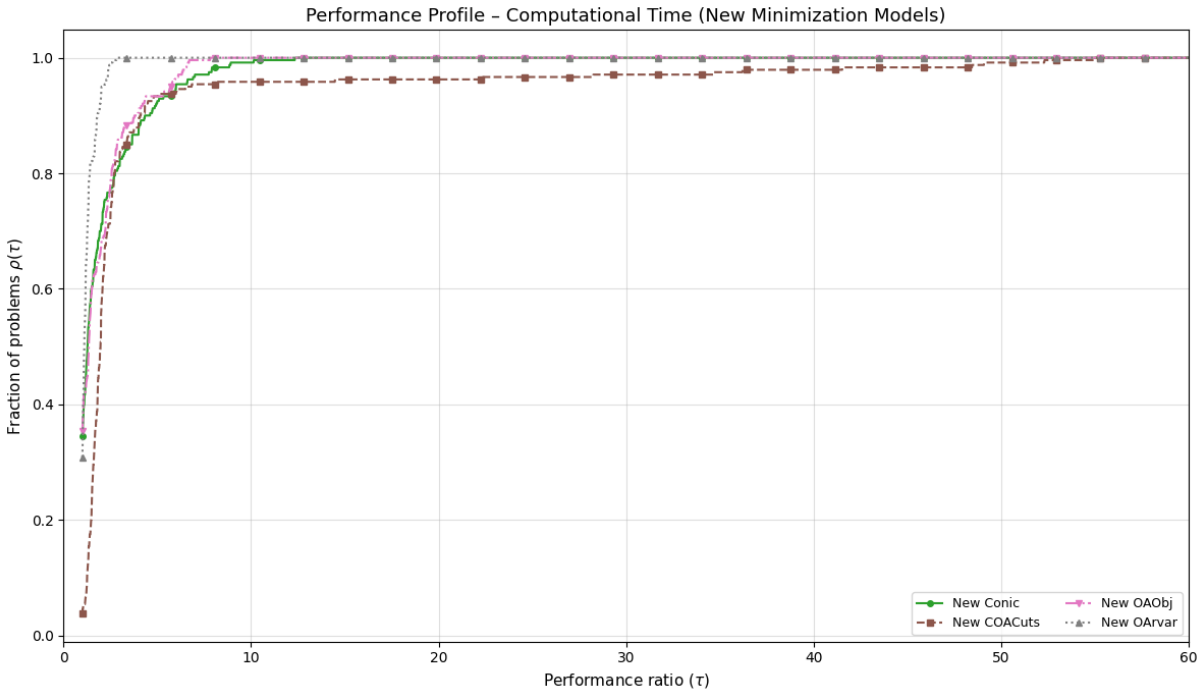

Figure 5.11: Performance profile for new models up to 60 nodes

Having established the computational efficiency and robustness of the proposed formulations, the following section turns to a qualitative and quantitative analysis of the resulting hub-and-spoke networks configurations. This analysis aims to illustrate how the inclusion or removal of hubs affects the market share captured by the entrant, as well as how variations in key parameters of the utility function influence the competitive behavior of the network.

5.4 Analysis of Resulting Hub-and-Spoke Networks on Competitive MPMAPHLP

After establishing the computational efficiency and robustness of the proposed formulations, this section shifts the focus from the algorithmic performance to the structural and behavioral interpretation of the resulting networks. The analysis aims to provide a quantitative and qualitative understanding of how the configuration of hub locations and the associated market shares evolve under competitive conditions.

In particular, we investigate how the insertion or removal of hubs in the entrant's network influences its market capture, as well as how variations in the key parameters of the utility function — the economy-of-scale factor (α) and the passenger sensitivity coefficient (γ) to repulsion factors — affect the balance of service coverage. Selected instances are presented through illustrative maps to highlight these dynamics and to provide managerial insights into the structural behavior of competitive hub networks.

5.4.1 Effect of the Number of Hubs on Entrant's Market Share

For this analysis, we selected a network scenario with 20 airports ($n = 20$) and varied the number of hubs across $p = \{2, 3, 4\}$, as illustrated in Figure 5.12. All maps were generated under $\alpha = 0.1$ (strongest economy-of-scale setting) and $\gamma = 0.5$ (balanced passenger sensitivity), ensuring a consistent behavioral and cost structure across all network configurations. The results show that the market share captured by the entrant airline increases with the number of hubs, even when the incumbent also expands its hub network. However, the extent of market capture is significantly affected by whether the incumbent optimizes the positioning of its hubs or locates them at random, revealing the strategic importance of hub location decisions in competitive environments.

Initially, with $p = 2$ hubs (Figures 5.12.a and 5.12.b), the incumbent's hub selection is optimal, leading the entrant airline to choose the same pair of hubs, located at nodes 13 and 19. In this configuration, market share is evenly distributed between the two companies, each capturing 50.00% of the total demand. When one additional hub is introduced in both networks ($p = 3$), but the competitor's third hub is randomly located (Figures 5.12.c and 5.12.d), the entrant's market share increases by an average of 11.88%, reaching 61.88% of capture. Finally, when four hubs are installed ($p = 4$), but two of the competitor's hubs are non-optimal, the entrant achieves a market share of 71.05% (Figures 5.12.e and 5.12.f). These results are consistent with the findings of Eiselt and Marianov (2009), who demonstrated that, first, installing the same number of hubs as the leader is an effective strategy for market entry, and second, that suboptimal hub placement by the incumbent further favors the entrant's market capture.

From a spatial perspective, these maps reveal a clear expansion pattern in the entrant's network as the number of hubs increases. Starting from the same configuration with $p = 2$, the entrant significantly broadens its geographic coverage when the third hub is added, more extensively than the incumbent does. The same behavior is observed with the introduction of the fourth hub, where the incumbent maintains a relatively clustered distribution, while the entrant adopts a more dispersed configuration, prioritizing shorter access distances over shorter inter-hub distances. This spatial strategy explains the observed increase in the entrant's market share to 71.05%, as greater network connectivity and territorial reach enhance its ability to attract demand. Under the strong economy-of-scale regime ($\alpha = 0.1$), inter-hub connections become comparatively inexpensive, making proximity to origin and destination nodes the dominant factor driving passenger choice and, consequently, the entrant's competitive advantage.

The identified spatial strategies also reveal how structural parameters in the model translate into competitive outcomes. The next analysis focuses on how variations in the economy-of-scale factor (α) and passenger sensitivity (γ) affect market equilibrium, highlighting the managerial implications of adjusting these parameters in real-world hub location planning.

5.4.2 Effects of Passenger Sensitivity and Discount on Market Share

Before analyzing the quantitative results, it is essential to recall the distinct role that the parameter γ plays in the utility formulation of the competitive hub location problem. It captures passenger sensitivity to repulsive factors, which in this study are represented by distances serving as proxies for both travel time and cost. When considered together with the discount effect of parameter α reducing the effective cost of inter-hub travel, it determines the trade-off between network efficiency and accessibility, influencing whether passengers prefer shorter access/egress distances or cheaper inter-hub routes.

All results presented so far were obtained under the balanced setting $\gamma = 0.5$, in which passengers value all distance-based repulsive factors equally, and the entrant benefits from combining short access/egress legs with a competitive inter-hub geometry. By varying this parameter, we can observe how changes in passenger sensitivity reshape competitive advantages, particularly when access and egress distances become more or less relevant relative to inter-hub travel distances.

Figure 5.13 illustrates the combined effect of the parameters γ and α on the entrant's market capture for the network with 20 nodes and four hubs, assuming random hub locations for the incumbent. It is important to highlight that the hub locations of both the entrant and the incumbent in this case remain fixed across all parameter variations, corresponding to the configuration presented in Figures 5.12.e and 5.12.f. Additional

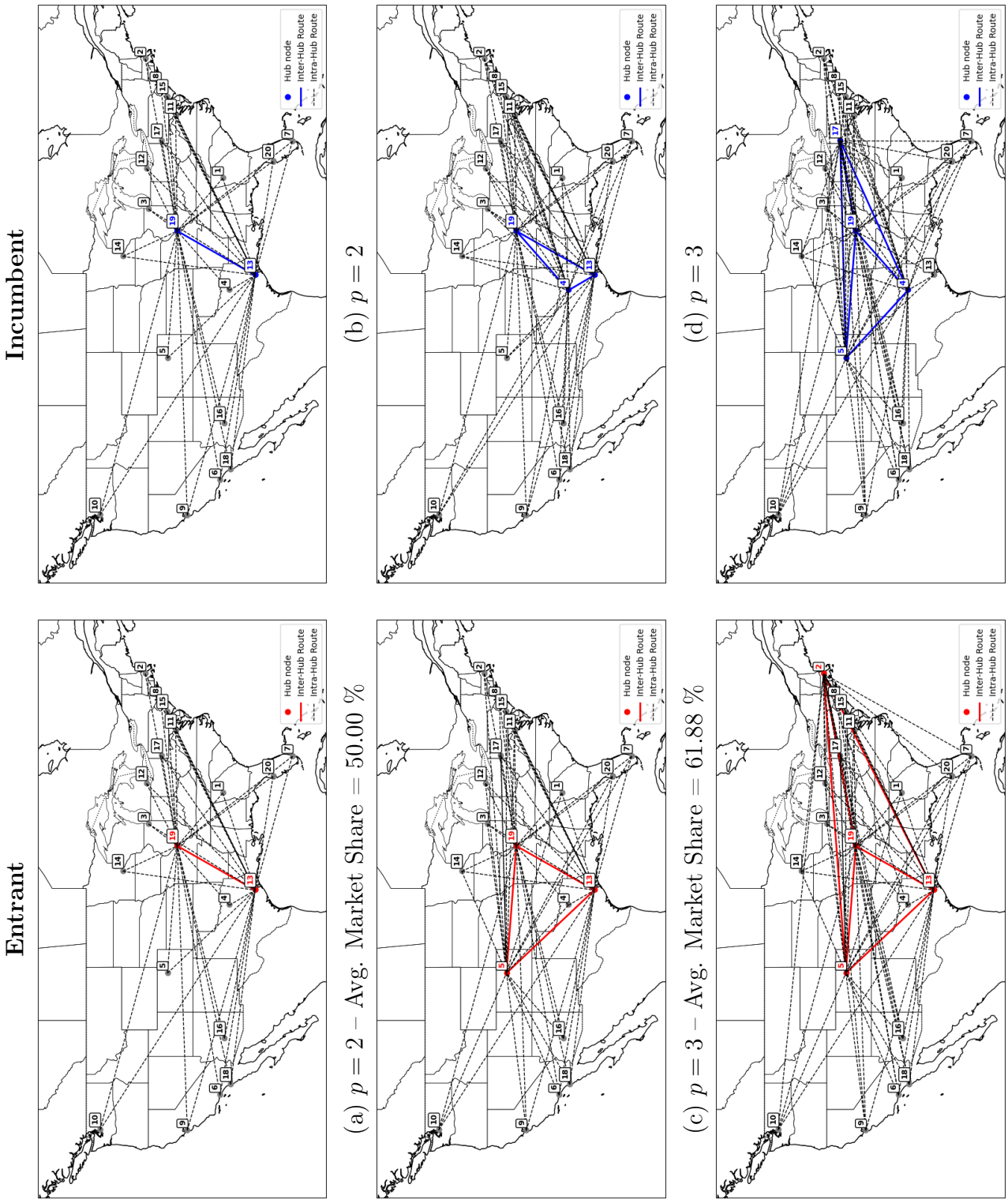

(a) $p = 2$ – Avg. Market Share = 50.00 %
(b) $p = 2$
(c) $p = 3$ – Avg. Market Share = 61.88 %
(d) $p = 3$
(e) $p = 4$ – Avg. Market Share = 71.05 %
(f) $p = 4$

Figure 5.12: Visualization of the network configurations obtained for $n = 20$, comparing the solutions of the entrant (left) and incumbent (right) companies across different number of hubs (p).

analyses for networks with 30- and 40- nodes confirmed the same behavioral patterns and are provided in Appendix E for completeness.

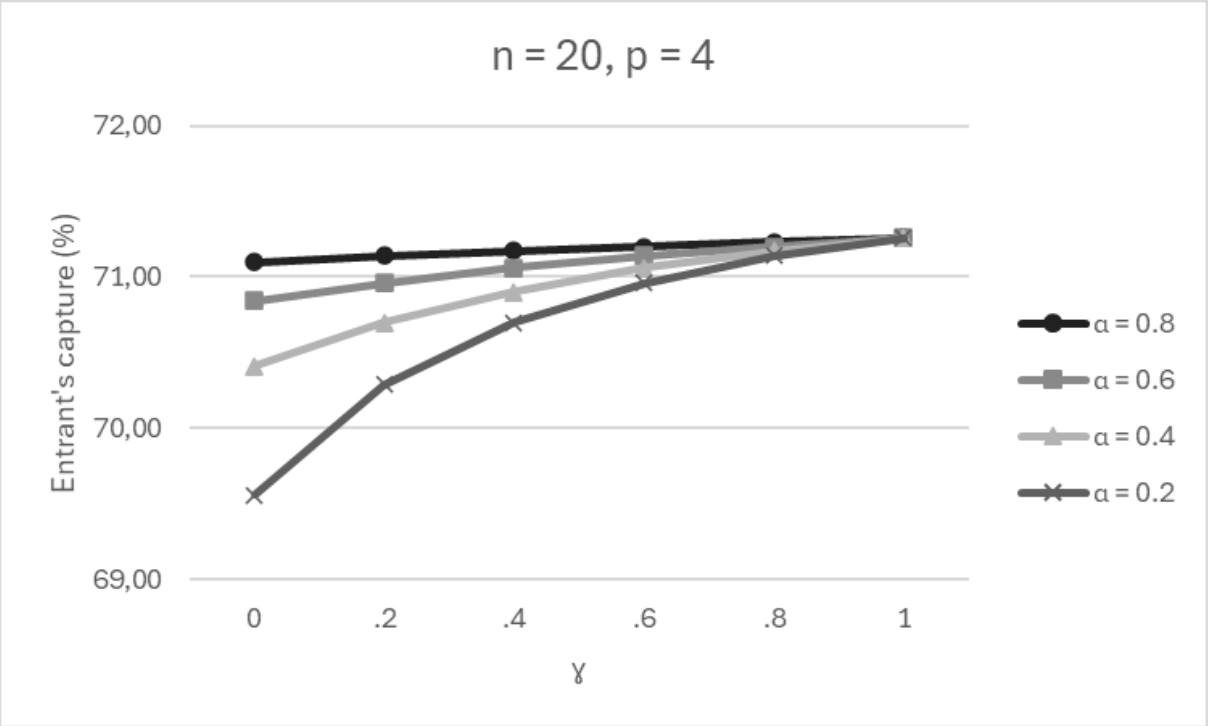

Figure 5.13: Effects of parameter variation on market share gain by an entrant in a 20-node network with 4 hubs and random competitor's hub location.

The monotonic increase in market share with rising γ indicates that the entrant airline benefits from higher passenger sensitivity to access and egress distances between hubs and origin/destination nodes, as its hubs are more spatially dispersed than those of the incumbent. Since the incumbent maintains a more concentrated hub configuration, resulting in longer access/egress distances but shorter inter-hub connections, when $\gamma = 0$, the passenger's perceived utility of paths is dominated by the discounted component and therefore by the cheap hub–hub corridors. In this regime, smaller α values amplify the attractiveness of the incumbent's short hub–hub links, reducing the entrant's market share.

In the extreme case where $\gamma = 1$, the discount on inter-hub segments becomes irrelevant to passengers, and all functions converge to the maximum achievable market share for the entrant. This result contrasts with that reported by Eiselt and Marianov (2009), who incorporated fixed waiting times at hubs in their model, penalizing time-sensitive passengers, whereas in our formulation only travel distances are considered. Nevertheless, our findings are consistent with their general conclusion that large inter-hub discounts combined with passengers who are less sensitive to immaterial costs (time, or distance) do not necessarily benefit the entrant.

Therefore, we conclude that for passengers, economies of scale are less relevant than the topological quality of the network itself. In other words, strategically positioning hubs

to minimize travel distances provides greater competitive advantage than merely reducing the monetary cost of travel. From a practical perspective, this insight suggests that in markets where total travel distance and network accessibility are perceptible to passengers, strategic hub placement can outperform cost-based strategies, reinforcing the managerial relevance of spatial optimization in competitive network design.

Finally, it is important to emphasize that the interpretation of the parameters α and γ must be aligned with the specific characteristics of the target market. A realistic calibration of these parameters is essential for accurately representing passenger behavior, as we can expect that leisure or younger travelers tend to be more price-sensitive, while business or older travelers generally value shorter total travel times and fewer connections. Therefore, understanding the predominant passenger profile in a given market allows the model to better reflect competitive dynamics and to provide more reliable managerial insights for network planning.

The insights gained from both the computational performance and the behavioral analysis highlight how advanced optimization models can inform strategic decisions in competitive network design. The next chapter consolidates these findings, outlining the main contributions, managerial implications, and directions for future research.

Chapter 6

Conclusions and Directions for Future Research

This work addressed the Competitive Multiple Allocation p-Hub Location Problem, with a specific application to the air transportation industry, in which a new airline seeks to enter an already consolidated market. In such a context, the strategic design of hub-and-spoke networks becomes a key determinant for the acquisition of market share. To capture passenger choice behavior, a probabilistic model based on a gravity-type utility function was adopted to represent the attractiveness of alternative paths between origins and destinations. This approach allows modeling the competitive dynamics between incumbent and entrant carriers, simultaneously accounting for spatial and accessibility factors within the network.

To date, the literature has approached competitive hub location problems primarily from the perspective of market share maximization (Marianov et al., 1999; Eiselt and Marianov, 2009; Tiwari et al., 2021a). The main contribution of this research lies in proposing novel mathematical formulations and exact solution strategies that enhance both computational efficiency and interpretative understanding of competitive hub networks. To the best of our knowledge, this is the first study to reformulate the problem from the perspective of minimizing market share loss, which proved to be a more stable and computationally superior alternative. Furthermore, an improved minimization formulation was proposed, introducing aggregated connectivity constraints, setting a new benchmark in efficiency for the competitive MPMAPHLP. This reformulation streamlined the model's structure and significantly enhanced its numerical performance, yielding substantial reductions in both processing time and branch-and-bound nodes explored.

The original formulations are characterized as Mixed-Integer Nonlinear Programming (MINLP), type Linear Fractional Programming (LFP) models, and computationally intractable for off-the-shelf solvers. They were reformulated as Mixed-Integer Second-Order Cone Programs (MISOCP) and solved exactly using a commercial solver capable of exploiting the problem's structural properties. A series of computational experiments were conducted on the well-known CAB benchmark dataset. The main results are:

- A direct reformulation of the maximization model into an equivalent minimization

version accelerated computational processing time by up to 113 times on average;

- The new proposed formulation demonstrated even better results, accelerating processing time by up to 1081 times on average when compared to the maximization model and by up to 597 times on average when compared to our initial minimization model;
- Our new model solves instances of up to 60 nodes in minutes, while the maximization model fails to solve instances of 40 nodes.

After validating the conic formulations, three alternative exact formulations based on the Outer Approximation (OA) technique were developed to further improve scalability and strengthen solution robustness for larger instances. The results showed evidence that:

- Computational results provide no evidence that it is advantageous to apply outer approximation cuts to the original conic minimization formulation;
- The new model solved using the simple conic formulation performed better than any external approximation cut made to the original minimization model;
- The models that showed the best performance were the OA-rvar, followed by the OA-Obj, and the uncut conic model, all applied to the new minimization formulation.

The findings of this research lead to a clear managerial insight: for passengers, economies of scale are less relevant than the topological quality of the network itself. In other words, strategically positioning hubs to minimize overall travel distances provides a stronger competitive advantage than merely reducing the monetary cost of inter-hub connections. In practical terms, this indicates that in markets where total travel distance and network accessibility are perceptible to passengers, well-designed spatial configurations can outperform purely cost-oriented strategies, reinforcing the importance of spatial optimization in competitive network design.

It is also important to emphasize that the interpretation of the parameters α and γ must be consistent with the specific characteristics of the market under study. Realistic calibration of these parameters is essential to accurately represent passenger behavior. Therefore, understanding the predominant passenger profile within a given market allows the model to better capture competitive dynamics and to generate more reliable managerial insights for strategic network planning.

6.1 Directions for Future Research

Building on the findings and methodological advances achieved in this research, several promising directions for future work are worth exploring. These opportunities can be

grouped into three complementary perspectives: methodological, behavioral, and empirical.

From a methodological perspective, future studies should further investigate the potential of the OA-Obj formulation by incorporating initial cuts, as this model already demonstrated strong performance in solving large-scale instances even without warm-start strategies. Implementing structured initial cuts could further enhance its convergence behavior and numerical stability. It also would be an improvement the use of cut-strengthening mechanisms, particularly strategies that control the direction and informativeness of the outer-approximation cuts. Another promising direction is the development of hybrid solution strategies, particularly the integration of the Outer Approximation and Benders Decomposition methods (De Camargo et al., 2011; O'Kelly et al., 2015). Such hybrid frameworks could substantially improve scalability and enable the efficient resolution of even larger and more complex competitive hub location instances.

From a behavioral standpoint, future research could explore alternative passenger choice modeling approaches, moving beyond the traditional gravity-based utility function. Incorporating discrete choice models, such as logit models, would allow for a more realistic representation of heterogeneous passenger preferences behaviors. Moreover, new formulations of economies-of-scale could be developed, replacing fixed hub-to-hub discounts with technology-dependent cost structures, such as the relationship between aircraft size and flow. Additionally, incorporating stochastic demand effects, including seasonality and uncertainty, would enable the design of stochastic optimization variants of the competitive MPMAPHLP, producing solutions that remain effective under fluctuating market conditions.

Finally, from an applied and empirical perspective, future work could extend the proposed framework to include competitive pricing strategies, environmental and sustainability criteria, and validation using real-world data. Integrating operational costs, and observed air traffic patterns would enhance the practical applicability of the models and strengthen their managerial relevance for the strategic planning of competitive transportation networks. Another promising direction involves reformulating the competitive MPMAPHLP to allow direct flights between origins and destinations without mandatory connection through hubs. This extension would require a revised network structure and cost formulation, enabling a flexible trade-off between hub-based and point-to-point operations, and potentially revealing new equilibrium patterns in competitive settings.

References

Ahn, W. C. (2023). Study on improvement in logistics industry in gangwon province: Focusing on yangyang international airport. *The Asian Journal of Shipping and Logistics*, 39(1):23–29.

Akturk, S., Atamturk, A., and Gürel, S. (2014). Aircraft rescheduling with cruise speed control. *Operations Research*, 62:829–845.

Alumur, S. and Kara, B. Y. (2008). Network hub location problems: The state of the art. *European journal of operational research*, 190(1):1–21.

Alumur, S. A. (2019). Hub location and related models. *Contributions to Location Analysis: In Honor of Zvi Drezner's 75th Birthday*, pages 237–252.

Alumur, S. A., Campbell, J. F., Contreras, I., Kara, B. Y., Marianov, V., and O'Kelly, M. E. (2021). Perspectives on modeling hub location problems. *European Journal of Operational Research*, 291(1):1–17.

Atamtürk, A., Berenguer, G., and Shen, Z.-J. (2012). A conic integer programming approach to stochastic joint location-inventory problems. *Operations Research*, 60(2):366–381.

Basallo-Triana, M. J., Vidal-Holguín, C. J., and Bravo-Bastidas, J. J. (2021). Planning and design of intermodal hub networks: A literature review. *Computers & Operations Research*, 136:105469.

Basso, L. J. and Jara-Díaz, S. R. (2006a). Are returns to scale with variable network size adequate for transport industry structure analysis? *Transportation Science*, 40(3):259–268.

Basso, L. J. and Jara-Díaz, S. R. (2006b). Distinguishing multiproduct economies of scale from economies of density on a fixed-size transport network. *Networks and Spatial Economics*, 6:149–162.

Ben-Akiva, M., McFadden, D., Abe, M., Bockenholt, U., Bolduc, D., Gopinath, D., Morikawa, T., Ramaswamy, V., Rao, V., Revelt, D., and Steinberg, D. (1997). Modeling methods for discrete choice analysis. *Marketing Letters*, 8(3):273–286.

Ben-Tal, A. and Nemirovski, A. (2001). *Lectures on modern convex optimization: analysis, algorithms, and engineering applications*. SIAM.

Benson, H. Y. and Ümit Sağlam (2014). *Mixed-Integer Second-Order Cone Programming: A Survey*, chapter Chapter 2, pages 13–36. Informs.

Bryan, D. (1998). Extensions to the hub location problem: Formulations and numerical examples. *Geographical Analysis*, 30(4):315–330.

Campbell, J. F. (2013). Modeling economies of scale in transportation hub networks. In *2013 46th Hawaii International Conference on System Sciences*, pages 1154–1163. IEEE.

Campbell, J. F., Ernst, A. T., and Krishnamoorthy, M. (2002). Hub location problems. *Handbook of transportation science*, pages 373–408.

Campbell, J. F. and O'Kelly, M. E. (2012). Twenty-five years of hub location research. *Transportation Science*, 46(2):153–169.

Contreras, I. and O'Kelly, M. (2019). Hub location problems. *Location science*, pages 327–363.

de Araújo, A. C. A., Roboredo, M. C., Pessoa, A. A., and Pereira, V. (2020). Exact methods for the discrete multiple allocation (r|p) hub-centroid problem. *Computers and Operations Research*, 116.

De Camargo, R. S., de Miranda Jr, G., and Ferreira, R. P. (2011). A hybrid outer-approximation/benders decomposition algorithm for the single allocation hub location problem under congestion. *Operations Research Letters*, 39(5):329–337.

De Camargo, R. S., de Miranda Jr, G., and Luna, H. P. L. (2009). Benders decomposition for hub location problems with economies of scale. *Transportation Science*, 43(1):86–97.

Dolan, E. D. and Moré, J. J. (2002). Benchmarking optimization software with performance profiles. *Mathematical programming*, 91:201–213.

Drezner, T. and Drezner, Z. (2001). A note on applying the gravity rule to the airline hub problem. *Journal of Regional Science*, 41(1):67–72.

Drezner, Z. and Eiselt, H. (2024). Competitive location models: A review. *European Journal of Operational Research*, 316(1):5–18.

Duran, M. A. and Grossmann, I. E. (1986). An outer-approximation algorithm for a class of mixed-integer nonlinear programs. *Mathematical programming*, 36:307–339.

Eiselt, H. A., Laporte, G., and Thisse, J.-F. (1993). Competitive location models: A framework and bibliography. *Transportation science*, 27(1):44–54.

Eiselt, H. A. and Marianov, V. (2009). A conditional p-hub location problem with attraction functions. *Computers & Operations Research*, 36(12):3128–3135.

Eiselt, H. A., Marianov, V., and Drezner, T. (2019). *Competitive location models*. Springer.

Elhedhli, S. (2005). Exact solution of a class of nonlinear knapsack problems. *Operations research letters*, 33(6):615–624.

Farahani, R. Z., Hekmatfar, M., Arabani, A. B., and Nikbakhsh, E. (2013). Hub location problems: A review of models, classification, solution techniques, and applications. *Computers & industrial engineering*, 64(4):1096–1109.

Farham, M. S., Rostami, B., and Haughton, M. (2023). Vehicle utilization in hub network design: Exploiting economies of scale in transportation. *arXiv preprint arXiv:2301.04207*.

Floudas, C. A. (1995). *Nonlinear and mixed-integer optimization: fundamentals and applications*. Oxford University Press.

Grossmann, I. E. and Kravanja, Z. (1995). Mixed-integer nonlinear programming techniques for process systems engineering. *Computers & Chemical Engineering*, 19:189–204.

Hotelling, H. (1929). Stability in competition, kecon. *The Economic Journal*, Vol. 39, No. 153:41–57.

Huff, D. L. (1964). Defining and estimating a trading area. *Journal of marketing*, 28(3):34–38.

Huff, D. L. (1966). A Programmed Solution for Approximating an Optimum Retail Location. *Land Economics*, 42(3):293–303.

Jara-Díaz, S. R., Cortés, C. E., and Morales, G. A. (2013). Explaining changes and trends in the airline industry: Economies of density, multiproduct scale, and spatial scope. *Transportation Research Part E: Logistics and Transportation Review*, 60:13–26.

Kelley, Jr, J. E. (1960). The cutting-plane method for solving convex programs. *Journal of the society for Industrial and Applied Mathematics*, 8(4):703–712.

Kimms, A. (2006). Economies of scale in hub & spoke network design models: We have it all wrong. *Perspectives on operations research: essays in honor of Klaus Neumann*, pages 293–317.

Laporte, G., Nickel, S., and Saldanha-da Gama, F. (2019). *Location Science*, volume 2nd Edition. Springer.

Mahmoodjanloo, M., Tavakkoli-Moghaddam, R., Baboli, A., and Jamiri, A. (2020). A multi-modal competitive hub location pricing problem with customer loyalty and elastic demand. *Computers and Operations Research*, 123.

Marianov, V., Serra, D., and ReVelle, C. (1999). Location of hubs in a competitive environment. *European journal of operational research*, 114(2):363–371.

O'kelly, M. E. (1986). The location of interacting hub facilities. *Transportation science*, 20(2):92–106.

O'Kelly, M. E. and Bryan, D. (1998). Hub location with flow economies of scale. *Transportation research part B: Methodological*, 32(8):605–616.

O'Kelly, M. E., Luna, H. P. L., de Camargo, R. S., and de Miranda Jr, G. (2015). Hub location problems with price sensitive demands. *Networks and Spatial Economics*, 15(4):917–945.

Real, L. B., Contreras, I., Cordeau, J.-F., de Camargo, R. S., and de Miranda, G. (2021). Multimodal hub network design with flexible routes. *Transportation Research Part E: Logistics and Transportation Review*, 146:102188.

ReVelle, C. S. and Eiselt, H. A. (2005). Location analysis: A synthesis and survey. *European journal of operational research*, 165(1):1–19.

Ricard, L. and Bierlaire, M. (2025). 50 years of behavioral models for transportation and logistics. *EURO Journal on Transportation and Logistics*, page 100156.

Sharma, A., Jakhar, S. K., Vlachos, I., and Kumar, S. (2025). Advances in hub location problems: a literature review and research agenda. *International Journal of Productivity and Performance Management*, 74(1):24–55.

Sharma, A., Kohar, A., Jakhar, S. K., et al. (2021). Profit maximizing hub location problem in the airline industry under coopetition. *Computers & Industrial Engineering*, 160:107563.

Tiwari, R., Jayaswal, S., and Sinha, A. (2021a). Alternate solution approaches for competitive hub location problems. *European Journal of Operational Research*, 290:68–80.

Tiwari, R., Jayaswal, S., and Sinha, A. (2021b). Competitive hub location problem: Model and solution approaches. *Transportation Research Part B: Methodological*, 146:237–261.

Von Stackelberg, H. (1951). *Grundlagen der theoretischen Volkswirtschaftslehre*. Mohr Siebeck.

Walley, K. (2007). Coopetition: An introduction to the subject and an agenda for research. *International Studies of Management & Organization*, 37(2):11–31. Accessed 7 January 2019.

Wandelt, S., Dai, W., Zhang, J., and Sun, X. (2022). Toward a reference experimental benchmark for solving hub location problems. *Transportation Science*, 56(2):543–564.

Wang, S., Kong, N. N., and Gao, Y. (2024). Use mobile location data to infer airport catchment areas and calibrate huff gravity model in the new york metropolitan area. *Journal of Transport Geography*, 114:103790.

Appendix A

Generating an *a priori* set of OA cuts for the conic model

To initialize the solution process of the OA-rvar and COACuts algorithms, a finite set of pre-generated outer-approximation (OA) cuts is constructed for the nonlinear function $f(r) = \frac{1}{r}$. This procedure, adapted from Elhedhli (2005), aims to provide a piecewise linear approximation $\hat{f}(r)$ that bounds the nonlinear function within a small and uniform error tolerance $\varepsilon > 0$:

$$0 \leq f(r) - \hat{f}(r) \leq \varepsilon, \qquad \forall r > 1.$$

The domain of r is discretized into a finite sequence of breakpoints

$$R_1, R_2, \ldots, R_{n(\varepsilon)},$$

and associated tangent points

$$r_1, r_2, \ldots, r_{n(\varepsilon)},$$

such that

$$R_{h-1} \leq r_h \leq R_h, \qquad \forall h \in \mathcal{H}_0.$$

At each tangent point r_h, a linearization (OA cut) is generated using the first derivative of $f(r)$:

$$f'(r_h) = -\frac{1}{r_h^2}.$$

The recursive construction of these initial OA cuts (Figure A.1) ensures that the piecewise linear function $\hat{f}(r)$ maintains a maximum deviation of ε from $f(r)$ across the entire interval of interest. The condition

$$f(R_1) = \hat{f}(R_1) + \varepsilon$$

defines the next breakpoint R_1, such that the linearization tangent at r_1 and the nonlinear curve intersect within the prescribed error tolerance.

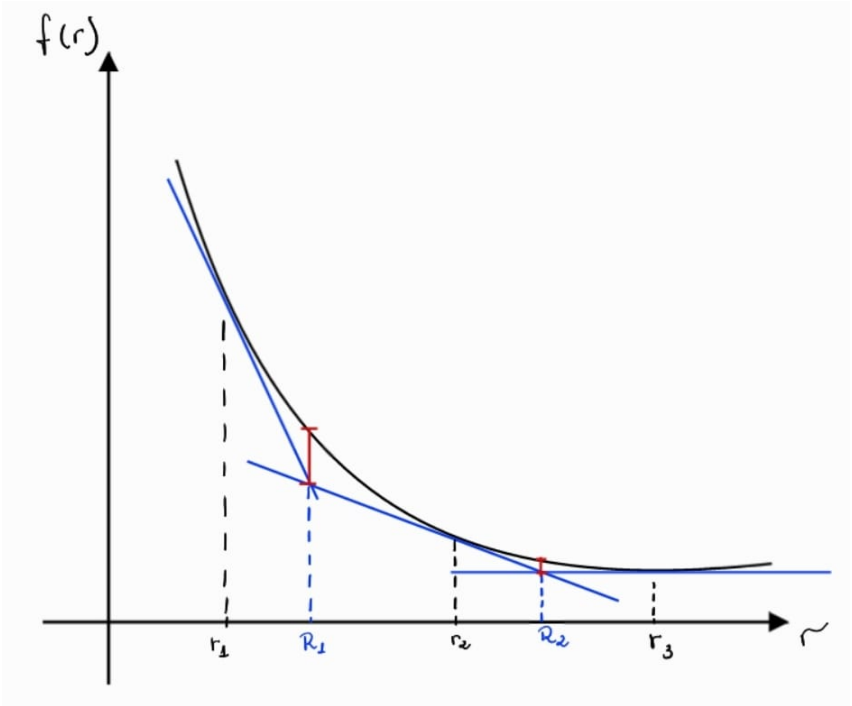

Figure A.1: Recursive construction of OA cuts for the function $f(r) = \frac{1}{r}$.

Developing the linearization of $f(r)$ at r_1 and evaluating it at R_1, we obtain:

$$\hat{f}(R_1) = \frac{1}{r_1} - \frac{1}{r_1^2}(R_1 - r_1).$$

Substituting this into the approximation condition $f(R_1) - \hat{f}(R_1) = \varepsilon$ gives:

$$\frac{1}{R_1} - \left(\frac{1}{r_1} - \frac{1}{r_1^2}(R_1 - r_1)\right) = \varepsilon,$$

which simplifies to:

$$\frac{1}{R_1} + \left(\frac{R_1}{r_1^2} - \frac{2}{r_1}\right) = \varepsilon.$$

Rearranging terms yields a quadratic equation in R_1:

$$\frac{1}{r_1^2}R_1^2 - \left(\frac{2}{r_1} + \varepsilon\right)R_1 + 1 = 0.$$

Through the Bhaskara formula, the root R_1 is given by the positive solution:

$$R_1 = \frac{\left(\frac{2}{r_1} + \varepsilon\right) + \sqrt{\left(\frac{2}{r_1} + \varepsilon\right)^2 - 4\frac{1}{r_1^2}}}{\frac{2}{r_1^2}} \tag{A.1}$$

It is important to note that $R_1, r_1 \geq 1$ during the procedure to ensure the validity of the function domain.

The subsequent tangent point r_2 is computed from the intersection between the linearization at R_1 and the curve $f(r)$. Starting from the linearization

$$\bar{y} = \hat{f}(R_1) = f(r_2) + f'(r_2)(R_1 - r_2),$$

we have:

$$\bar{y} = \frac{1}{r_2} - \frac{1}{r_2^2}(R_1 - r_2),$$

which expands to:

$$\bar{y} = \frac{2}{r_2} - \frac{R_1}{r_2^2}.$$

Multiplying by r_2^2 to eliminate fractions and rearranging terms gives:

$$\bar{y}\, r_2^2 - 2r_2 + R_1 = 0,$$

whose positive root determines the next tangent point:

$$r_2 = \frac{2 + \sqrt{4 - 4\bar{y}R_1}}{2\bar{y}}. \tag{A.2}$$

The recursive process begins with the first tangent point r_1, typically defined at the lower bound of the domain ($r_1 = 1$), which represents the initial point where the function $f(r) = 1/r$ is linearized. From this tangent, the first breakpoint R_1 is computed by solving Equation A.1, ensuring that the deviation between $f(r)$ and its linear approximation does not exceed the prescribed tolerance ε. Next, using Equation A.2, the subsequent tangent point r_2 is determined based on the intersection between the linearization at R_1 and the nonlinear function.

The procedure is then repeated iteratively, alternating between the computation of each breakpoint R_h and its corresponding tangent point r_{h+1}. Specifically, for a given tangent point r_h, the next breakpoint R_h is obtained by solving Equation A.1, and the subsequent tangent point r_{h+1} is then computed using Equation A.2.

This recursive process continues until the domain of interest is fully covered or the approximation error ε is satisfied for all segments. The resulting set of tangent points $\{r_h\}_{h\in\mathcal{H}_0}$ defines the initial OA cuts incorporated into the conic formulations of the OA-rvar and COACuts algorithms.

Appendix B

Detailed Results of Conic Models

Table B.1: Detailed computational results of the conic formulations by α, reporting CPU time (s) and optimality gaps (%) on instances of sizes $n = \{10, 15, 20, 25, 30, 40\}$.

n	p	α	Market Share (%)	Conic formulations		
				MAXMPMAPHLP cpu (gap %)	MINMPMAPHLP cpu (gap %)	NEW MINMPMAPHLP cpu (gap %)
	2	0.1	66.01	1.21	0.23	**0.20**
	2	0.2	66.10	1.16	0.15	**0.11**
	2	0.3	66.18	1.32	0.27	**0.13**
	2	0.4	66.25	0.93	**0.24**	0.37
	2	0.5	66.31	1.44	0.24	**0.12**
	2	0.6	66.36	1.17	0.17	**0.12**
	2	0.7	66.41	0.95	0.16	**0.11**
	2	0.8	66.45	1.62	0.17	**0.11**
	2	0.9	66.49	1.19	0.17	**0.11**
	2	1.0	66.52	1.06	0.23	**0.12**
			averages	1.21	0.20	0.15
	3	0.1	60.70	1.72	0.16	**0.10**
	3	0.2	60.74	2.20	0.20	**0.11**
	3	0.3	60.79	1.47	0.15	**0.11**
	3	0.4	60.82	1.10	0.21	**0.12**
10	3	0.5	60.85	4.00	0.21	**0.11**
	3	0.6	60.88	1.43	0.15	**0.13**
	3	0.7	60.91	1.53	0.24	**0.11**
	3	0.8	60.93	1.87	0.26	**0.12**
	3	0.9	60.95	1.88	0.23	**0.12**
	3	1.0	60.96	3.90	0.19	**0.12**
			averages	2.11	0.20	0.12
	4	0.1	64.70	2.80	0.20	**0.07**
	4	0.2	64.87	18.97	0.16	**0.08**
	4	0.3	65.03	3.02	0.14	**0.05**
	4	0.4	65.17	3.24	0.15	**0.05**
	4	0.5	65.29	8.26	0.28	**0.07**
	4	0.6	65.41	5.62	0.17	**0.04**
	4	0.7	65.51	2.32	0.17	**0.05**
	4	0.8	65.61	13.88	0.17	**0.10**
	4	0.9	65.69	1.58	0.13	**0.09**
	4	1.0	65.77	3.99	0.18	**0.08**
			averages	6.37	0.18	0.07
	2	0.1	50.00	13.36	1.30	**0.16**
	2	0.2	50.00	11.80	1.11	**0.16**
	2	0.3	50.00	10.12	1.49	**0.17**
	2	0.4	50.00	9.73	1.16	**0.16**
	2	0.5	50.00	28.20	1.50	**0.93**
	2	0.6	50.00	11.46	1.69	**0.17**
	2	0.7	50.00	11.47	1.30	**0.18**
	2	0.8	50.00	12.42	1.69	**0.56**
	2	0.9	50.00	25.63	1.34	**0.77**
	2	1.0	50.00	11.74	1.60	**0.72**
			averages	14.59	1.42	0.40
	3	0.1	60.77	15.00	1.26	**0.23**
	3	0.2	60.82	14.38	1.43	**1.07**
	3	0.3	60.85	14.46	1.64	**0.26**
	3	0.4	60.89	15.25	1.38	**0.24**
15	3	0.5	60.92	12.66	1.19	**0.25**
	3	0.6	60.94	58.07	1.38	**0.22**
	3	0.7	60.96	14.89	1.11	**0.25**
	3	0.8	60.98	21.38	1.43	**0.25**
	3	0.9	61.00	9.99	1.45	**0.79**
	3	1.0	61.02	20.04	1.11	**0.25**
			averages	19.61	1.34	0.38
	4	0.1	63.23	28.27	1.72	**1.50 (0.01)**
	4	0.2	63.37	20.06	1.59	**1.04**
	4	0.3	63.50	19.54	1.67	**0.62**
	4	0.4	63.61	19.94	1.17	**0.22**
	4	0.5	63.72	15.92	1.43	**0.23**

	4	0.6	63.82	58.01	1.47	**0.23**
	4	0.7	63.91	57.90	1.97	**0.25**
	4	0.8	64.00	20.22	1.44	**0.32**
	4	0.9	64.08	16.08	1.55	**0.76**
	4	1.0	64.15	18.32	1.30	**0.24**
			averages	27.43	1.53	0.54
	2	0.1	50.00	80.48	5.12	**0.48**
	2	0.2	50.00	78.37	6.72	**0.62**
	2	0.3	50.00	89.48	5.40	**0.53**
	2	0.4	50.00	156.09	4.17	**0.51**
	2	0.5	50.00	81.65	3.94	**0.48**
	2	0.6	50.00	77.56	6.19	**0.44**
	2	0.7	50.00	86.18	5.33	**0.47**
	2	0.8	50.00	76.31	6.08	**0.44**
	2	0.9	50.00	70.77	4.97	**0.50**
	2	1.0	50.00	69.51	6.15	**0.50**
			averages	86.64	5.41	0.50
	3	0.1	61.84	779.87	6.70	**3.89**
	3	0.2	61.85	301.14	6.95	**3.40**
	3	0.3	61.87	107.15	6.47	**2.08**
	3	0.4	61.88	116.63	5.42	**2.29**
20	3	0.5	61.89	97.49	7.70	**2.09**
	3	0.6	61.89	101.62	12.86	**0.50**
	3	0.7	61.89	98.19	11.44	**2.22**
	3	0.8	61.90	170.26	6.76	**2.09**
	3	0.9	61.90	211.28	5.96	**0.51**
	3	1.0	61.90	542.30	6.86	**0.71**
			averages	252.59	7.71	1.98
	4	0.1	70.76	701.29	8.78	**0.60**
	4	0.2	70.84	130.29	9.21	**0.61**
	4	0.3	70.92	791.75	8.56	**0.77**
	4	0.4	70.99	629.55	7.89	**0.57**
	4	0.5	71.04	1928.29	8.35	**1.76 (0.01)**
	4	0.6	71.10	587.43	10.21	**1.85**
	4	0.7	71.14	289.61	7.27	**2.02**
	4	0.8	71.19	593.98	6.43	**0.70**
	4	0.9	71.22	353.99	9.40	**0.67**
	4	1.0	71.26	3095.10	7.60	**0.71**
			averages	910.13	8.37	1.03
	2	0.1	50.00	545.88	22.17	**9.73**
	2	0.2	50.00	536.47	21.11	**1.12**
	2	0.3	50.00	453.64	20.50	**1.23**
	2	0.4	50.00	487.65	21.39	**1.29**
	2	0.5	50.00	512.03	21.27	**1.32**
	2	0.6	50.00	533.96	22.14	**1.36**
	2	0.7	50.00	541.49	18.79	**1.22**
	2	0.8	50.00	506.87	17.95	**1.20**
	2	0.9	50.00	611.17	20.05	**1.21**
	2	1.0	50.00	632.75	18.43	**1.15**
			averages	536.19	20.38	2.08
	3	0.1	64.88	1084.14	31.94	**1.31**
	3	0.2	64.91	1054.59	36.58	**1.22**
	3	0.3	64.93	755.35	32.82 (0.01)	**1.23**
	3	0.4	64.94	1178.34	37.67	**1.27**
25	3	0.5	64.96	985.82	33.33	**1.36**
	3	0.6	64.97	1179.65	38.53	**1.30**
	3	0.7	64.97	962.30	33.80	**1.30**
	3	0.8	64.98	1848.15	24.90	**1.34**
	3	0.9	64.99	1136.87	24.28	**1.31**
	3	1.0	64.99	1039.38	34.45	**1.33**
			averages	1122.46	32.83	1.30
	4	0.1	71.69	3944.40	51.93	**2.89**
	4	0.2	71.73	2177.03 (0.01)	46.58	**2.74**
	4	0.3	71.76	7045.85	52.61	**3.08**
	4	0.4	71.78	4425.40	43.52	**3.07**
	4	0.5	71.80	3558.05	55.00	**14.65**
	4	0.6	71.82	9327.59 (0.01)	46.50	**8.61**
	4	0.7	71.83	3383.84	51.72	**2.99**

	4	0.8	71.84	3243.43	42.85	**2.82**
	4	0.9	71.85	3306.63	45.72	**14.55**
	4	1.0	71.87	3737.64	38.09	**13.45**
			averages	4414.99	47.45	6.89
	4	0.1	63.41	3591.06 (36.56)	703.73	**5.28**
	4	0.2	63.60	3594.69 (37.12)	655.74	**5.32**
	4	0.3	63.78	3594.28 (37.55)	657.54	**4.06**
	4	0.4	63.95	3593.80 (33.99)	635.84	**5.74**
	4	0.5	64.10	3594.25 (32.63)	669.16	**4.58**
	4	0.6	64.25	3594.41 (37.53)	610.03	**6.12**
	4	0.7	64.40	3592.98 (38.43)	488.48	**4.59**
	4	0.8	64.53	3592.80 (38.00)	581.22	**6.64**
	4	0.9	64.66	3594.48 (32.05)	598.38 (0.01)	**5.25**
	4	1.0	64.78	3592.48 (36.76)	646.75	**10.56**
			averages	3593.52 (36.06)	624.69	5.81
	5	0.1	57.46	3594.47 (45.69)	1424.37 (0.01)	**2.54**
	5	0.2	57.56	3592.65 (40.52)	1364.51 (0.01)	**2.44**
	5	0.3	57.66	3601.83 (52.20)	1123.48 (0.01)	**2.28**
	5	0.4	57.75	3594.64 (42.92)	1055.58 (0.01)	**2.23**
30	5	0.5	57.84	3592.14 (47.31)	967.40 (0.01)	**1.95**
	5	0.6	57.92	3595.14 (30.31)	1115.47 (0.01)	**2.15**
	5	0.7	58.00	3594.12 (51.45)	915.76 (0.01)	**2.58**
	5	0.8	58.08	3595.41 (42.94)	833.14	**2.11 (0.01)**
	5	0.9	58.15	3594.29 (40.43)	645.93	**2.20 (0.01)**
	5	1.0	58.22	3602.49 (49.82)	714.05	**2.66**
			averages	3595.72 (44.36)	1015.97 (0.01)	2.31
	6	0.1	64.15	3596.47 (32.59)	1680.56	**4.77**
	6	0.2	64.44	3594.65 (28.10)	2037.58 (0.01)	**4.00**
	6	0.3	64.71	3599.89 (33.86)	1474.13	**2.43**
	6	0.4	64.97	3593.15 (30.29)	1732.33 (0.01)	**2.37**
	6	0.5	65.21	3595.18 (34.64)	1313.87	**2.28**
	6	0.6	65.43	3592.90 (27.12)	1741.71 (0.01)	**2.10**
	6	0.7	65.65	3592.64 (28.07)	1215.02	**2.41**
	6	0.8	65.85	3594.17 (28.82)	1675.00 (0.01)	**2.06**
	6	0.9	66.04	3593.02 (27.92)	1083.26	**2.03**
	6	1.0	66.23	3594.36 (24.80)	1069.06 (0.01)	**2.08**
			averages	3594.64 (29.62)	1502.25 (0.01)	2.65
	4	0.1	63.27	3591.95 (79.89)	3596.49 (55.01)	**33.09**
	4	0.2	63.47	3591.46 (67.49)	3597.60 (51.93)	**39.99**
	4	0.3	63.65	3591.36 (79.63)	3597.61 (52.05)	**60.92**
	4	0.4	63.82	3592.20 (59.35)	3595.89 (50.25)	**38.14**
	4	0.5	63.99	3592.12 (58.26)	3597.69 (48.21)	**19.51 (0.01)**
	4	0.6	64.14	3592.40 (71.40)	3596.76 (48.89)	**37.03**
	4	0.7	64.29	3592.68 (77.79)	3596.99 (47.36)	**38.15**
	4	0.8	64.43	3591.60 (79.06)	3597.94 (48.19)	**40.61**
	4	0.9	64.56	3591.64 (76.01)	3597.36 (45.87)	**25.39**
	4	1.0	64.69	3592.20 (65.42)	3597.58 (47.32)	**38.55**
			averages	3591.96 (71.43)	3597.19 (49.51)	37.14
	5	0.1	64.86	-	3598.12 (51.05)	**19.30**
	5	0.2	65.02	-	3598.24 (49.48)	**25.04**
	5	0.3	65.18	-	3597.28 (47.85)	**28.14**
	5	0.4	65.32	-	3597.45 (48.91)	**19.20**
40	5	0.5	65.47	-	3597.84 (47.34)	**32.92**
	5	0.6	65.60	-	3597.55 (47.93)	**40.43**
	5	0.7	65.73	-	3597.72 (46.78)	**21.78**
	5	0.8	65.85	-	3597.16 (46.41)	**17.48**
	5	0.9	65.97	-	3597.73 (47.76)	**15.11**
	5	1.0	66.08	-	3597.83 (47.10)	**16.71**
			averages		3597.69 (48.06)	23.61
	6	0.1	65.27	-	3598.50 (44.70)	**14.11**
	6	0.2	65.49	-	3597.97 (44.22)	**24.07**
	6	0.3	65.70	-	3597.60 (44.64)	**18.78**
	6	0.4	65.90	-	3597.89 (44.50)	**16.30**

6	0.5	66.10	-	3597.95 (44.91)	**14.51**
6	0.6	66.28	-	3597.90 (44.58)	**17.72**
6	0.7	66.46	-	3597.72 (42.81)	**17.76**
6	0.8	66.63	-	3598.10 (43.95)	**15.22**
6	0.9	66.79	-	3597.49 (42.25)	**11.18**
6	1.0	66.94	-	3598.44 (41.46)	**17.72**
		averages		3597.96 (43.80)	16.74

[]

Table B.2: Detailed computational results of the conic formulations by α, reporting the number of branch-and-bound nodes explored for each (n, p) instance.

n	p	α	Branch-and-bound nodes		
			MAX	MIN	NEW MIN
	2	0.1	38	48	1
	2	0.2	38	42	2
	2	0.3	40	42	2
	2	0.4	34	38	2
	2	0.5	29	41	1
	2	0.6	32	38	1
	2	0.7	36	37	2
	2	0.8	33	32	1
	2	0.9	36	35	2
	2	1.0	35	41	1
		averages	35.10	39.40	1.50
	3	0.1	67	51	2
	3	0.2	68	59	2
	3	0.3	50	48	2
	3	0.4	54	49	2
10	3	0.5	54	49	2
	3	0.6	51	51	2
	3	0.7	49	45	2
	3	0.8	58	57	2
	3	0.9	37	40	2
	3	1.0	54	50	1
		averages	54.20	49.90	1.90
	4	0.1	41	54	0
	4	0.2	43	44	0
	4	0.3	53	39	0
	4	0.4	51	45	0
	4	0.5	73	56	0
	4	0.6	64	52	0
	4	0.7	44	41	0
	4	0.8	42	38	0
	4	0.9	29	45	0
	4	1.0	36	37	0
		averages	47.60	45.10	0.00
	2	0.1	89	70	0
	2	0.2	62	65	0
	2	0.3	71	67	0
	2	0.4	67	75	0
	2	0.5	67	73	0
	2	0.6	57	69	0
	2	0.7	59	68	0
	2	0.8	67	57	0
	2	0.9	65	59	0
	2	1.0	54	76	0
		averages	65.80	67.90	0.00
	3	0.1	135	115	0
	3	0.2	122	127	0
	3	0.3	129	124	0
	3	0.4	125	117	0

15	3	0.5	93	93	0
	3	0.6	130	97	0
	3	0.7	96	92	0
	3	0.8	122	98	0
	3	0.9	92	95	0
	3	1.0	109	92	0
		averages	115.30	105.00	0.00
	4	0.1	175	175	4
	4	0.2	169	149	1
	4	0.3	145	147	2
	4	0.4	113	109	0
	4	0.5	113	147	0
	4	0.6	154	105	0
	4	0.7	115	162	0
	4	0.8	116	135	0
	4	0.9	119	104	0
	4	1.0	116	100	0
		averages	133.50	133.30	0.70
	2	0.1	105	115	0
	2	0.2	109	134	0
	2	0.3	127	122	0
	2	0.4	112	97	0
	2	0.5	112	99	0
	2	0.6	96	98	0
	2	0.7	105	91	0
	2	0.8	114	114	0
	2	0.9	96	108	0
	2	1.0	83	104	0
		averages	105.90	108.20	0.00
	3	0.1	246	176	0
	3	0.2	176	221	0
	3	0.3	152	169	0
	3	0.4	192	152	0
20	3	0.5	126	152	0
	3	0.6	155	189	0
	3	0.7	168	162	0
	3	0.8	214	210	0
	3	0.9	167	185	0
	3	1.0	148	165	0
		averages	174.40	178.10	0.00
	4	0.1	235	279	0
	4	0.2	303	273	0
	4	0.3	227	272	0
	4	0.4	256	221	0
	4	0.5	243	276	0
	4	0.6	274	270	0
	4	0.7	204	192	0
	4	0.8	259	168	0
	4	0.9	171	213	0
	4	1.0	238	189	0
		averages	241.00	235.30	0.00
	2	0.1	206	204	0
	2	0.2	215	193	0
	2	0.3	187	192	0

	2	0.4	167	188	0
	2	0.5	197	191	0
	2	0.6	217	183	0
	2	0.7	213	182	0
	2	0.8	206	178	0
	2	0.9	210	221	0
	2	1.0	232	181	0
		averages	205.00	191.30	0.00
	3	0.1	561	494	0
	3	0.2	509	442	0
	3	0.3	367	426	0
	3	0.4	483	411	0
25	3	0.5	391	388	0
	3	0.6	421	402	0
	3	0.7	403	412	0
	3	0.8	505	300	0
	3	0.9	379	331	0
	3	1.0	465	380	0
		averages	448.40	398.60	0.00
	4	0.1	608	667	5
	4	0.2	777	646	1
	4	0.3	630	527	3
	4	0.4	597	625	1
	4	0.5	557	679	3
	4	0.6	616	536	5
	4	0.7	490	721	3
	4	0.8	492	495	3
	4	0.9	656	534	5
	4	1.0	550	484	5
		averages	597.30	591.40	3.40

	4	0.1		9717	1
	4	0.2		10211	1
	4	0.3		8901	1
	4	0.4		8022	1
	4	0.5		8354	1
	4	0.6		7728	2
	4	0.7		6951	1
	4	0.8		7152	3
	4	0.9		7568	1
	4	1.0		6741	3
		averages		8134.50	1.50
	5	0.1		15983	1
	5	0.2		16681	1
	5	0.3		13413	1
	5	0.4		12978	0
30	5	0.5		11645	0
	5	0.6		11467	0
	5	0.7		11375	1
	5	0.8		9044	0
	5	0.9		7944	0
	5	1.0		7759	1
		averages		11828.90	0.50
	6	0.1		21481	3
	6	0.2		23324	2
	6	0.3		18649	0

	6	0.4	17695	0
	6	0.5	16615	0
	6	0.6	18730	0
	6	0.7	14379	0
	6	0.8	17584	0
	6	0.9	11965	0
	6	1.0	11586	0
		averages	17200.80	0.50
	4	0.1		9
	4	0.2		4
	4	0.3		7
	4	0.4		8
	4	0.5		3
	4	0.6		4
	4	0.7		5
	4	0.8		6
	4	0.9		4
	4	1.0		4
		averages		5.40
	5	0.1		5
	5	0.2		5
	5	0.3		5
	5	0.4		5
40	5	0.5		5
	5	0.6		3
	5	0.7		5
	5	0.8		4
	5	0.9		8
	5	1.0		3
		averages		4.80
	6	0.1		7
	6	0.2		5
	6	0.3		4
	6	0.4		3
	6	0.5		1
	6	0.6		1
	6	0.7		1
	6	0.8		2
	6	0.9		1
	6	1.0		2
		averages		2.70

Table B.3: Detailed results of the relative speed-ups among the conic formulations by α for each (n, p) instance.

n	**p**	α	**Speed-ups**		
			MAX/MIN	**MAX/NEW**	**MIN/NEW**
	2	0.1	5.26	6.05	1.15
	2	0.2	7.73	10.55	1.36
	2	0.3	4.89	10.15	2.08
	2	0.4	3.88	2.51	0.65
	2	0.5	6.00	12.00	2.00
	2	0.6	6.88	9.75	1.42
	2	0.7	5.94	8.64	1.45
	2	0.8	9.53	14.73	1.55
	2	0.9	7.00	10.82	1.55
	2	1.0	4.61	8.83	1.92
		averages	6.17	9.40	1.51
	3	0.1	10.75	17.20	1.60
	3	0.2	11.00	20.00	1.82
	3	0.3	9.80	13.36	1.36
	3	0.4	5.24	9.17	1.75
10	3	0.5	19.05	36.36	1.91
	3	0.6	9.53	11.00	1.15
	3	0.7	6.38	13.91	2.18
	3	0.8	7.19	15.58	2.17
	3	0.9	8.17	15.67	1.92
	3	1.0	20.53	32.50	1.58
		averages	10.76	18.48	1.74
	4	0.1	14.00	40.00	2.86
	4	0.2	118.56	237.13	2.00
	4	0.3	21.57	60.40	2.80
	4	0.4	21.60	64.80	3.00
	4	0.5	29.50	118.00	4.00
	4	0.6	33.06	140.50	4.25
	4	0.7	13.65	46.40	3.40
	4	0.8	81.65	138.80	1.70
	4	0.9	12.15	17.56	1.44
	4	1.0	22.17	49.88	2.25
		averages	36.79	91.35	2.77
	2	0.1	10.28	83.50	8.13
	2	0.2	10.63	73.75	6.94
	2	0.3	6.79	59.53	8.76
	2	0.4	8.39	60.81	7.25
	2	0.5	18.80	30.32	1.61
	2	0.6	6.78	67.41	9.94
	2	0.7	8.82	63.72	7.22
	2	0.8	7.35	22.18	3.02
	2	0.9	19.13	33.29	1.74
	2	1.0	7.34	16.31	2.22
		averages	10.43	51.08	5.68
	3	0.1	11.90	65.22	5.48
	3	0.2	10.06	13.44	1.34
	3	0.3	8.82	55.62	6.31
	3	0.4	11.05	63.54	5.75
15	3	0.5	10.64	50.64	4.76
	3	0.6	42.08	263.95	6.27

	3	0.7	13.41	59.56	4.44
	3	0.8	14.95	85.52	5.72
	3	0.9	6.89	12.65	1.84
	3	1.0	18.05	80.16	4.44
		averages	14.79	75.03	4.63
	4	0.1	16.44	18.85	1.15
	4	0.2	12.62	19.29	1.53
	4	0.3	11.70	31.52	2.69
	4	0.4	17.04	90.64	5.32
	4	0.5	11.13	69.22	6.22
	4	0.6	39.46	252.22	6.39
	4	0.7	29.39	231.60	7.88
	4	0.8	14.04	63.19	4.50
	4	0.9	10.37	21.16	2.04
	4	1.0	14.09	76.33	5.42
		averages	17.63	87.40	4.31
	2	0.1	15.72	167.67	10.67
	2	0.2	11.66	126.40	10.84
	2	0.3	16.57	168.83	10.19
	2	0.4	37.43	306.06	8.18
	2	0.5	20.72	170.10	8.21
	2	0.6	12.53	176.27	14.07
	2	0.7	16.17	183.36	11.34
	2	0.8	12.55	173.43	13.82
	2	0.9	14.24	141.54	9.94
	2	1.0	11.30	139.02	12.30
		averages	16.89	175.27	10.95
	3	0.1	116.40	200.48	1.72
	3	0.2	43.33	88.57	2.04
	3	0.3	16.56	51.51	3.11
	3	0.4	21.52	50.93	2.37
20	3	0.5	12.66	46.65	3.68
	3	0.6	7.90	203.24	25.72
	3	0.7	8.58	44.23	5.15
	3	0.8	25.19	81.46	3.23
	3	0.9	35.45	414.27	11.69
	3	1.0	79.05	763.80	9.66
		averages	36.66	194.52	6.84
	4	0.1	79.87	1168.82	14.63
	4	0.2	14.15	213.59	15.10
	4	0.3	92.49	1028.25	11.12
	4	0.4	79.79	1104.47	13.84
	4	0.5	230.93	1095.62	4.74
	4	0.6	57.53	317.53	5.52
	4	0.7	39.84	143.37	3.60
	4	0.8	92.38	848.54	9.19
	4	0.9	37.66	528.34	14.03
	4	1.0	407.25	4359.30	10.70
		averages	113.19	1.080.78	10.25
	2	0.1	24.62	56.10	2.28
	2	0.2	25.41	478.99	18.85
	2	0.3	22.13	368.81	16.67
	2	0.4	22.80	378.02	16.58
	2	0.5	24.07	387.90	16.11

	2	0.6	24.12	392.62	16.28
	2	0.7	28.82	443.84	15.40
	2	0.8	28.24	422.39	14.96
	2	0.9	30.48	505.10	16.57
	2	1.0	34.33	550.22	16.03
		averages	26.50	398.40	14.97
	3	0.1	33.94	827.59	24.38
	3	0.2	28.83	864.42	29.98
	3	0.3	23.01	614.11	26.68
	3	0.4	31.28	927.83	29.66
25	3	0.5	29.58	724.87	24.51
	3	0.6	30.62	907.42	29.64
	3	0.7	28.47	740.23	26.00
	3	0.8	74.22	1379.22	18.58
	3	0.9	46.82	867.84	18.53
	3	1.0	30.17	781.49	25.90
		averages	35.69	863.50	25.39
	4	0.1	75.96	1364.84	17.97
	4	0.2	46.74	794.54	17.00
	4	0.3	133.93	2287.61	17.08
	4	0.4	101.69	1441.50	14.18
	4	0.5	64.69	242.87	3.75
	4	0.6	200.59	1083.34	5.40
	4	0.7	65.43	1131.72	17.30
	4	0.8	75.69	1150.15	15.20
	4	0.9	72.32	227.26	3.14
	4	1.0	98.13	277.89	2.83
		averages	93.52	1.000.17	11.38

	4	0.1	133.28
	4	0.2	123.26
	4	0.3	161.96
	4	0.4	110.77
	4	0.5	146.10
	4	0.6	99.68
	4	0.7	106.42
	4	0.8	87.53
	4	0.9	113.98
	4	1.0	61.25
		averages	114.42
	5	0.1	560.78
	5	0.2	559.23
	5	0.3	492.75
	5	0.4	473.35
30	5	0.5	496.10
	5	0.6	518.82
	5	0.7	354.95
	5	0.8	394.85
	5	0.9	293.60
	5	1.0	268.44
		averages	441.29
	6	0.1	352.32
	6	0.2	509.40
	6	0.3	606.64
	6	0.4	730.94
	6	0.5	576.26

6	0.6	829.39
6	0.7	504.16
6	0.8	813.11
6	0.9	533.63
6	1.0	513.97
	averages	596.98

Appendix C

Detailed Results of OA-based Formulations

Table C.1: Computational results for the OA-Obj MIN and NEW formulations on instances of sizes $n = \{10, 15, 20, 25, 30, 40\}$.

n	p	α	Market share (%)	OA-Obj					
				MIN			NEW		
				cpu (s)	gap (%)	#bbn	cpu (s)/ratio	gap (%)	#bbn
		0.1	66.01	0.19		4	**0.04 / 4.75**		3
		0.2	66.10	0.20		4	**0.04 / 5.00**		3
		0.3	66.18	0.20		4	**0.04 / 5.00**		3
		0.4	66.25	0.18		4	**0.03 / 6.00**		3
	2	0.5	66.31	0.18		4	**0.03 / 6.00**		3
		0.6	66.36	0.16		4	**0.03 / 5.33**		3
		0.7	66.41	0.14		4	**0.03 / 4.67**		3
		0.8	66.45	0.15		4	**0.03 / 5.00**		3
		0.9	66.49	0.17		4	**0.03 / 5.67**		3
		1	66.52	0.13		4	**0.02 / 6.50**		3
		averages		0.17		4.00	0.03 / 5.39		3.00
		0.1	60.70	0.19		5	**0.06 / 3.17**		4
		0.2	60.74	0.20		5	**0.06 / 3.33**		4
		0.3	60.79	0.19		5	**0.06 / 3.17**		4
		0.4	60.82	0.19		5	**0.06 / 3.17**		4
10	3	0.5	60.85	0.18		5	**0.04 / 4.5**		3
		0.6	60.88	0.12		4	**0.03 / 4**		3
		0.7	60.91	0.11		4	**0.03 / 3.67**		3
		0.8	60.93	0.11		4	**0.04 / 2.75**		3
		0.9	60.95	0.11		4	**0.03 / 3.67**		3
		1	60.96	0.10		4	**0.04 / 2.5**		3
		averages		0.15		4.50	0.05 / 3.39		3.40
		0.1	64.70	0.11		4	**0.03 / 3.67**		3
		0.2	64.87	0.12		4	**0.03 / 4**		3
		0.3	65.03	0.11		4	**0.02 / 5.5**		3
		0.4	65.17	0.11		4	**0.03 / 3.67**		3
	4	0.5	65.29	0.11		4	**0.03 / 3.67**		3
		0.6	65.41	0.12		4	**0.03 / 4**		3
		0.7	65.51	0.10		4	**0.03 / 3.33**		3
		0.8	65.61	0.11		4	**0.03 / 3.67**		3
		0.9	65.69	0.11		4	**0.03 / 3.67**		3
		1	65.77	0.11		4	**0.03 / 3.67**		3
		averages		0.11		4.00	0.03 / 3.88		3.00
		0.1	50.00	0.60		3	**0.11 / 5.45**		3
		0.2	50.00	0.83		3	**0.11 / 7.55**		3
		0.3	50.00	0.58		3	**0.13 / 4.46**		3
		0.4	50.00	0.57		3	**0.11 / 5.18**		3
	2	0.5	50.00	0.51		3	**0.12 / 4.25**		3
		0.6	50.00	0.49		3	**0.11 / 4.45**		3
		0.7	50.00	0.69		3	**0.13 / 5.31**		3
		0.8	50.00	0.48		3	**0.11 / 4.36**		3
		0.9	50.00	0.43		3	**0.11 / 3.91**		3
		1	50.00	0.38		3	**0.12 / 3.17**		3
		averages		0.56		3.00	0.12 / 4.81		3.00
		0.1	60.77	0.83		4	**0.12 / 6.92**		3
		0.2	60.82	0.99		4	**0.12 / 8.25**		3
		0.3	60.85	0.80		4	**0.12 / 6.67**		3
		0.4	60.89	0.85		4	**0.12 / 7.08**		3
15	3	0.5	60.92	0.72		4	**0.12 / 6**		3
		0.6	60.94	0.83		4	**0.12 / 6.92**		3
		0.7	60.96	0.68		4	**0.12 / 5.67**		3
		0.8	60.98	0.67		4	**0.12 / 5.58**		3
		0.9	61	0.68		4	**0.12 / 5.67**		3
		1	61.02	0.67		4	**0.12 / 5.58**		3
		averages		0.77		4.00	0.12 / 6.43		3.00
		0.1	63.23	0.82		4	**0.29 / 2.83**		4
		0.2	63.37	0.86		4	**0.27 / 3.19**		4
		0.3	63.50	0.83		4	**0.26 / 3.19**		4
		0.4	63.61	0.77		4	**0.26 / 2.96**		4
	4	0.5	63.72	0.81		4	**0.13 / 6.23**		3

n	p	α	Market share (%)	OA-Obj					
				MIN			NEW		
				cpu (s)	gap (%)	#bbn	cpu (s)/ratio	gap (%)	#bbn
		0.6	63.82	0.83		4	**0.12 / 6.92**		3
		0.7	63.91	0.85		4	**0.13 / 6.54**		3
		0.8	64	0.77		4	**0.12 / 6.42**		3
		0.9	64.08	0.76		4	**0.13 / 5.85**		3
		1	64.15	0.74		4	**0.14 / 5.29**		3
		averages		0.80		4.00	0.19 / 4.94		3.40
		0.1	50.00	1.70		3	**0.40 / 4.25**		3
		0.2	50.00	1.75		3	**0.42 / 4.17**		3
		0.3	50.00	1.77		3	**0.41 / 4.32**		3
		0.4	50.00	1.74		3	**0.43 / 4.05**		3
	2	0.5	50.00	1.54		3	**0.42 / 3.67**		3
		0.6	50.00	1.9		3	**0.45 / 4.22**		3
		0.7	50.00	2.36		3	**0.42 / 5.62**		3
		0.8	50.00	1.87		3	**0.42 / 4.45**		3
		0.9	50.00	1.97		3	**0.42 / 4.69**		3
		1	50.00	1.80		3	**0.43 / 4.19**		3
		averages		1.84		3.00	0.42 / 4.36		3.00
		0.1	61.84	3.46		4	**0.44 / 7.86**		3
		0.2	61.85	3.41		4	**0.43 / 7.93**		3
		0.3	61.87	3.54		4	**0.44 / 8.05**		3
		0.4	61.88	3.21		4	**0.43 / 7.47**		3
20	3	0.5	61.89	3.52		4	**0.43 / 8.19**		3
		0.6	61.89	3.42		4	**0.43 / 7.95**		3
		0.7	61.89	3.08		4	**0.47 / 6.55**		3
		0.8	61.9	3.21		4	**0.44 / 7.3**		3
		0.9	61.9	3.12		4	**0.43 / 7.26**		3
		1	61.9	3.17		4	**0.46 / 6.89**		3
		averages		3.31		4.00	0.44 / 7.54		3.00
		0.1	70.76	4.73		4	**0.46 / 10.28**		3
		0.2	70.84	4.21		4	**0.52 / 8.1**		3
		0.3	70.92	4.23		4	**0.44 / 9.61**		3
		0.4	70.99	4.07		4	**0.51 / 7.98**		3
	4	0.5	71.04	3.94		4	**0.43 / 9.16**		3
		0.6	71.10	4.16		4	**0.43 / 9.67**		3
		0.7	71.14	3.95		4	**0.49 / 8.06**		3
		0.8	71.19	3.80		4	**0.48 / 7.92**		3
		0.9	71.22	3.9		4	**0.48 / 8.13**		3
		1	71.26	4.07		4	**0.48 / 8.48**		3
		averages		4.11		4.00	0.47 / 8.74		3.00
		0.1	50.00	5.27		3	**1.26 / 4.18**		3
		0.2	50.00	4.81		3	**1.29 / 3.73**		3
		0.3	50.00	5.12		3	**1.30 / 3.94**		3
		0.4	50.00	4.9		3	**1.29 / 3.8**		3
	2	0.5	50.00	5.03		3	**1.27 / 3.96**		3
		0.6	50.00	5.35		3	**1.28 / 4.18**		3
		0.7	50.00	4.92		3	**1.23 / 4**		3
		0.8	50.00	4.96		3	**1.26 / 3.94**		3
		0.9	50.00	5.04		3	**1.25 / 4.03**		3
		1	50.00	6.07		3	**1.29 / 4.71**		3
		averages		5.15		3.00	1.27 / 4.05		3.00
		0.1	64.88	18.37		4	**1.34 / 13.71**		3
		0.2	64.91	17.61		4	**1.25 / 14.09**		3
		0.3	64.93	17.36		4	**1.29 / 13.46**		3
		0.4	64.94	18.27		4	**1.31 / 13.95**		3
25	3	0.5	64.96	14.09		4	**1.29 / 10.92**		3
		0.6	64.97	16.58		4	**1.26 / 13.16**		3
		0.7	64.97	14.47		4	**1.27 / 11.39**		3
		0.8	64.98	14.71		4	**1.29 / 11.4**		3
		0.9	64.99	13.22		4	**1.28 / 10.33**		3
		1	64.99	5.71		3	**1.30 / 4.39**		3
		averages		15.04		3.90	1.29 / 11.68		3.00

n	p	α	Market share (%)	OA-Obj					
				MIN			NEW		
				cpu (s)	gap (%)	#bbn	cpu (s)/ratio	gap (%)	#bbn
		0.1	71.69	38.91		5	**3.13** / **12.43**		4
		0.2	71.73	37.02		5	**3.33** / **11.12**		4
		0.3	71.76	39.75		5	**3.26** / **12.19**		4
		0.4	71.78	35.74		5	**3.07** / **11.64**		4
	4	0.5	71.80	35.30		5	**5.44** / **6.49**		5
		0.6	71.82	34.20		5	**5.42** / **6.31**		5
		0.7	71.83	56.82		6	**5.57** / **10.2**		5
		0.8	71.84	57.98		6	**5.42** / **10.7**		5
		0.9	71.85	54.73		6	**5.39** / **10.15**		5
		1	71.87	56.17		6	**5.62** / **9.99**		5
		averages		44.66		5.40	4.57 / 10.12		4.60
		0.1	63.41	817.74		6	**3.34** / **244.83**		3
		0.2	63.60	530.73		5	**3.35** / **158.43**		3
		0.3	63.78	485.66		5	**3.43** / **141.59**		3
		0.4	63.95	513.97		5	**3.28** / **156.7**		3
	4	0.5	64.10	509.77		5	**3.47** / **146.91**		3
		0.6	64.25	467.41		5	**3.26** / **143.38**		3
		0.7	64.40	565.69		5	**3.43** / **164.92**		3
		0.8	64.53	511.27		5	**7.39** / **69.18**		4
		0.9	64.66	442		5	**6.98** / **63.32**		4
		1	64.78	423.02		5	**7.11** / **59.5**		4
		averages		526.73		5.10	4.50 / 134.88		3.30
		0.1	57.46	720.30		5	**3.02** / **238.51**		3
		0.2	57.56	350.89		4	**2.92** / **120.17**		3
		0.3	57.66	313.56		4	**2.93** / **107.02**		3
		0.4	57.75	331.83		4	**3.27** / **101.48**		3
30	5	0.5	57.84	318.21		4	**2.97** / **107.14**		3
		0.6	57.92	265.81		4	**3** / **88.6**		3
		0.7	58	265.39		4	**3.02** / **87.88**		3
		0.8	58.08	262.51		4	**3.16** / **83.07**		3
		0.9	58.15	270.69		4	**2.96** / **91.45**		3
		1	58.22	220.86		4	**2.83** / **78.04**		3
		averages		332.01		4.10	3.01 / 110.34		3.00
		0.1	64.15	1309.96		5	**6.9** / **189.85**		4
		0.2	64.44	1418.44		5	**6.99** / **202.92**		4
		0.3	64.71	611.91		4	**3.20** / **191.22**		3
		0.4	64.97	629.11		4	**3.07** / **204.92**		3
	6	0.5	65.21	484.76		4	**3.07** / **157.9**		3
		0.6	65.43	601.60		4	**3.05** / **197.25**		3
		0.7	65.65	542.17		4	**3.04** / **178.35**		3
		0.8	65.85	566.67		4	**2.98** / **190.16**		3
		0.9	66.04	464.05		4	**2.96** / **156.77**		3
		1	66.23	499.85		4	**2.89** / **172.96**		3
		averages		712.85		4.20	3.82 / 184.23		3.20
		0.1	63.27	6644.93		5	**52.73** / **126.02**		5
		0.2	63.47	7423.67		5	**52** / **142.76**		5
		0.3	63.65	7076.47		5	**28.94** / **244.52**		4
		0.4	63.82	5989.69		5	**29.35** / **204.08**		4
	4	0.5	63.99	6085.71		5	**27.69** / **219.78**		4
		0.6	64.14	6630.94		5	**28.48** / **232.83**		4
		0.7	64.29	6452.59		5	**28.58** / **225.77**		4
		0.8	64.43	6087.87		5	**28.85** / **211.02**		4
		0.9	64.56	5723.23		5	**27.97** / **204.62**		4
		1	64.69	5215.13		5	**27.30** / **191.03**		4
		averages		6333.02		5.00	33.19 / 200.24		4.20
		0.1	64.86	66951.30		7	**83.57** / **801.14**		6
		0.2	65.02	54093.25		7	**53.54** / **1010.33**		5
		0.3	65.18	36013.41		6	**52.64** / **684.15**		5
		0.4	65.32	34423.79		6	**53.49** / **643.56**		5
40	5	0.5	65.47	29467.40		6	**52.92** / **556.83**		5
		0.6	65.60	18885.04		5	**53.50** / **352.99**		5
		0.7	65.73	25831.85		6	**54.66** / **472.59**		5

n	p	α	Market share (%)	OA-Obj					
				MIN			NEW		
				cpu (s)	gap (%)	#bbn	cpu (s)/ratio	gap (%)	#bbn
		0.8	65.85	30447.85		6	**54.62** / **557.45**		5
		0.9	65.97	23115.12		6	**54.20** / **426.48**		5
		1	66.08	26628.59		6	**53.29** / **499.69**		5
		averages		34585.76		6.10	56.64 / 600.52		5.10
		0.1	65.27	64410.27		6	**53.37** / **1206.86**		5
		0.2	65.49	73650.78		6	**53.89** / **1366.69**		5
		0.3	65.70	65488.47		6	**51.9** / **1261.82**		5
		0.4	65.9	76638.82		6	**52.31** / **1465.09**		5
	6	0.5	66.10	27130.17		5	**30.10**/ **901.33**		4
		0.6	66.28	38051.24		5	**30.07** / **1265.42**		4
		0.7	66.46	18145.48		4	**15.31** / **1185.2**		3
		0.8	66.63	22647.89		4	**15.12** / **1497.88**		3
		0.9	66.79	19309.39		4	**27.72** / **696.59**		4
		1	66.94	16149.13		4	**27.30** / **591.54**		4
		averages		42162.16		5.00	35.71 / 1143.84		4.20

Table C.2: Computational results for the OA-rvar MIN and NEW formulations on instances of sizes $n = \{10, 15, 20, 25, 30, 40\}$.

n	p	α	Market share (%)	OA-rvar					
				MIN			NEW		
				cpu (s)	gap (%)	#bbn	cpu (s)/ratio	gap (%)	#bbn
		0.1	66.01	0.09		2	**0.05 / 1.8**		2
		0.2	66.10	0.09		2	**0.05 / 1.8**		2
		0.3	66.18	0.11		2	**0.04 / 2.75**		2
		0.4	66.25	0.10		2	**0.05 / 2**		2
	2	0.5	66.31	0.11		2	**0.04 / 2.75**		2
		0.6	66.36	0.12		2	**0.05 / 2.4**		2
		0.7	66.41	0.13		2	**0.04 / 3.25**		2
		0.8	66.45	0.11		2	**0.05 / 2.2**		2
		0.9	66.49	0.09		2	**0.05 / 1.8**		2
		1	66.52	0.10		2	**0.05 / 2**		2
		averages		0.11		2.00	0.05 / 2.28		2.00
		0.1	60.70	0.13		3	**0.08 / 1.63**		3
		0.2	60.74	0.13		3	**0.07 / 1.86**		3
		0.3	60.79	0.12		3	**0.07 / 1.71**		3
		0.4	60.82	0.12		3	**0.07 / 1.71**		3
10	3	0.5	60.85	0.12		3	**0.07 / 1.71**		3
		0.6	60.88	0.08		2	**0.06 / 1.33**		2
		0.7	60.91	0.08		2	**0.04 / 2**		2
		0.8	60.93	0.10		2	**0.05 / 2**		2
		0.9	60.95	0.08		2	**0.05 / 1.6**		2
		1	60.96	0.09		2	**0.05 / 1.8**		2
		averages		0.11		2.50	0.06 / 1.74		2.50
		0.1	64.70	0.08		2	**0.03 / 2.67**		2
		0.2	64.87	0.07		2	**0.04 / 1.75**		2
		0.3	65.03	0.07		2	**0.04 / 1.75**		2
		0.4	65.17	0.07		2	**0.04 / 1.75**		2
	4	0.5	65.29	0.08		2	**0.03 / 2.67**		2
		0.6	65.41	0.08		2	**0.04 / 2**		2
		0.7	65.51	0.08		2	**0.04 / 2**		2
		0.8	65.61	0.07		2	**0.03 / 2.33**		2
		0.9	65.69	0.07		2	**0.03 / 2.33**		2
		1	65.77	0.06		2	**0.03 / 2**		2
		averages		0.07		2.00	0.04 / 2.13		2.00
		0.1	50.00	0.53		2	**0.13 / 4.08**		2
		0.2	50.00	0.53		2	**0.14 / 3.79**		2
		0.3	50.00	0.56		2	**0.14 / 4**		2
		0.4	50.00	0.48		2	**0.14 / 3.43**		2
	2	0.5	50.00	0.67		2	**0.14 / 4.79**		2
		0.6	50.00	0.69		2	**0.13 / 5.31**		2
		0.7	50.00	0.53		2	**0.13 / 4.08**		2
		0.8	50.00	0.54		2	**0.14 / 3.86**		2
		0.9	50.00	0.52		2	**0.14 / 3.71**		2
		1	50.00	0.63		2	**0.14 / 4.5**		2
		averages		0.57		2.00	0.14 / 4.15		2.00
		0.1	60.77	0.47		2	**0.14 / 3.36**		2
		0.2	60.82	0.46		2	**0.13 / 3.54**		2
		0.3	60.85	0.46		2	**0.13 / 3.54**		2
		0.4	60.89	0.52		2	**0.13 / 4**		2
15	3	0.5	60.92	0.43		2	**0.13 / 3.31**		2
		0.6	60.94	0.45		2	**0.12 / 3.75**		2
		0.7	60.96	0.48		2	**0.13 / 3.69**		2
		0.8	60.98	0.50		2	**0.14 / 3.57**		2
		0.9	61	0.46		2	**0.12 / 3.83**		2
		1	61.02	0.42		2	**0.14 / 3**		2
		averages		0.47		2.00	0.13 / 3.56		2.00
		0.1	63.23	0.48		2	**0.19 / 2.53**		2
		0.2	63.37	0.46		2	**0.18 / 2.56**		2
		0.3	63.50	0.46		2	**0.18 / 2.56**		2
		0.4	63.61	0.43		2	**0.16 / 2.69**		2
	4	0.5	63.72	0.44		2	**0.15 / 2.93**		2
		0.6	63.82	0.45		2	**0.15 / 3**		2
		0.7	63.91	0.45		2	**0.15 / 3**		2
		0.8	64	0.43		2	**0.15 / 2.87**		2

n	p	α	Market share (%)	OA-rvar					
				MIN			NEW		
				cpu (s)	gap (%)	#bbn	cpu (s)/ratio	gap (%)	#bbn
		0.9	64.08	0.44		2	**0.15 / 2.93**		2
		1	64.15	0.42		2	**0.15 / 2.8**		2
		averages		0.45		2.00	0.16 / 2.79		2.00
		0.1	50.00	1.89		2	**0.38 / 4.97**		2
		0.2	50.00	2.46		2	**0.39 / 6.31**		2
		0.3	50.00	1.95		2	**0.42 / 4.64**		2
		0.4	50.00	2.78		2	**0.42 / 6.62**		2
	2	0.5	50.00	1.77		2	**0.43 / 4.12**		2
		0.6	50.00	1.93		2	**0.46 / 4.2**		2
		0.7	50.00	2.48		2	**0.45 / 5.51**		2
		0.8	50.00	2.40		2	**0.45 / 5.33**		2
		0.9	50.00	2.02		2	**0.43 / 4.7**		2
		1	50.00	2.06		2	**0.44 / 4.68**		2
		averages		2.17		2.00	0.43 / 5.11		2.00
		0.1	61.84	2.07		2	**0.46 / 4.5**		2
		0.2	61.85	2.31		2	**0.46 / 5.02**		2
		0.3	61.87	2.42		2	**0.46 / 5.26**		2
		0.4	61.88	2.34		2	**0.45 / 5.2**		2
20	3	0.5	61.89	2.04		2	**0.47 / 4.34**		2
		0.6	61.89	1.99		2	**0.45 / 4.42**		2
		0.7	61.89	2		2	**0.45 / 4.44**		2
		0.8	61.9	1.67		2	**0.45 / 3.71**		2
		0.9	61.9	1.91		2	**0.44 / 4.34**		2
		1	61.9	1.93		2	**0.46 / 4.2**		2
		averages		2.07		2.00	0.46 / 4.54		2.00
		0.1	70.76	2.21		2	**0.51 / 4.33**		2
		0.2	70.84	2.37		2	**0.51 / 4.65**		2
		0.3	70.92	2.24		2	**0.58 / 3.86**		2
		0.4	70.99	2.18		2	**0.58 / 3.76**		2
	4	0.5	71.04	2.14		2	**0.57 / 3.75**		2
		0.6	71.10	2.03		2	**0.54 / 3.76**		2
		0.7	71.14	1.85		2	**0.51 / 3.63**		2
		0.8	71.19	1.80		2	**0.51 / 3.53**		2
		0.9	71.22	1.72		2	**0.51 / 3.37**		2
		1	71.26	1.93		2	**0.56 / 3.45**		2
		averages		2.05		2.00	0.54 / 3.81		2.00
		0.1	50.00	5.13		2	**0.96 / 5.34**		2
		0.2	50.00	5.42		2	**0.93 / 5.83**		2
		0.3	50.00	5.40		2	**0.95 / 5.68**		2
		0.4	50.00	5.59		2	**0.95 / 5.88**		2
	2	0.5	50.00	5.41		2	**0.94 / 5.76**		2
		0.6	50.00	5.51		2	**0.96 / 5.74**		2
		0.7	50.00	5.12		2	**0.93 / 5.51**		2
		0.8	50.00	5.19		2	**0.96 / 5.41**		2
		0.9	50.00	5.40		2	**0.95 / 5.68**		2
		1	50.00	5.39		2	**0.98 / 5.5**		2
		averages		5.36		2.00	0.95 / 5.63		2.00
		0.1	64.88	9.08		2	**1.26 / 7.21**		2
		0.2	64.91	8.88		2	**1.26 / 7.05**		2
		0.3	64.93	7.97		2	**1.26 / 6.33**		2
		0.4	64.94	8.84		2	**1.24 / 7.13**		2
25	3	0.5	64.96	8		2	**1.26 / 6.35**		2
		0.6	64.97	7.43		2	**1.26 / 5.9**		2
		0.7	64.97	7.80		2	**1.26 / 6.19**		2
		0.8	64.98	8.07		2	**1.21 / 6.67**		2
		0.9	64.99	7.55		2	**1.23 / 6.14**		2
		1	64.99	6.67		2	**1.22 / 5.47**		2
		averages		8.03		2.00	1.25 / 6.44		2.00
		0.1	71.69	9.82		2	**1.39 / 7.06**		2
		0.2	71.73	9.39		2	**1.36 / 6.9**		2
		0.3	71.76	14.98		3	**2.14 / 7**		3
		0.4	71.78	13.71		3	**2.20 / 6.23**		3
	4	0.5	71.80	14.70		3	**2.12 / 6.93**		3
		0.6	71.82	13.83		3	**2.14 / 6.46**		3
		0.7	71.83	14.87		3	**2.22 / 6.7**		3

n	p	α	Market share (%)	OA-rvar					
				MIN			NEW		
				cpu (s)	gap (%)	#bbn	cpu (s)/ratio	gap (%)	#bbn
		0.8	71.84	13.84		3	**2.29 / 6.04**		3
		0.9	71.85	13		3	**2.20 / 5.91**		3
		1	71.87	12.37		3	**2.25 / 5.5**		3
		averages		13.05		2.80	2.03 / 6.47		2.80
		0.1	63.41	173.96		2	**3.59 / 48.46**		2
		0.2	63.60	171.22		2	**3.67 / 46.65**		2
		0.3	63.78	161.84		2	**2.56 / 63.22**		2
		0.4	63.95	156.82		2	**2.71 / 57.87**		2
	4	0.5	64.10	155.34		2	**2.44 / 63.66**		2
		0.6	64.25	163.06		2	**2.67 / 61.07**		2
		0.7	64.40	150.47		2	**2.77 / 54.32**		2
		0.8	64.53	148.13		2	**2.66 / 55.69**		2
		0.9	64.66	137.92		2	**3.03 / 45.52**		2
		1	64.78	217.01		3	**4.05 / 53.58**		3
		averages		163.58		2.10	3.02 / 55		2.10
		0.1	57.46	322.07		2	**2.88 / 111.83**		2
		0.2	57.56	302.75		2	**2.95 / 102.63**		2
		0.3	57.66	263.18		2	**2.93 / 89.82**		2
		0.4	57.75	256.40		2	**3 / 85.47**		2
30	5	0.5	57.84	226.87		2	**2.94 / 77.17**		2
		0.6	57.92	246.16		2	**2.98 / 82.6**		2
		0.7	58	225.85		2	**2.98 / 75.79**		2
		0.8	58.08	199.62		2	**3 / 66.54**		2
		0.9	58.15	183.51		2	**2.9 / 63.28**		2
		1	58.22	192.88		2	**2.95 / 65.38**		2
		averages		241.93		2.00	2.95 / 82.05		2.00
		0.1	64.15	630.16		3	**3.95 / 159.53**		3
		0.2	64.44	604.55		3	**4.05 / 149.27**		3
		0.3	64.71	353.39		2	**2.69 / 131.37**		2
		0.4	64.97	289.07		2	**2.66 / 108.67**		2
	6	0.5	65.21	256.20		2	**2.61 / 98.16**		2
		0.6	65.43	227.45		2	**2.49 / 91.35**		2
		0.7	65.65	223.78		2	**2.42 / 92.47**		2
		0.8	65.85	262.72		2	**2.42 / 108.56**		2
		0.9	66.04	184.73		2	**2.41 / 76.65**		2
		1	66.23	180.12		2	**2.25 / 80.05**		2
		averages		321.22		2.20	2.80 / 109.61		2.20
		0.1	63.27	2778.86		3	**18.25 / 152.27**		3
		0.2	63.47	2979.26		3	**18.27 / 163.07**		3
		0.3	63.65	2012.61		2	**13.18 / 152.7**		2
		0.4	63.82	1921.28		2	**13.07 / 147**		2
	4	0.5	63.99	1727.86		2	**12.26 / 140.93**		2
		0.6	64.14	1734.06		2	**12.88 / 134.63**		2
		0.7	64.29	1628.83		2	**12.21 / 133.4**		2
		0.8	64.43	1710.91		2	**12.27 / 139.44**		2
		0.9	64.56	1488.52		2	**11.86 / 125.51**		2
		1	64.69	1538.73		2	**12.03 / 127.91**		2
		averages		1952.09		2.20	13.63 / 141.69		2.20
		0.1	64.86	15851.18		4	**27.07 / 585.56**		4
		0.2	65.02	14314.67		4	**32 / 447.33**		4
		0.3	65.18	13635.32		4	**30.86 / 441.84**		4
		0.4	65.32	11954.01		4	**27.23 / 439**		4
40	5	0.5	65.47	12038		4	**26.40 / 455.98**		4
		0.6	65.60	12148.08		4	**26.95 / 450.76**		4
		0.7	65.73	10612.77		4	**26.72 / 397.18**		4
		0.8	65.85	11579.91		4	**27.73 / 417.6**		4
		0.9	65.97	7163.50		4	**26.76 / 267.69**		4
		1	66.08	6921.59		4	**27.41 / 252.52**		4
		averages		11621.90		4.00	27.91 / 415.55		4.00
		0.1	65.27	20337.98		4	**33.72 / 603.14**		4
		0.2	65.49	19121.99		4	**43.72 / 437.37**		4
		0.3	65.70	17930.96		4	**37.51 / 478.03**		4
		0.4	65.9	12813.55		3	**32.97 / 388.64**		3
	6	0.5	66.10	7454.98		2	**24.89 / 299.52**		2
		0.6	66.28	9055.13		2	**18.51 / 489.2**		2

n	p	α	Market share (%)	OA-rvar					
				MIN			NEW		
				cpu (s)	gap (%)	#bbn	cpu (s)/ratio	gap (%)	#bbn
		0.7	66.46	7548.56		2	**18.32** / **412.04**		2
		0.8	66.63	6135.52		2	**21.15** / **290.1**		2
		0.9	66.79	4826.79		2	**19.08** / **252.98**		2
		1	66.94	6278.63		2	**18.92** / **331.85**		2
		averages		11150.41		2.70	26.88 / 398.29		2.70

Table C.3: Computational results for the COACuts MIN and NEW formulations on instances of sizes $n = \{10, 15, 20, 25, 30, 40\}$.

n	p	α	Market share (%)	Conic OA cuts					
				MIN			NEW		
				cpu (s)	gap (%)	#bbn	cpu (s)/ratio	gap (%)	#bbn
		0.1	66.01	0.41		44	**0.12** / **3.42**		1
		0.2	66.10	0.42		39	**0.12** / **3.50**		1
		0.3	66.18	0.37		37	**0.15** / **2.47**		1
		0.4	66.25	0.28		31	**0.12** / **2.33**		1
	2	0.5	66.31	0.34		34	**0.13** / **2.62**		1
		0.6	66.36	0.37		34	**0.12** / **3.08**		1
		0.7	66.41	0.30		27	**0.13** / **2.31**		1
		0.8	66.45	0.28		41	**0.13** / **2.15**		1
		0.9	66.49	0.35		39	**0.12** / **2.92**		1
		1	66.52	0.43		40	**0.13** / **3.31**		1
		averages		0.355		36.60	0.13 / 2.81		1
		0.1	60.70	0.47		54	**0.13** / **3.62**		3
		0.2	60.74	0.34		44	**0.15** / **2.27**		1
		0.3	60.79	0.41		43	**0.16** / **2.56**		1
		0.4	60.82	0.37		52	**0.12** / **3.08**		1
10	3	0.5	60.85	0.28		41	**0.11** / **2.55**		1
		0.6	60.88	0.33		47	**0.12** / **2.75**		1
		0.7	60.91	0.32		43	**0.06** / **5.33**		0
		0.8	60.93	0.37		43	**0.12** / **3.08**		1
		0.9	60.95	0.37		43	**0.07** / **5.29**		0
		1	60.96	0.25		38	**0.07** / **3.57**		0
		averages		0.351		44.80	0.11 / 3.41		0.9
		0.1	64.70	0.21		42	**0.05** / **4.20**		0
		0.2	64.87	0.22		38	**0.06** / **3.67**		0
		0.3	65.03	0.26		53	**0.05** / **5.20**		0
		0.4	65.17	0.23		27	**0.06** / **3.83**		0
	4	0.5	65.29	0.40		49	**0.06** / **6.67**		0
		0.6	65.41	0.23		38	**0.05** / **4.60**		0
		0.7	65.51	0.20		35	**0.06** / **3.33**		0
		0.8	65.61	0.31		33	**0.06** / **5.17**		0
		0.9	65.69	0.35		33	**0.06** / **5.83**		0
		1	65.77	0.21		32	**0.06** / **3.50**		0
		averages		0.262		38	0.06 / 4.60		0
		0.1	50.00	1.91		73	**0.23** / **8.30**		0
		0.2	50.00	2.43		68	**0.24** / **10.13**		0
		0.3	50.00	2.04		63	**0.23** / **8.87**		0
		0.4	50.00	1.73		63	**0.23** / **7.52**		0
	2	0.5	50.00	3.19		68	**0.25** / **12.76**		0
		0.6	50.00	2.93		56	**0.24** / **12.21**		0
		0.7	50.00	3.45		65	**0.22** / **15.68**		0
		0.8	50.00	1.99		57	**0.24** / **8.29**		0
		0.9	50.00	2.37		59	**0.23** / **10.3**		0
		1	50.00	2.56		59	**0.24** / **10.67**		0
		averages		2.46		63.10	0.24 / 10.47		0
		0.1	60.77	2.08		122	**0.33** / **6.30**		0
		0.2	60.82	2.30		120	**0.54** / **4.26**		0
		0.3	60.85	2.72		116	**0.32** / **8.50**		0
		0.4	60.89	2.34		127	**0.32** / **7.31**		0
15	3	0.5	60.92	1.76		116	**0.31** / **5.68**		0
		0.6	60.94	1.76		103	**0.33** / **5.33**		0
		0.7	60.96	2.03		106	**0.30** / **6.77**		0
		0.8	60.98	1.81		79	**0.32** / **5.66**		0
		0.9	61	1.75		73	**0.32** / **5.47**		0
		1	61.02	2.34		113	**0.31** / **7.55**		0
		averages		2.089		107.50	0.34 / 6.28		0
		0.1	63.23	2.47		124	**0.91** / **2.71**		1
		0.2	63.37	3.06		127	**0.61** / **5.02**		1
		0.3	63.50	2.45		129	**0.62** / **3.95**		1
		0.4	63.61	2.95		126	**0.42** / **7.02**		0
	4	0.5	63.72	2.41		107	**0.30** / **8.03**		0

n	p	α	Market share (%)	Conic OA cuts					
				MIN			NEW		
				cpu (s)	gap (%)	#bbn	cpu (s)/ratio	gap (%)	#bbn
		0.6	63.82	3.04		137	**0.30 / 10.13**		0
		0.7	63.91	2.35		108	**0.31 / 7.58**		0
		0.8	64	2.87		120	**0.31 / 9.26**		0
		0.9	64.08	2.08		90	**0.31 / 6.71**		0
		1	64.15	2.07		78	**0.31 / 6.68**		0
		averages		2.575		114.60	0.44 / 6.71		0.3
		0.1	50.00	7.40		115	**0.55 / 13.45**		0
		0.2	50.00	10.27		127	**0.56 / 18.34**		0
		0.3	50.00	7.94		136	**0.74 / 10.73**		0
		0.4	50.00	5.97		118	**0.77 / 7.75**		0
	2	0.5	50.00	5.50		110	**0.76 / 7.24**		0
		0.6	50.00	6.66		127	**0.80 / 8.33**		0
		0.7	50.00	6.94		109	**0.74 / 9.38**		0
		0.8	50.00	6.83		106	**0.77 / 8.87**		0
		0.9	50.00	7.44		88	**0.95 / 7.83**		0
		1	50.00	7.67		96	**0.89 / 8.62**		0
		averages		7.262		113.20	0.75 / 10.05		0
		0.1	61.84	9.97		192	**0.69 / 14.45**		0
		0.2	61.85	11.24		184	**0.68 / 16.53**		0
		0.3	61.87	9.83		176	**0.68 / 14.46**		0
		0.4	61.88	10.27		158	**0.70 / 14.67**		0
20	3	0.5	61.89	7.89		151	**0.69 / 11.43**		0
		0.6	61.89	8.39		164	**0.68 / 12.34**		0
		0.7	61.89	8.78		123	**0.68 / 12.91**		0
		0.8	61.9	12.33		210	**0.71 / 17.37**		0
		0.9	61.9	7.40		128	**0.65 / 11.38**		0
		1	61.9	11.50		176	**0.69 / 16.67**		0
		averages		9.76		166.20	0.69 / 14.22		0
		0.1	70.76	15.61		333	**0.97 / 16.09**		0
		0.2	70.84	12.50		276	**0.93 / 13.44**		0
		0.3	70.92	13.13		226	**0.96 / 13.68**		0
		0.4	70.99	9.67		196	**0.95 / 10.18**		0
	4	0.5	71.04	11.05		270	**0.94 / 11.76**		0
		0.6	71.10	15.05		255	**0.86 / 17.5**		0
		0.7	71.14	11.24		227	**0.90 / 12.49**	0.01	0
		0.8	71.19	11.35		223	**1.21 / 9.38**		0
		0.9	71.22	10.91		167	**1.24 / 8.80**		0
		1	71.26	12		200	**1.31 / 9.16**		0
		averages		12.251		237.30	1.03 / 12.25		0
		0.1	50.00	30.67		230	**1.86 / 16.49**		0
		0.2	50.00	29.97		232	**1.80 / 16.65**	0.01	0
		0.3	50.00	32.16		222	**1.87 / 17.20**		0
		0.4	50.00	33.93		225	**1.82 / 18.64**		0
	2	0.5	50.00	35.54		218	**1.82 / 19.53**		0
		0.6	50.00	26.57		237	**1.83 / 14.52**		0
		0.7	50.00	22.83		195	**1.84 / 12.41**		0
		0.8	50.00	34.83		217	**1.86 / 18.73**		0
		0.9	50.00	29.55		217	**1.92 / 15.39**		0
		1	50.00	29.92		186	**1.90 / 15.75**		0
		averages		30.597		217.90	1.85 / 16.53		0
		0.1	64.88	56.05		522	**2.51 / 22.33**		0
		0.2	64.91	55.89		523	**2.21 / 25.29**		0
		0.3	64.93	45.35		497	**2.00 / 22.68**		0
		0.4	64.94	48.51		428	**2.57 / 18.88**		0
25	3	0.5	64.96	45.41		430	**2.08 / 21.83**		0
		0.6	64.97	56.56		418	**2.55 / 22.18**		0
		0.7	64.97	38.55		342	**2.17 / 17.76**		0
		0.8	64.98	42.23		407	**2.09 / 20.21**		0
		0.9	64.99	49.12		419	**2.65 / 18.54**		0
		1	64.99	42.87		343	**2.61 / 16.43**		0
		averages		48.054		432.9	2.34 / 20.61		0

n	p	α	Market share (%)	Conic OA cuts					
				MIN			NEW		
				cpu (s)	gap (%)	#bbn	cpu (s)/ratio	gap (%)	#bbn
		0.1	71.69	85.41		600	**6.68 / 12.79**		0
		0.2	71.73	76.02	0.01	760	**6.87 / 11.07**		1
		0.3	71.76	69.50		652	**6.72 / 10.34**		1
		0.4	71.78	69.95		675	**9.07 / 7.71**	0.01	4
	4	0.5	71.80	58.78		526	**7.94 / 7.40**		3
		0.6	71.82	66.11		520	**7.10 / 9.31**		3
		0.7	71.83	59.33		446	**7.82 / 7.59**		3
		0.8	71.84	49.55		459	**18.84 / 2.63**		3
		0.9	71.85	58.17		566	**9.68 / 6.01**		5
		1	71.87	64.53		613	**15.38 / 4.20**		5
		averages		65.735		581.70	9.61 / 7.9		2.8
		0.1	63.41	743.01		9881	**7.65 / 97.13**		1
		0.2	63.60	659.73		9273	**7.59 / 86.92**		1
		0.3	63.78	663.23		8533	**5.46 / 121.47**		0
		0.4	63.95	709.45		8800	**7.93 / 89.46**		1
	4	0.5	64.10	631.51	0.01	7850	**6.24 / 101.20**		0
		0.6	64.25	687.57		7718	**7.35 / 93.55**		1
		0.7	64.40	561.29		6974	**8.50 / 66.03**		1
		0.8	64.53	592.03		7001	**8.96 / 66.07**		1
		0.9	64.66	568.36		6572	**7.14 / 79.60**		1
		1	64.78	506.95		6240	**24.45 / 20.73**		3
		averages		632.313		7884.20	9.13 / 82.22		1
		0.1	57.46	999.19	0.01	15228	**5.77 / 173.17**		1
		0.2	57.56	1144.60		14711	**4.90 / 233.59**		0
		0.3	57.66	1349.70	0.01	14852	**4.90 / 275.45**		1
		0.4	57.75	1401.79	0.01	14485	**4.64 / 302.11**		1
30	5	0.5	57.84	1033.78		11903	**2.93 / 352.83**		1
		0.6	57.92	1001.72	0.01	10727	**3.12 / 321.06**		0
		0.7	58	808.39	0.01	10277	**5.08 / 159.13**		1
		0.8	58.08	978.83		8954	**5.28 / 185.38**		1
		0.9	58.15	877.41		8221	**5.47 / 160.4**		1
		1	58.22	986.85		7949	**4.92 / 200.58**		1
		averages		1058.226		11730.70	4.70 / 236.37		0.8
		0.1	64.15	1593.11		21283	**4.93 / 323.15**		3
		0.2	64.44	2052.01		21987	**4.92 / 417.08**		2
		0.3	64.71	1731.61	0.01	17979	**3.37 / 513.83**		0
		0.4	64.97	1636.36		15868	**3.54 / 462.25**		0
	6	0.5	65.21	1973.69	0.01	19193	**3.13 / 630.57**		0
		0.6	65.43	1209.45	0.01	15813	**2.76 / 438.21**		0
		0.7	65.65	1906.36		17550	**2.81 / 678.42**		0
		0.8	65.85	1837.07	0.01	15495	**2.82 / 651.44**		0
		0.9	66.04	1072.12	0.01	10786	**3.66 / 292.93**		1
		1	66.23	1149.93		11171	**2.78 / 413.64**		0
		averages		1616.171		16712.50	3.47 / 482.15		0.6
		0.1	63.27	8147.84		30503	**264.17 / 30.84**		14
		0.2	63.38	8003.09		30166	**515.96 / 15.51**		48
		0.3	63.65	7727.24		30050	**26.69 / 289.52**		7
		0.4	63.66	7590.73		27824	**473.19 / 16.04**		34
	4	0.5	63.99	7647.81		26344	**672.94 / 11.36**		42
		0.6	63.94	7771.99	0.01	30488	**534.87 / 14.53**		33
		0.7	64.08	8755.05	0.01	24623	**599.18 / 14.61**		32
		0.8	64.20	6155.33		24684	**641.67 / 9.59**		35
		0.9	64.56	6084.36	0.01	22038	**21.79 / 279.23**		4
		1	64.32	6680.29		22144	**582.66 / 11.47**		32
		averages		7456.373		26886.40	433.312 / 69.27		28.1
		0.1	64.86	22802.25		87776	**429.51 / 53.09**		42
		0.2	64.88	26800.50	0.01	79974	**19.27 / 1390.79**		9
		0.3	65.18	27476.83	0.01	75834	**53.00 / 518.43**		5
		0.4	65.31	22865.57	0.01	70586	**78.27 / 292.14**		6
40	5	0.5	65.45	22390.91	0.01	71975	**35.23 / 635.56**		7
		0.6	65.59	20374.59	0.01	64138	**34.32 / 593.67**		7
		0.7	65.72	29358.19	0.01	60340	**35.95 / 816.64**		16

n	p	α	Market share (%)	Conic OA cuts					
				MIN			NEW		
				cpu (s)	gap (%)	#bbn	cpu (s)/ratio	gap (%)	#bbn
		0.8	65.52	51905.27	0.01	59598	**18.29** / **2837.9**		12
		0.9	65.63	43062.82		58460	**18.13** / **2375.22**		6
		1	66.08	52360.68	0.01	51484	**34.11** / **1535.05**		7
		averages		31939.761		68016.50	75.608 / 1104.85		11.7
		0.1	65.19	103578.68		163001	**488.99** / **211.82**		47
		0.2	65.48	115223.00	0.01	127365	**24.61** / **4681.96**		3
		0.3	65.47	120905.97	0.01	120931	**24.26** / **4983.76**		3
		0.4	65.83	121014.65	0.01	121380	**26.45** / **4575.22**		3
	6	0.5	65.87	99455.95	0.01	104562	**21.90** / **4541.37**		1
		0.6	66.03	79339.45	0.01	97897	**22.29** / **3559.42**		1
		0.7	66.18	103089.10	0.01	94544	**52.11** / **1978.3**	0.01	3
		0.8	66.63	73347.01	0.01	80190	**19.75** / **3713.77**		1
		0.9	66.56	71872.46	0.01	84406	**20.29** / **3542.26**		1
		1	66.88	60059.98	0.01	76423	**22.00** / **2730.00**		1
		averages		94788.625		107069.9	72.265 / 3451.79		6.4

Appendix D

Detailed Results on Larger Instances

Table D.1: Computational results for the New MPMAPHLP formulations on instances of size $n = \{50\}$.

p	α	MS (%)	Conic			COAcuts			OA r var			OA-Obj		
			cpu(s)	gap(%)	#bbn	cpu(s)	gap(%)	#bbn	cpu(s)	gap(%)	#bbn	cpu(s)	gap(%)	#bbn
	0.1	58.69	150.97		4	115.58		1	121.12		0	233.97		0
	0.2	58.83	117.52		1	143.11		1	120.75		0	230.02		0
	0.3	58.96	114.13		1	139.54		1	124.16		0	230.97		0
	0.4	59.09	109.64		4	89.21		1	117.16		0	229.1		0
4	0.5	59.21	107.82		1	144.67		1	119.34		0	241.99		0
	0.6	59.33	115.45		1	103.85		1	119.38		0	220.89		0
	0.7	59.44	99.76		1	148.15		1	119.64		0	224.56		0
	0.8	59.54	114.25		1	110.15		1	122.13		0	408.7		0
	0.9	59.64	113.24		1	105.95		1	117.54		0	240.81		0
	1	59.74	116.78		1	147.19		1	116.38		0	222.58		0
	averages		115.956		1.6	124.74		1	119.76		0	248.359		0
	0.1	61.59	36.04		0	54.3		0	85.28		0	98.17		0
	0.2	61.84	35.47		0	48.95		0	84.39		0	94.33		0
	0.3	62.09	37.3		0	53.82		0	87.94		0	95.89		0
	0.4	62.32	37.28		0	47.82		0	88.82		0	95.57		0
5	0.5	62.54	66.4		0	48.59		0	85.83		0	93.5		0
	0.6	62.75	33.28		0	49.39		0	87.31		0	95.12		0
	0.7	62.95	30.39		0	55.14		0	85.84		0	94.66		0
	0.8	63.14	36.82		0	55.66		0	83.85		0	96.3		0
	0.9	63.32	35.84		0	55.16		0	87.03		0	94.78		0
	1	63.5	36.51		0	68.76		1	82.02		0	85.46		0
	averages		38.533		0	53.759		0.1	85.831		0	94.378		0
	0.1	54	65.99		3	100.47		3	132.78		0	260.94		0
	0.2	54.1	68.86		3	412.83		5	136.71		0	445.98		0
	0.3	54.2	104.59		5	105.77		1	137.84		0	451.35		0
	0.4	54.29	73.79		5	115.36		5	141.77		0	451.64		0
6	0.5	54.39	70.55		4	118.63		6	139.85		0	445.39		0
	0.6	54.49	112.21		4	218.85		5	138.66		0	451.53		0
	0.7	54.58	113.03		3	119.62		3	138.51		0	454.47		0
	0.8	54.67	108.63		1	126.33		1	145.86		0	457.46		0
	0.9	54.76	67.4		1	104.81		1	92.02		0	451.03		0
	1	54.84	81.01		1	117.82		1	93.25		0	431.77		0
	averages		86.606		3	154.049		3.1	129.725		0	430.156		0

Table D.2: Computational results for the New MPMAPHLP formulations on instances of size $n = \{60\}$.

p	α	MS (%)	Conic			COAcuts			OA r var			OA-Obj		
			cpu(s)	gap(%)	#bbn	cpu(s)	gap(%)	#bbn	cpu(s)	gap(%)	#bbn	cpu(s)	gap(%)	#bbn
	0.1	59.82	181.23		0	312.2		1	182.94		0	251.56		0
	0.2	60.02	175.84		0	221.44		1	183.83		0	243.42		0
	0.3	60.2	211.9		0	167.68		0	181.04		0	248.52		0
	0.4	60.38	174.71		0	164.38		0	178.12		0	239.72		0
4	0.5	60.55	477.08		2	235.56		0	176.89		0	235.89		0
	0.6	60.71	173.81		0	260.33		0	178.86		0	235.61		0
	0.7	60.87	152.38		0	191.57		1	182.64		0	241.64		0
	0.8	61.02	163.37		0	243.54		0	356.19		0	237.76		0
	0.9	61.16	170.89		0	250.28		0	177.87		0	239.71		0
	1	61.3	144.56		0	295.35		1	178.54		0	206.7		0
	averages		202.577		0.2	234.233		0.4	197.692		0	238.053		0
	0.1	58.36	332.71		3	383.42		3	337.98		0	1086.36		0
	0.2	58.55	453.62		3	455.94		3	344.61		0	1065.63		0
	0.3	58.74	164.08		2	333.89		3	291.23		0	1044.01		0
	0.4	58.93	165.63		1	258.76		2	288.62		0	1086.68		0
5	0.5	59.1	177.76		1	477.78		3	196.72		0	1002.87		0
	0.6	59.27	176.73		1	244.54		1	197.94		0	1023.87		0
	0.7	59.44	129.41		0	330.06		1	199.26		0	1011.05		0
	0.8	59.59	151.54		0	283.22		1	199.61		0	1005.95		0
	0.9	59.74	169.42		1	263.23		1	201.3		0	1010.42		0
	1	59.89	354.75		3	799.4		3	303.16		0	545.11		0
	averages		227.565		1.5	383.024		2.1	256.043		0	988.195		0
	0.1	58.73	595.89		3	607.59		3	276		0	1028.35		0
	0.2	58.94	348.61		3	356.94		3	270.41		0	533.34		0
	0.3	59.13	130.8		0	199.55		0	170.89		0	540.98		0
	0.4	59.32	122.83		0	198.58		0	172.79		0	538.26		0
6	0.5	59.49	90.8		0	161.36		0	175.28		0	537.36		0
	0.6	59.66	98.96		0	159.86		0	173.89		0	530.06		0
	0.7	59.83	95.58		0	160.18		0	168.7		0	549.2		0
	0.8	59.98	94.86		0	159.73		0	169.97		0	538.62		0
	0.9	60.13	88.08		0	192.95		1	170.62		0	251.24		0
	1	60.28	90.71		0	163.05		0	169.06		0	223.21		0
	averages		175.712		0.6	235.979		0.7	191.761		0	527.062		0

Table D.3: Computational results for the New MPMAPHLP formulations on instances of size $n = \{70\}$.

p	α	MS (%)	Conic			COAcuts			OA r var			OA-Obj		
			cpu(s)	gap(%)	#bbn	cpu(s)	gap(%)	#bbn	cpu(s)	gap(%)	#bbn	cpu(s)	gap(%)	#bbn
	0.1	58.41	1260.71		22	13325.38		76	551.58		0	-	-	-
	0.2	58.57	1035.72		50	7105.98		44	497.85		0	-	-	-
	0.3	58.73	16626.53		74	14841.98		74	542.69		0	-	-	-
	0.4	58.89	23581.1		90	1202.37		7	553.11		0	-	-	-
4	0.5	59.03	3814.64		93	18187.52		73	531.69		0	-	-	-
	0.6	59.17	1447.6		12	19200.44		73	835.6		0	-	-	-
	0.7	59.31	2846.13		30	36266.7		151	819.35		0	-	-	-
	0.8	59.44	4421.68		31	21947.25		60	823.24		0	-	-	-
	0.9	59.56	3093.15		28	3120.79		16	817.89		0	-	-	-
	1	59.68	2935.56		29	25286.91		72	803.9		0	-	-	-
	averages		6106.282		45.9	16048.532		64.6	677.69		0			
	0.1	56.18	16903.33		69	1227.23	0.01	21	514.33		0	560.78		0
	0.2	56.35	15292.51		60	1439.82		24	519.65		0	561.42		0
	0.3	56.52	1445.88		6	11459.34		63	512.02		0	558.62		0
	0.4	56.68	1369.05		8	536.6		7	799.58		0	555.75		0
5	0.5	56.83	19912.27		57	919.86		5	803.36		0	544.48		0
	0.6	56.98	612.97		4	3225.83		53	804.45		0	552.25		0
	0.7	57.12	16626.98		61	3631.76		45	801.34		0	1372.73		0
	0.8	57.26	19258.91		55	564.45		9	789.09		0	564.61		0
	0.9	57.39	3605.07	0.01	19	1465.1		21	780.93		0	565.73		0
	1	57.52	4278.12	0.01	33	1392.98		19	773.44		0	487.23		0
	averages		9930.509		37.2	2586.297		26.7	709.819		0	632.36		0
	0.1	58.01	27960.19		130	11601.65		62	1006.1		0	-	-	-
	0.2	58.27	3132.91		28	3428.79		54	1016.28		0	-	-	-
	0.3	58.52	1962.22		24	2382.9	0.01	42	1005.19		0	-	-	-
	0.4	58.76	19013.73		72	24372.38		95	1029.83		0	-	-	-
6	0.5	58.99	16440.72		62	1868.54		29	996.53		0	-	-	-
	0.6	59.21	16796.51		75	26796.33		102	1005.69		0	-	-	-
	0.7	59.42	23534.26		76	4264.21		50	1020.92		0	-	-	-
	0.8	59.61	2920.69		17	5422.56	0.01	40	1035.07		0	-	-	-
	0.9	59.8	5830.37		43	3124.84		51	1010.34		0	-	-	-
	1	59.99	2972.23		36	51891.06		162	977.69		0	-	-	-
	averages		12056.383		56.3	13515.326		68.7	1010.364		0			

Appendix E

Extended Results on Parameter Sensitivity

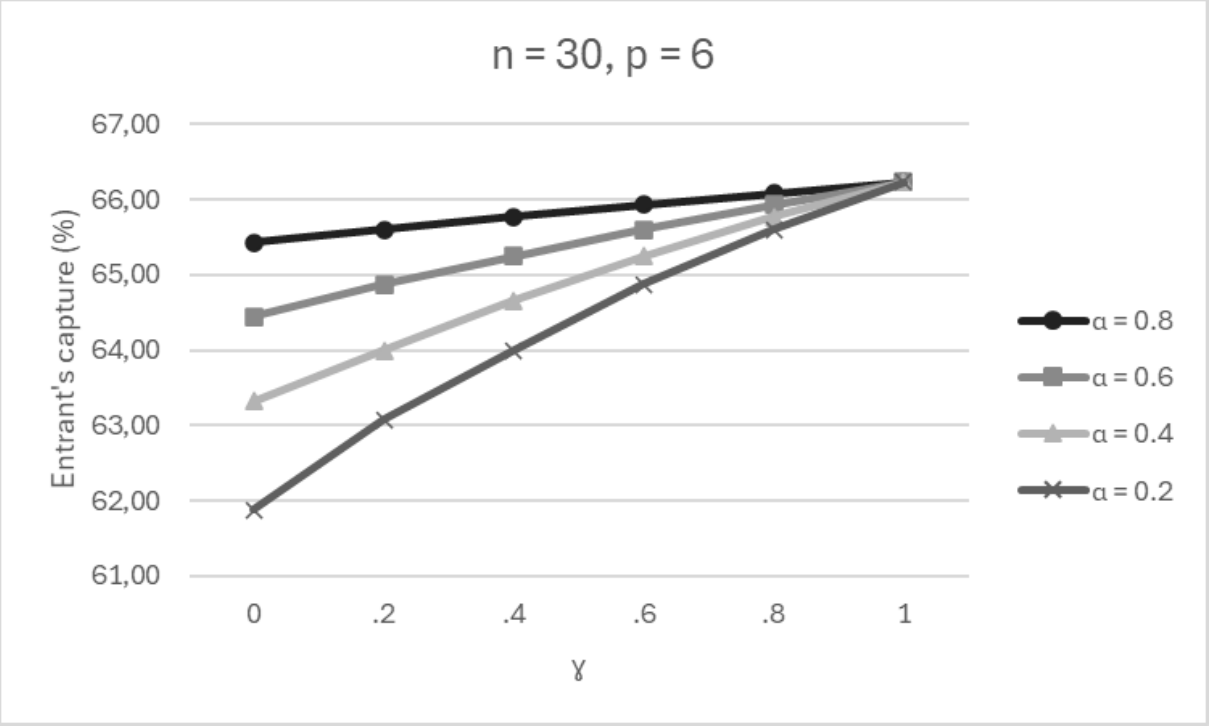

Figure E.1: Effects of parameter variation on market share gain by an entrant in a 30-node network with 6 hubs and random competitor's hub location.

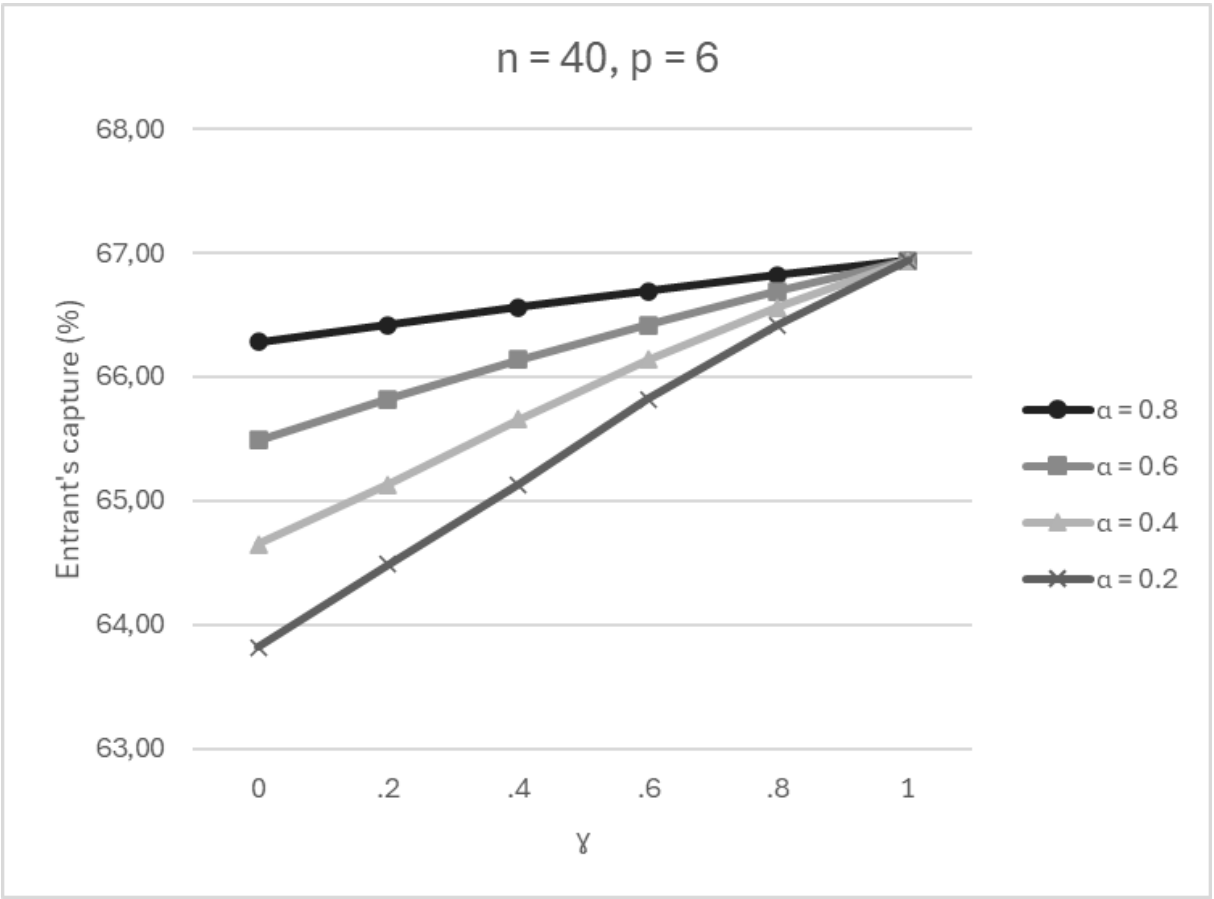

Figure E.2: Effects of parameter variation on market share gain by an entrant in a 40-node network with 6 hubs and random competitor's hub location.